Millennium Hotel • Tuesday, April 24 • 11:30 a.m.

CIRES

Rendezvous 2012

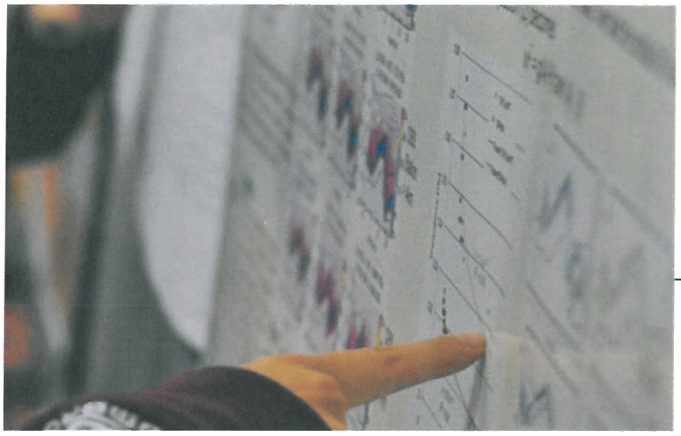

CIRES Annual Institute-wide Poster Symposium

Hosted by CIRES Members' Council
email: memberscouncil@ cires.colorado.edu

Come celebrate innovation, performance, and outstanding service with your CIRES colleagues!

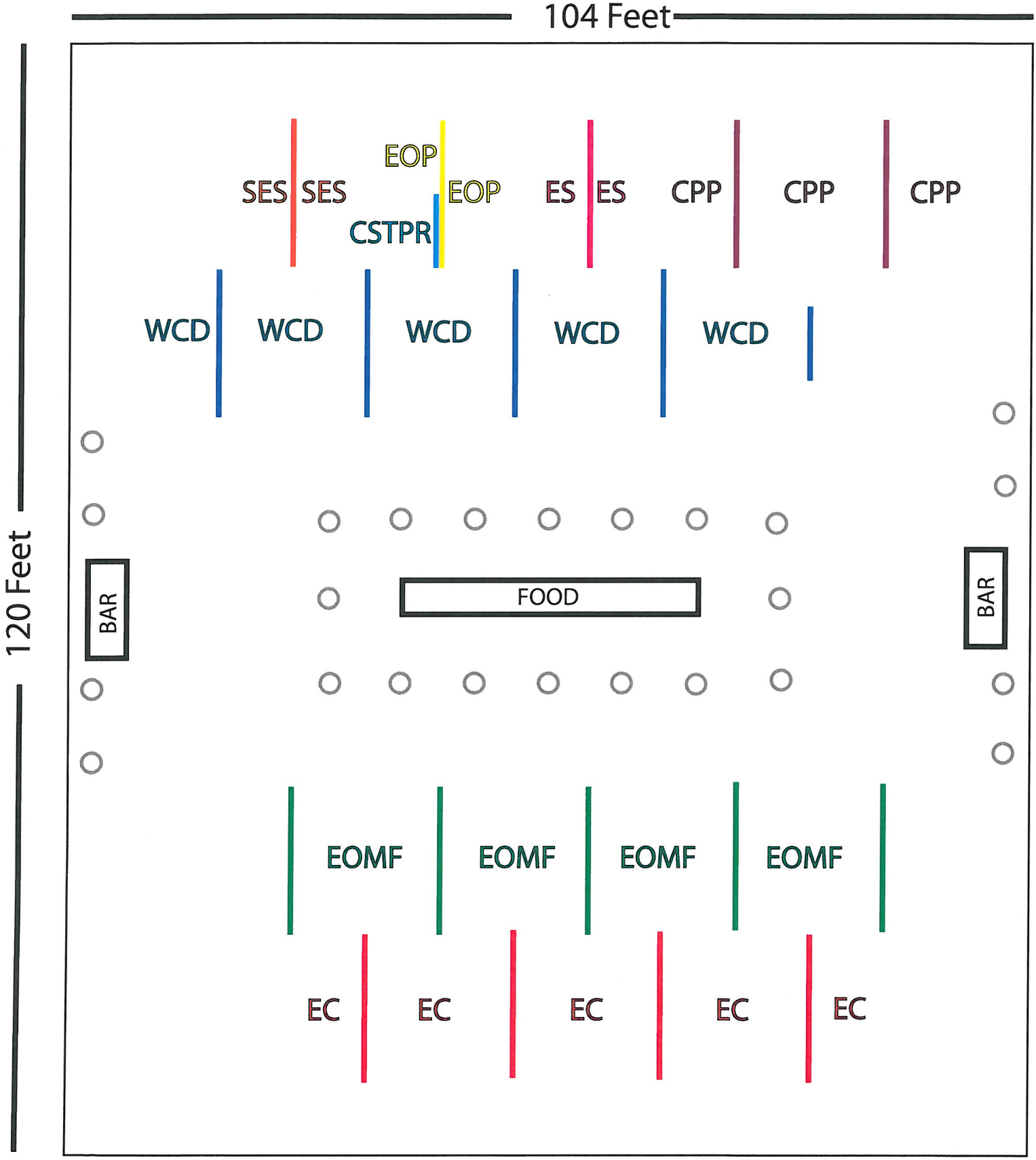
104 Feet
120 Feet
SES
SES
EOP
EOP
CSTPR
ES
ES
CPP
CPP
CPP
WCD
WCD
WCD
WCD
WCD
BAR
FOOD
BAR
EOMF
EOMF
EOMF
EOMF
EC
EC
EC
EC
EC
15mm=8'
Cocktail Tables

Poster Titles/Authors

Poster Session 1: 1.30pm - 3.00pm

Center for Science and Technology Policy

LB 1. Ecological Management and the Substitution Problem: People as Predators
Benjamin Hale (1), Alex Lee (2), Adam Hermans (2)

LB 2. Impacts of Thermoelectric Power Generation on Water Resources in the Coterminous US
K. Averyt (1), N. Madden (2), A. Huber-Lee (3), A. Lewis (4), S. Levental (3), J. Rogers (2)

Cryospheric and Polar Processes Division

PP 1. Collecting and Preserving Local and Traditional Climate Knowledge
Julia Collins, Peter L. Pulsifer, Shari Gearheard

PP 2. Characterizing the effects of changing slope on Greenland ice sheet mass balance estimates
Michael MacFerrin, Waleed Abdalati, Ted Scambos

PP 3. Challenges and decisions in producing a sea ice concentration Climate Data Record.
Matthew H Savoie, Donna J. Scott, Walter N. Meier

PP 4. Libre Systems: Making Data and Software More Available Through Re-usable Components
Scott Lewis (1), Jess Lacy (2), Stuart Reed (3), Ian Truslove (4), Luis Lopez (4), Margaret McNulty (5), Hanchao Wu (6), Miao Liu (7), Ruth Duerr (8)

PP 5. NSIDC Green Data Center Retrofit Project: Massive energy use reduction on a budget
David Gallaher(1), Ron Weaver (1), Ben Weerts (1)

PP 6. Is retreating Arctic sea ice affecting the body condition of bowhead whales?
Matthew L. Druckenmiller (1) and J. Craighead George (2)

PP 7. Establishing a Collaborative Effort to Assess the Role of Glaciers and Seasonal Snow Cover in the Hydrology of the Mountains of High Asia
R. Armstrong (1), A. Barrett (1), M.J. Brodzik (1), F. Fetterer (1), S.J.S. Khalsa (1), A. Racoviteanu (2), B. Raup (1), M. Williams (2)

PP 8. LiDAR for Snow Depth Mapping
Jeffrey S. Deems (1,2), Thomas H. Painter (3), David C. Finnegan (4)

PP 9. Changes in Arctic atmospheric moisture as shown by six reanalyses
Andrew P. Barrett, Mark C. Serreze, Julienne Stroeve

PP 10. Simulation of ICESat-2 micro-pulse laser measurements over polar ice/snow surfaces of different geophysical parameters
Mahsa S.Moussavi (1), Waleed Abdalati (2), Ted Scambos (3)

PP 11. Global Policy Implications of Thawing Permafrost
Kevin Schaefer (1), Tingjun Zhang (1), Lori Bruhwiler (2), Andrew P. Barrett (1), Zhuxiao Li (1)

PP 12. Algorithm Development for Analysis of Multi-Beam Photon-Counting Laser Altimeter Data as a Means to Maximize Expected Science Return From the ICESat-2 Mission
Ute C Herzfeld (1,2), Brian McDonald (2), Bruce F Wallin (1,6), Stephen P Palm (3), Alexander Marshak (4), Thorsten Markus (5), Thomas Neumann (5), Phillip Chen (1,2), Matt Goo (1,2)

PP 13. Bering Glacier Surge 2011 - Observation, Analysis and Parameterization
Brian McDonald (1,2), Ute C. Herzfeld(1,2), Maciej Stachura (3), Alexander Weltmann (1), Robert Grifin Hale (1), William Alex Yearsley (1), Sean O'Grady (1)

Ecosystem Science Division

PK 1. High Elevation Lakes of the Western US: Are we Studying Systems Recovering from Excess Atmospheric Deposition of Acids and Nutrients?
James O. Sickman

PK 2. Pentachlorophenol hydroxylase
Why is it such a poor catalyst and how could it do better?
Klara Hlouchova (1), Johannes Rudolph (2), Shelley Copley (1)

PK 3. Accelerating Education in Interdisciplinary Geographic Science and Technology in India: Proposal to the Obama-Singh 21st Century Knowledge Initiative.
Dr. John J. Kineman

PK 4. Resistance and resilience mediate disturbance interactions: A synthesis and modeling exercise.
Brian Buma (1), Carol Wessman (2)

PK 5. Effects of fish introductions on lakes at high elevations in the Colorado Rockies: Seasonal variability in biomass and production of macroinvertebrates
Thomas M. Detmer (1), James H. McCutchan, Jr. (2), and William M. Lewis, Jr. (3)

PK 6. Assessing the benefits of green infrastructure: The dynamics of landscape decision, built morphology, and ecosystem services
Carol Wessman(1), Brian Muller(2), Mahda Bagher(2), Brian Buma(1), Travis Flohr(2), Mehdi Heris(2),

PK 7. Ice Analysis and Seal Identification with Image Analysis
Betsy Weatherhead (1), Ute Herzfeld (1), Lance Bradbury (1), Jim Maslanik (1)

Education Outreach Program

YL 1. Project EXTREMES (Exploration, Teaching and Research for Excellence in Middle and Elementary Science)
Cooper, Leigh

YL 2. Inspiring Climate Education Excellence(ICEE): Developing Elearning professional development modules - secondary science teachers
Emily Kellagher, Susan Buhr, Susan Lynds

Poster Titles/Authors

Poster Session 1: 1.30pm - 3.00pm

YL 3. Addressing climate and energy misconceptions – teaching tools offered by the Climate Literacy and Energy Awareness Network (CLEAN)
Anne U. Gold (1), Tamara Shapiro Ledley (2), Karin Kirk (3), Marian Grogan (2), Susan M. Buhr (1), Cathryn A. Manduca (3), Sean Fox (3), Frank Niepold (4), Cynthia Howell (5), Susan E. Lynds (1)

YL 4. The Role of Photography in the Study of Climate Change
Natasha Vizcarra, Allaina Wallace

YL 5. Partnering with the CIRES Education and Outreach Group on Broader Impacts
Susan Buhr (1), Jessica Feld (1), Anne Gold (1), Emily Kellagher (1), Susan Lynds (1), Amanda Morton (1), David Oonk (1), Lesley Smith (1)

YL 6. The National Ocean Sciences Bowl (NOSB): More Than Just A Competition
Emily Kellagher (1), Amanda Morton (2)

Environmental Chemistry Division

Poster Session 2: 3.00pm - 4.40pm

RD 1. Global Model Study of Isocyanic Acid (HNCO)
Paul J. Young(1,2), Louisa K. Emmons(3), Jean-Francois Lamarque(3), James M. Roberts(2), Christine Wiedinmyer(3), Patrick Veres(4) and John J. Orlando(3)

RD 2. Organic Aerosol Formation and Processing in the Los Angeles Basin: Role of Gasoline vs. Diesel Emissions
R. Bahreini (1,2), A.M. Middlebrook (2), J. de Gouw (1,2), C. Warneke (1,2), M.K. Trainer (2), S.S. Brown (2), W.P. Dube (1,2), J.S. Holloway (1,2), A.E. Perring (1,2), J.P. Schwarz (1,2), J.R. Spackman (1,2), H. Stark (1,2,3), N.L. Wagner (1,2), D.D. Parrish (2)

RD 3. Potential Aerosol Mass (PAM) flow-through reactor measurements of SOA formation from BEACHON-RoMBAS
Brett B. Palm (1,2), Amber M. Ortega (1,3), Pedro Campuzano-Jost (1,2), Douglas A. Day (1,2), Thomas Karl (4), Lisa Kaser (5), Werner Jud (5), Armin Hansel (5), Juliane L. Fry (1,6), Steven S. Brown (7), Kyle Zarzana (1,2), William Dube (1,7), Nick Wagner (1,7), Danielle Draper (6), William H. Brune (8), and Jose L. Jimenez (1,2)

RD 4. Real-time gas and particle-phase organic acids measurement at a forest site using chemical ionization high-resolution time-of-flight mass spectrometry during BEACHON-RoMBAS
R.L.N. Yatavelli (1), H. Stark (1,2), J.R. Kimmel (2,3), M.J. Cubison(3), D.A. Day(1), J.T. Jayne(2), J. A. Thornton(4), D.R. Worsnop(2), J.L. Jimenez(1)

RD 5. The signature of aqSOA: Aerosol modification by secondary organic aerosol formation in the aqueous phase
Barbara Ervens (1,2), Annmarie Carlton (3)

RD 6. Addressing Science and Policy Needs with Community Emissions Efforts
Gregory Frost (1), Leonor Tarrasón (2), Claire Granier (1,3,4), Paulette Middleton (5), and the ECCAD and CIERA teams

RD 7. NO3-initiated oxidation of biogenic hydrocarbons: An important nighttime sink of volatile organic compounds and source of secondary organic aerosol
Juliane L. Fry (1), Danielle Draper (1), Steven S. Brown (2), James N. Smith (3), Kyle Zarzana (4), Brett B. Palm (4), Pedro Campuzano-Jost (4), Jose L. Jimenez (4), Lisa Kaser (5), Armin Hansel (5), Bill Brune (6), Peter Edwards (2), John Ortega (3), Paul Winkler (3)

RD 8. Twenty-five years of ozonesonde measurements at South Pole: An assessment of changing loss rates
Birgit Hassler (1,2), John S. Daniel (2), Bryan J. Johnson (3), Susan Solomon (4), Samuel J. Oltmans (1)

RD 9. Importance of Biotic vs Abiotic Controls on VOC Emissions from Ponderosa Pine
Allyson S.D. Eller (1), Peter C. Harley (2), Russell K. Monson (1,3)

RD 10. Influence of Benzene on the Optical Properties of Titan Haze Laboratory Analogs in the Mid-Visible
Y. Heidi Yoon (1), Melissa G. Trainer (2), Margaret A. Tolbert (1,3)

RD 11. Volatile organic compounds (VOCs) in the South Coast Air Basin (SoCAB): Characterizing the gas-phase chemical evolution of air masses during CalNex 2010
J.B. Gilman (1,2), B.M. Lerner (1,2), W.C. Kuster (1,2), D. Bon (1,2,3), C. Warneke (1,2), E.J. Williams (1,2), J.S. Holloway (1,2), I.B. Pollack (1,2), T.B. Ryerson (1), E.L. Atlas (4), D.R. Blake (5), S.C. Herndon (6), M.S. Zahniser (6), A. Vlasenko (7), S.M. Li (7), S. Alvarez (8), B. Rappenglueck (8), J. Flynn (8), N. Grossberg (8), B. Lefer (8), J.A. de Gouw (1,2)

RD 12. Depositional ice nucleation on monocarboxylic acids: effect of the O:C ratio
Gregory Schill and Margaret Tolbert

RD 13. Winter Ozone Production: Uintah Basin, Utah
Russ Schnell(1), Samuel Oltmans(2), Ryan Neeley(2) and Thomas Mefford(2)

RD 14. Absorption Cross Sections of Ozone and Hydrogen Peroxide Between 350 nm and 470 nm
Jessica L. Axson (1)(2), Steve S. Brown (3), Greg Frost (2)(3), Tara F. Kahan (3), Veronica Vaida (1)(2), Rebecca A. Washenfelder (2)(3), and Cora J. Young (2)(3)

RD 15. Long term variations in springtime Arctic boundary layer ozone depletion events at Barrow, Alaska (1973-2012)
Samuel J. Oltmans (1,2), Joyce M. Harris (2), Laura C. Patrick (1,2), Bryan J. Johnson(2)

RD 16. Evaluation of turbulence of marine stratocumulus in large-eddy simulations against ship-borne data
Takanobu Yamaguchi (1)(2), Alan Brewer (2), Graham Feingold (2)

RD 17. A revised look at the oceanic sink for atmospheric carbon tetrachloride (CCl4)
James H. Butler (1), Shari A. Yvon-Lewis (2,6), Jurgen M. Lobert (3,6), Daniel B. King (3,6), Stephen A. Montzka (1,6), James W. Elkins (1), Bradley D. Hall (1), Valentin Koropalov (5), John L. Bullister (7)

RD 18. Shorter-lived trace-gases: opportunities for mitigating ozone depletion and climate change
S. Montzka (1,2), G. Dutton (2), B. Miller (2), C. Siso (2), D. Mondeel (2), T. Conway (1), E. Dlugokencky (1), B. Hall (1), D. Nance (2), J. Elkins (1), and J. Butler (1)

RD 19. The glyoxal budget and its contribution to organic aerosol for Los Angeles, California during CalNex 2010
R. A. Washenfelder (1, 2), C. J. Young (1,2), S. S. Brown (2), W. M. Angevine (1,2), E. L. Atlas (3), D. R. Blake (4), D. M. Bon (1,2), M. J. Cubison (1,5), J. A. de Gouw (1,2), S. Dusanter (6,7,8), J. Flynn (9), J. B. Gilman (1,2), M. Graus (1,2), S. Griffith (6), N. Grossberg (9), P. L. Hayes (1,5), J. L. Jimenez (1,5), W. C. Kuster (1,2), B. L. Lefer (9), I. B. Pollack (1,2), T. B. Ryerson (2), H. Stark (1, 10), P. S. Stevens (6), and M. K. Trainer (2)

RD 20. Comparisons between aircraft, balloon and remote sensing measurements of UT/LS water vapor during the NASA MACPEX mission
A. W. Rollins (1,2), T. D. Thornberry (1,2), R.-S. Gao (2), L. A. Watts (1,2), D. W. Fahey (1,2), E. G. Hall (1,3), A. F. Jordan (1,3), D. F. Hurst (1,3), J. B. Smith (4), M. R. Sargent (4), D. S. Sayres (4), C. Schiller (5), N. Spelten (5), M. Krämer (5)

RD 21. Medical Aerosols for Global Health: New Needle-Free Methods of HPV Vaccine Delivery of Dry Powders and Aerosols
Stephen P. Cape (1), David H. McAdams (1,2), Elizabeth Gersch (4), David Chen (1,2), Nisha K. Shah (1,2), Robert L. Garcea (3,4) and Robert E. Sievers (1,2,3)

RD 22. Application of a volatility basis set model to secondary organic aerosol simulations across the U.S.
R. Ahmadov (1,2), S. McKeen (1,2), R. Bahreini (1,2), A. Middlebrook (2), J.A. de Gouw (1,2), J.L. Jimenez (1,3), P.L. Hayes (1,3), M. Trainer (2)

RD 23. BioCORN Study 2011 – Eddy covariance fluxes over energy crop ecosystems
Martin Graus (1, 2), Carsten Warneke (1, 2), Eric J Williams (1, 2), Brian M Lerner (1, 2), Jessica B Gilman (1, 2), Rui Li (1, 2), Allyson SD Eller (1, 3), Christopher Gray (1, 3), Noah Fierer (1, 3), Ray Fall (1, 4), Peter C Harley (5), James M Roberts (2), Christopher Fryrear (6), Mark Collins (6), Karl Whitman (6), Joost De Gouw (1, 2)

RD 24. Decadal Change and Regional Trends of PH Throughout the Southern Ocean
Andrew R. Margolin (1,2), Nicole S. Lovenduski (2,3), Jose-Luis Jimenez (1,4), Cortlandt G. Pierpont (1)

RD 25. Vertical profiles of HONO during NACHTT 2011: Relative importance of heterogeneous production on aerosol versus the ground surface
C. J. Young (1,2), T. C. VandenBoer (3), N. L. Wagner (1,2), W. P. Dube (1,2), T. P. Riedel (4), R. Bahreini ((1,2), F. Ozturk ((1,2), C. Warneke (1,2), J. de Gouw (1,2), W. C. Keene (5), A. A. P. Pszenny (6), J. A. Thornton (4), D. Wolfe (1), S. S. Brown (1), A. M. Middlebrook (1), and J. M. Roberts (1)

RD 26. N2O5 uptake coefficients determined from ambient wintertime measurements
N. L. Wagner (1, 2), T. P. Riedel (3,4), J. M. Roberts (1), J. A. Thornton (3), T. C. VandenBoer (1), W. P. Dubé (1,2), A. M. Middlebrook (1), B. C. Sive (5), R. S. Russo (5), C. A. Brock (1), C. J. Young (1,2), F. Ozturk (1), R. Bahreini (1,2), Y. Zhou (6), R. Swarthout (6), S. S. Brown (1)

RD 27. Henry's law coefficients and hydrolysis rate coefficients of atmospheric trace gases
Ranajit K Talukdar (1,2)*, Bartlomiej Witkowski (1,2,3), A. R. Ravishankara (2), and James B. Burkholder (2)

Environmental Observations, Modeling and Forecasting Division

GR 1. Multi-scale observations of small cloud systems
Allison McComiskey (1,2), Graham Feingold (2), Andrew Vogelmann (3)

GR 2. Processing and presentation of high-resolution DART® data for recent significant tsunami events
George Mungov(1,4), Marie C. Eblé(2), Kelly J. Stroker(3)

GR 3. Decadal Variability in the Background Stratospheric Aerosol Layer
R.R. Neely III(1,2,3), R. Michael Hardesty (1,2), S. Solomon(4), Owen B. Toon (3,5), Jeffrey P. Thayer (6), John E. Barnes(2), Karen Rosenlof(2), E.G. Dutton(2), Michael O'Neill(1)

Poster Titles/Authors

GR 4. Feasibility of US National Wind and Solar Energy Production System
Alexander E. MacDonald (1), Anneliese Alexander (2), Christopher Clack (1), Adam Dunbar (1), Yuanfu Xie (1)

GR 5. ncISO Facilitating Metadata and Scientific Data Discovery
David Neufeld (1), Ted Habermann (2)

GR 6. Application of Wave Interferometry to Experimental Investigation of Infragravity Waves off New Zealand
Nikolay Zabotin (1,2), Oleg Godin (2,3), Anne Sheehan (4,2), Zhaohui Yang (4,2), and John Collins (5)

GR 7. Long term changes in the upper stratospheric ozone at Syowa, Antarctica
Koji Miyagawa (1), Irina Petropavlovskikh(2), Robert D. Evans (3), C. Long(4), J. Wild (4), G. Manney (5)and W. Daffer (5)

GR 8. Lightning NOx Parameterization for Synoptic Meteorological-scale Predictions with Convective Parameterization in WRF-Chem
John Wong (1), David Noone (1), Mary Barth (2)

GR 9. Diurnal variations of meteoric Fe layers in the mesosphere and lower thermosphere at McMurdo (77.8°S, 166.7°E), Antarctica
Zhibin Yu1, Xinzhao Chu1, Wentao Huang1, Weichun Fong1, and Zhangjun Wang1

GR 10. Impact of Atmospheric Tides on Ionosphere-Thermosphere System
T.-W. Fang(1), T. J. Fuller-Rowell(1), R. A. Akmaev(2), and F. Wu(1)

GR 11. Diurnal and Seasonal Variations of Temperatures from Lower to Upper Atmosphere at McMurdo, Antarctica from 2010 to 2011
Weichun Fong (1), Xinzhao Chu (1), Zhibin Yu (1), Cao Chen (1), Wentao Huang (1)

GR 12. Quantifying Digital Elevation Model (DEM) Uncertainty Introduced by Interpolative Gridding
Christopher Amante (1,2), Barry Eakins (1,2)

GR 13. Lidar and radar investigation of gravity wave characteristics, propagation and dissipation from the stratosphere to the lower thermosphere over McMurdo, Antarctica
Cao Chen (1), Xinzhao Chu (1), Weichun Fong (1), Zhibin Yu (1), Adrian J. McDonald (2) and Xian Lu (3)

GR 14. Observed Ocean Spectra from Argo Profiling Floats
Katherine McCaffrey (1,2), Baylor Fox-Kemper (1,2)

GR 15. Ozone depletion in filaments of the Arctic Polar Vortex observed during the first Global Hawk UAS science mission
James W. Elkins (1), Eric J. Hintsa (1,2), Geoffrey S. Dutton (1,2), Bradley D. Hall (1), Fred L. Moore (1,2), Ru-shan Gao (1), Samuel J. Oltmans (1,2), Bryan Johnson (1), Eric A. Ray (1,2), David W. Fahey (1) , and Paul A. Newman (3) plus GloPac, HIPPO, and MLS teams.

GR 16. Three Decades of Continuous Monitoring of Long-lived Halocarbons
Geoff Dutton (1), Brad Hall (2), J. David Nance (1), Debra J. Modeel (1), James W. Elkins (2)

GR 17. A Comparison of Solar and Lunar Position Algorithms
Allen Jordan (1,2), Emiel Hall (1,2), Jim Wendell (2), Ellsworth Dutton (2)

Poster Titles/Authors

Poster Session 2: 3.00pm - 4.40pm

GR 18. Simultaneous and Common-Volume Lidar Observations of the Mesospheric Fe and Na Layers at Boulder (40°N, 105°W)
Wentao Huang(1), Xinzhao Chu(1), Zhangjun Wang(1), Weichun Fong(1),
Zhibin Yu(1), John A. Smith(1), Brendan Roberts(1)

GR 19. Improving our understanding of ozone depleting substances (ODS) in the upper atmosphere
J. D. Nance (1,2), J. W. Elkins (2), F. L. Moore (1,2), G. S. Dutton (1,2), E. J. Hinsta (1,2), B. D. Hall (2), D. J. Mondeel (1,2), B. J. Miller (1,2), C Siso (1,2), and S. A. Montzka (2)

GR 20. Studying the 'cold pole' problem in WACCM and comparisons to lidar temperature morphology
Bo Tan(1)(2), Han-Li Liu(2), and Xinzhao Chu(1)

GR 21. Experimental Validation of a New Balloon-Borne Supercooled Liquid Sensor
Emrys Hall (1,2), Allen Jordan (1,2), Dave Serke (3), Frank McDonough (3), John Bognar (4), Spencer Abdo (4), Kirstin Baker (4), Tom Seitel (4), Randolph Ware (5), Marta Nelson (5), Andrew Reehorst (6)

GR 22. Determining constraints on aerosol parameter retrievals from direct and diffuse irradiances from 300 to 1050 nm
P. Kiedron (1), K. Lantz (1), P. Disterhoft (1), J. Michalsky (2)

GR 23. Comparison of Continuous Surface Ozone Measurements from Two Arctic Observatories
L. Patrick1, S.J. Oltmans1, I. Petropavlovskikh1

GR 24. Global Trends in Sulfur Hexafluoride
Brad Hall (1), Geoff Dutton (2), Debbie Mondeel (2, presenter), David Nance (2), Dale Hurst (2), Matt Rigby (3), Fred Moore (2), James Butler (1), James Elkins (1)

GR 25. Enhancing natural hazards data discovery with visual media
Heather L. McCullough (1), Evan McQuinn (2), Jesse Varner (2)

GR 26. Trace Gas Distributions Observed During the HIPPO Project
Eric J. Hintsa (1,2), Fred L. Moore (1,2), Geoff S. Dutton (1,2), Brad D. Hall (1), J. David Nance (1,2), and James W. Elkins (1)

GR 27. Sub-grid scale processes of the marine boundary layer cloud-aerosol system
Jan Kazil(1,2), Graham Feingold(2,1)

GR 28. An Information Management System for the U.S. Extended Continental Shelf Project
Jennifer Henderson(1), Elliot Lim(1), Evan McQuinn(1), Jesse Varner(1), Barry Eakins(1), John LaRocque(2), Anna Milan(2), Robin Warnken(2), and Susan McLean(2)

GR 29. Stochastic Weather Generator Based Ensemble Streamflow Forecasting
Nina Caraway (1), Balaji Rajagopalan (1),(3), Andy Wood (2), Kevin Werner (2)

GR 30. Global Stokes Drift and Climate Wave Modeling
Adrean Webb, Baylor Fox-Kemper

GR 31. Extreme Events: Pacemakers of Adaptation?
William R. Travis

GR 32. NGDC's first foray into CLASS: the transition of data archive and stewardship into an external archival facility
Francine Coloma (1), Robert Prentice (1), and Peter Elespuru (1)

GR 33. A real-time model of the equatorial ionospheric eastward electric field driven by ACE solar wind data.
Manoj Nair, Stefan Maus

GR 34. Student Training and Atmospheric Research (STAR) Na Doppler LIDAR at Boulder, Colorado
John A. Smith, Weichun Fong, Brendan Roberts, Wentao Huang, Xinzhao Chu

GR 35. Climate adaptation barriers and opportunities in the United States: A focus on policy and decision making at the sub-national scale
Lisa Dilling

GR 36. The ionospheric gravity and diamagnetic current systems
P. Alken (1), S. Maus (1), A. D. Richmond (2), A. Maute (2)

GR 37. Anomaly analysis of recent summer heat waves
Emily C. Gill (1), Emily P. Wilson(1), Thomas Chase(1)

GR 38. NOAA Mobile Laboratory's Unique Contribution to the Uintah Basin Study
Jonathan Kofler(1), Gabrielle Pétron(1), Bill Dubé(1), Peter Edwards(1), Steven S Brown(1), Felix Geiger(2), Carsten Warneke(1), Laura Patrick(1), Sara Crepinsek(1), Benjamin R Miller(1), Pat Lang(1), Tim Newberger(1), Jack Higgs(4), Colm Sweeny(1), Doug Guenther(1), Anna Karion(1), Sonja Wolter(1), James Salzman(3), Jonathan Williams(4), Mark Slovak(5), Allen Jordan(1), Pieter Tans(3), Russ Schnell(3)

GR 39. Hurricane Wake Restratification Mechanisms
Haney, S. R. (1,2), Fox-Kemper, B. (1,2), Bachman, S. (1,2), Cooper, B. (1,2), Kupper, S. (1,2), McCaffrey, K. L. (1,2), Stevenson, S. (1,2,3), Van Roekel, L. P. (1,2,4), Webb, A. (2,5), Ferrari, R. (6).

GR 40. The TropSat Observatory for Mesoscale Convective System Processes in the Global Maritime Tropics
David G. Long, Brigham Young University, Ernesto Rodriguez, Jet Propulsion Laboratory , Ralph F. Miliff, Visiting Fellow, CIRES , Robert Gaston, Jet Propulsion Laboratory
Brigham Young University, Jet Propulsion Laborator, Visiting Fellow, CIRES

Poster Titles/Authors

Poster Session 1: 1.30 pm - 3.00pm

Solid Earth Sciences Division

OG 1. Tracing the Geomorphic Signature of Lateral Faulting in New Zealand's Marlborough hill country
Alison R. Duvall (1), Gregory E. Tucker (1)

OG 2. Passive Tomography using a Dense Array of Single-Channel Seismic Recorders with applications to the Bighorn Mountains, Wyoming
Colin T. O'Rourke (1), Anne F. Sheehan (1), Joshua C. Stachnik (1,3), Lindsay L. Worthington (2) and the BASE Seismic Team

OG 3. Buoyancy sources in the Western U.S.
Will Levandowski (1), Craig Jones (1), Weisen Shen (2), Mike Ritzwoller (2)

OG 4. Constraining Mantle Anisotropy under the South Island of New Zealand
Daniel W. Zietlow(1), Anne F. Sheehan(1), Zhaohui Yang(1), Joshua C. Stachnik(1,4), John Collins(2), and Martha K. Savage(3)

OG 5. Reducing the Uncertainty in the Estimation of Deformation across the Rio Grande Rift Region
James Choe1, R. Steven Nerem1,3, Anne Sheehan2,3, Henry Berglund4, Mark H. Murray5

OG 6. Controls on the evolution of the Himalayan thrust belt
Delores M. Robinson

OG 7. Estimated Shallow Crustal Shear Velocity Structure Off the South Island, New Zealand from Seafloor Compliance Measurements
Justin S. Ball (1), Anne F. Sheehan (2)

Weather and Climate Dynamics Division

BL 1. Ground-based GPS Observation of SED-associated Irregularities Over CONUS
Yang-Yi Sun1,2,3 , Tomoko Matsuo1,2, Eduardo A. Araujo Pradere1,2, and Jann-Yenq Liu3

BL 2. Evaluation of the differential Doppler velocity approach for sizing particles in ice clouds
Sergey Matrosov

BL 3. Identifying Multiple Peaks in W-band Radar Doppler Spectra during Drizzle Events in VOCALS 2008
Christopher R. Williams (1, 2), Chris Fairall (2), and Ken Moran (1, 2)

BL 4. WRIT: Web Based Renanalyses Intercomparison Tools
Catherine A. Smith and Gilbert P. Compo

BL 5. The automated detection and analysis of short-term changes in coronal dimmings
Larisza Krista (1), Alysha Reinard (2)

BL 6. Physical Modeling of Neutral Winds in the Thermosphere: Initial Results
Mariangel Fedrizzi(1,2), Timothy J. Fuller-Rowell(1,2), Mihail Codrescu(2), Mark Conde(3), Kazuo Shiokawa(4)

BL 7. Auroral Forms that Extend Equatorward from the Persistent Midday Aurora during Geomagnetically Quiet Periods
J. V. Rodriguez (1), H. C. Carlson, Jr. (2), R. A. Heelis (3)

Poster Titles/Authors

BL 8. The effects of 3D error covariance and background model bias for an ionospheric data assimilation model
C. Y. Lin (1,2,3), T. Matsuo (1,2), E. A. Araujo-Pradere (1,2), and J. Y. Liu (3)

BL 9. New ways of discretizing global climate models
Shan Sun (1,2) and Rainer Bleck (1,2,3)

BL 10. High-resolution modeling approaches to understanding changes in extreme precipitation projections
Kelly Mahoney(1), Michael Alexander(2), Jamie Scott(1), Joe Barsugli(1)

BL 11. Adapting to Climate Change on the Shoshone National Forest: a science-management collaboration to develop planning and management tools
Janine Rice (1, 2), Linda Joyce (2), Bryan Armel (3), and Jeff Lukas (1)

BL 12. Turbulence profiles and cloud-surface coupling in Arctic stratiform clouds
Matthew D Shupe (1), P. Ola G Persson (1), Amy Solomon (1), Ian Brooks(2), Guylaine Canut (2)

BL 13. Inventory of NGDC high-resolution coastal tide gauge datasets for tsunami mitigation
Erica L. Harris, George Mungov

BL 14. Remote Sensing of the Mountain Snowpack: Integration of Observations and Models to Support Water Resource Management and Ecosystem Science
Noah Molotch (1,2), Jeff Deems (2), Bin Guan (3), Leann Lestak (4), Dominik Schneider (1), Michael Durand (5), Thomas Painter (3), and Jeff Dozier (6)

BL 15. Enhancing short term wind energy forecasting for improved utility operations: The Wind Forecast Improvement Project (WFIP)
Irina V. Djalalova (1), Laura Bianco (1), and James. M. Wilczak (2)

BL 16. Low-frequency variability of and impact of climate change on Southern California's Santa Ana winds
Mimi Hughes (1); Dan Cayan (2); Alex Hall (3)

BL 17. ENSO Diversity in the NCAR-CCSM4 Model
Antonietta Capotondi

BL 18. Global speleothem oxygen isotope measurements since the Last Glacial Maximum
Anju Shah (1), Carrie Morrill (1), Ed Gille (1), Wendy Gross (2), Dave Anderson (2), Bruce Bauer (2), Rodney Buckner (2), Mike Hartman (1)

BL 19. Evaluation of the impact of radar reflectivity data assimilation on RR and HRRR reflectivity and precipitation forecasts
Patrick Hofmann (1), Steve Weygandt (2), Ming Hu (1), Stan Benjamin (2), Haidao Lin (3), Curtis Alexander (1), David Dowell (2)

BL 20. A climatology of short-range weather forecasts from the High Resolution Rapid Refresh model
Eric James (1), Curtis Alexander (1), Brian Jamison (2), Stan Benjamin (3), Steve Weygandt (3)

BL 21. A Conditional Skill Mask for Improved Seasonal Predictions
Kathy Pegion(1,2), Arun Kumar (3)

Poster Titles/Authors

Poster Session 1: 1.30pm - 3.00pm

BL 22. Diagnosing a daily index of tornado variability with global reanalysis
Philip Pegion (1) and Martin Hoerling (2)

BL 23. Implementation of Space Environmental Anomalies Expert System Real Time
Jonathan Darnel (1), Janet Green (2), William Denig (2)

BL 24. Doppler Lidar Study of Wind Flow Characteristics in the Wake of Operating Wind Turbine
Pichugina Y.L.(1, 2), R. M. Banta (2), W. A. Brewer (2), J.K. Lundquist (3), N. D. Kelley (4), R. M. Hardesty (2), Andrew Clifton (4), R. J. Alvarez (2), M. L. Aitken (3), J. D. Mirocha (5), S. P. Sandberg (2), and A. M. Weickmann (1, 2)

BL 25. Relative contributions of synoptic and low-frequency eddies to time-mean atmospheric moisture transport, including the role of atmospheric rivers
Matthew Newman (1), George N. Kiladis (2), Klaus M. Weickmann, F. Martin Ralph (2), and Prashant D. Sardeshmukh (1)

BL 26. Evaluation of High Resolution Rapid Refresh (HRRR) Model Changes and Forecasts During 2011
Curtis Alexander (1), Steve Weygandt (2), Stan Benjamin (2), Tanya Smirnova (1), David Dowell (2), Patrick Hofmann (1), Eric James (1), Ming Hu (1), Haidao Lin (3), John Brown (2), and Joe Olson (1)

BL 27. Investigating North Pacific air-sea interaction using a local, empirical model
Dimitry Smirnov (1), Matt Newman (1), Mike Alexander (2)

BL 28. Snow and Ice Enhancements to the Land-Surface model used in WRF-based Rapid Refresh
Tatiana G. Smirnova (1,2), John M. Brown (2), Stan Benjamin (2)

BL 29. A Relationship Between Stochastic Forcing of Tropical SST and the North Atlantic Oscillation (NAO)
Leslie M. Hartten (1,2), Cécile Penland (2)

BL 30. Understanding the Causes of ENSO Asymmetry Using CMIP5 Runs
Tao Zhang and De-Zheng Sun

BL 31. Physical Processes Associated with Heavy Flooding Rainfall in Nashville, Tennessee, and Vicinity during 1–2 May 2010: The Role of an Atmospheric River and Mesoscale Convective Systems
Benjamin J. Moore (1), Paul J. Neiman (2), F. Martin Ralph (2), Faye E. Barthold (3**)**

BL 32. Toward Understanding the Climatic Role of Tropical Cyclones Using an Atmospheric General Circulation Model: Experiment Design and Model Evaluation
Henry R. Winterbottom (1), Phillip J. Pegion (2), and Robert E. Hart (3)
Upper Colorado Runoff Predictions in Support of NIDIS, Klaus Wolter (1,2,3)

BL 33. Upper Colorado Runoff Predictions in Support of NIDIS
Klaus Wolter, (1,2,3). (1) CIRES, (2) NOAA ESRL, (3) WWA

BL 34. Ionosphere-Plasmasphere-Electrodynamics (IPE) Model: An Impact of the Realistic Geomagnetic Field Model on the Ionospheric dynamics and energetics
Naomi Maruyama(1,2), Phil Richards(3), Tzu-Wei Fang(1,2), Catalin Negrea(1,2), Leslie Mayer(1,2), Tim Fuller-Rowell(1,2), Art Richmond(4), Astrid Maute(4), Rempel, Naomi

BL 35. The Western Water Assessment RISA Program: An Overview of Recent Accomplishments and Ongoing Research.
Eric Gordon(1), Jeff Lukas(1), Brad Udall(1), Kristin Averyt(1), and Tim Bardsley(1). (1) CIRES Western Water Assessment

LB 1. Ecological Management and the Substitution Problem: People as Predators

Benjamin Hale (1), Alex Lee (2), Adam Hermans (2). (1) ENVS/Philosophy, (2) ENVS

Management policies for America's National Parks require that "natural" conditions, as well as ecological and physical processes, are maintained and/or restored as much as possible. Shifts in the population of any critical species are often presumed to lead to "unnatural" conditions and disrupt critical ecological processes. For example, the Rocky Mountain National Park elk population, no longer kept in check by wolves, is thought to degrade the ecosystem by overgrazing and shifting foraging patterns of smaller fauna. To combat this degradation and manage trophic downgrading, National Park Service snipers act as surrogate predators, culling the elk population. In this paper, we argue that such practices fail to meet justificatory muster. Such strategies implicitly conflate the wolf component of the Rocky Mountain ecosystem with the function of wolf predation. Wolves are not just a means of predation, but an essential component of the collective ecosystem identity. We argue our position by presenting a series of thought experiments and intuition pumps. Hypothesizing similar policies that replace other species with their functional equivalents provides a consistency test for the practice. Though there are perhaps many non-ecological reasons for promoting this current culling policy, we conclude that wolf reintroduction is necessary to uphold our obligations to restore the Rocky Mountain National Park ecosystem's integrity.

LB 2. Impacts of Thermoelectric Power Generation on Water Resources in the Coterminous US

K. Averyt (1), N. Madden (2), A. Huber-Lee (3), A. Lewis (4), S. Levental (3), J. Rogers (2). (1) Western Water Assessment, CIRES, (2) Union of Concerned Scientists, (3) Tufts University, (4) Duke University

Water for thermoelectric cooling accounts for over 41% of all freshwater withdrawals in the US. Local water resources can be stressed by power plant water requirements when demand is imbalanced relative to surface and groundwater supplies. This research uses the Water Supply Stress Index, or WaSSI, to calculate the ratio of water demand to water supply for 2,106 8-digit hydrologic units nationwide (Sun et al. 2008). Water demand was determined by withdrawals from seven major user categories (commercial, domestic, industrial, irrigation, livestock, mining, thermoelectric), while supply is the sum of a) surface water supply; b) groundwater supply, based on historic rates of groundwater withdrawal; and c) return flows from major water users, including cities, agriculture and power plants. To identify basins where thermoelectric water use adds to the water burden, we calculate the WaSSI for each basin nationwide, both with and without power-plant water use included. We find that power plants exacerbate water stress in 44 basins. However, water transfers from other basins and reservoir storage were not taken into account, as robust data are unavailable. Work following on to this research delves into each "hotspot" to evaluate the utility of the WaSSI indicator in the context of its assumptions. References: Sun, G., S.G. McNulty, J.A. Moore Myers, and E.C. Cohen. 2008. Impacts of Multiple Stresses on Water Demand and Supply across the Southeastern United States. Journal of American Water Resources Association 44(6):1441-1457. http://www.forestthreats.org/tools/WaSSI

PP 1. Collecting and Preserving Local and Traditional Climate Knowledge

Julia Collins, Peter L. Pulsifer, Shari Gearheard, National Snow and Ice Data Center, CIRES

The Exchange for Local Observations and Knowledge of the Arctic (ELOKA) provides data management services and support to Arctic communities and others who are working with local and traditional knowledge (LTK) or who are gathering data from community-based monitoring systems. These data are at high risk of loss or, when preserved, may be difficult to access for a variety of reasons, including concerns regarding the distribution of sensitive or culturally important information and the difficulty of initiating or maintaining community-based research without an established data management infrastructure. LTK data are often presented in formats quite different from satellite or model data sources (e.g., interviews, maps, and photographs), which adds to the challenge of using LTK in concert with other climate data sets. The ELOKA team works together with local experts, indigenous organizations and researchers to design systems for responsibly curating these data, making them available to the contributing Arctic communities, and where possible, available to the climate research community in formats suitable for linking to satellite or model data. Where interest exists, we are helping our partners develop local data management programs. We will present examples of data management strategies used to date, lessons learned, and ideas for the future.

Note: Poster originally presented at 2011 World Climate Research Programme (WCRP) Open Science Conference.

PP 2. Characterizing the effects of changing slope on Greenland ice sheet mass balance estimates

Michael MacFerrin, Waleed Abdalati, Ted Scambos, CIRES, ESOC, University of Colorado, Department of Geography

Current Mass Balance estimates derived from satellite altimetry products use the assumption of constant slope to derive height change (dh/dt) measurements. However, with the rapid thinning of outlet glaciers across the ice sheet, this assumption may prove inadequate for deriving true mass balance estimates, especially along the ice sheet margins where changing topography is most pronounced. Using improved methods for processing ICESat data, with verification from airborne lidar data tracks, we can quantify the affects that changing topography have on mass balance estimates across the Greenland Ice Sheet.

PP 3. Challenges and decisions in producing a sea ice concentration Climate Data Record.

Matthew H Savoie, Donna J. Scott, Walter N. Meier, NSIDC

Historic sea ice concentrations derived from satellite passive microwave sensors are an important climatological data set. Trends in extent are often cited as evidence of fundamental changes in the Earth's climate. The general public is increasingly aware of climate change, yet climate change deniers continue to spread misinformation by casting doubts when misrepresenting both data and scientific findings. To ensure data quality while increasing public confidence, increased transparency and full reproducibility should be a goal for every researcher. In NSIDC's recent effort to create a sea ice concentration Climate Data Record (CDR), our goal was to create a completely automated, reproducible data set that matched the existing widely-used, published data sets. In this presentation, we review the challenges we encountered and the solutions selected in the creation of the CDR. These included unreproducible ancillary files, manual editing of data, and uncertainty about the input data. As we strive to meet CDRs production requirements for reproducibility, we acknowledge we are sacrificing data quality without manual processes. Researchers must understand the provenance and quality of a data set when choosing to use it

PP 4. Libre Systems: Making Data and Software More Available Through Re-usable Components

Scott Lewis (1), Jess Lacy (2), Stuart Reed (3), Ian Truslove (4), Luis Lopez (4), Margaret McNulty (5), Hanchao Wu (6), Miao Liu (7), Ruth Duerr (8)
(1) NASA, (2) PIC, (3) NSF

With the amount of stored data increasing at an exponential rate, it is becoming increasingly important for scientists and data managers to find effective ways to allow users to discover and use data effectively. Sharing software tools to assist in this effort is also becoming more vital in making this a reality. The National Snow and Ice Data Center's Libre project is solving this by creating a system of components including an aggregator, which will allow users to find data and services matching specified criteria more easily. While making it flexible enough to injest metadata from various sources is important, it is also important to make the concepts and actual software components available to others who wish to make their data and services more discoverable and accessible. The Libre system is designed to make this a reality, by componentizing the underlying mechanisms and thus allowing the pieces to be shared and reused by those who need them. These components can then be tailored to meet specific needs, allowing the individual data providers to avoid wasteful duplication of effort, and focus more on making their data available to the world. This componentization would also allow the data providers to replace specific pieces with other software if desired, while still preserving the overall functionality of the system. When finished, the various components of the Libre system will be released to the open source community, facilitating the easy inclusion and modification of the system, and allowing users to discover data and services more easily.

PP 5. NSIDC Green Data Center Retrofit Project: Massive energy use reduction on a budget

David Gallaher(1), Ron Weaver (1), Ben Weerts (1), (1) NSIDC

The Green Data Center Project was a successful effort to significantly reduce the energy use of the National Snow and Ice Data Center (NSIDC). Through a full retrofit of a traditional air conditioning system, the cooling energy required to meet the data center's constant load has been reduced by over 70% for summer months and over 90% for cooler winter months. The new cooling system design includes a unique cooling system that uses both airside economization and a new air conditioner that uses the efficient Maisotsenko Cycle. This cycle uses both direct and indirect evaporative cooling to produce a supply air state that is 30° to 40° Fahrenheit below the incoming air temperature. A patented heat and mass exchanger divides the incoming air stream into two streams: working air and product air. The working air is directed into channels with wetted surfaces and cooled by direct evaporation. At the same time, adjacent channels carry product air without any water added or wetted surface. The adjacency of these airstreams allows for indirect evaporative cooling of the product air. Working air, warm and saturated, is ultimately exhausted to the outside, or directed into the space when room humidity is below the humidity setpoint. The room humidity can drop below 25% relative humidity if the outside humidity is very low (which happens often in Colorado), and the AHU is in economizer mode, providing a significant amount of outdoor air to the room. In the winter months, this effect is even more pronounced and working air is directed into the space most of the time. One of the goals of this project was to create awareness of simple and effective energy reduction strategies for data centers. Although this particular project was able to maximize the positive effects of airside economization and indirect evaporative cooling because of its geographic location, similar strategies may also be relevant for many other sites and data centers in the U.S. The Green Data Center project was separated into several components: server consolidation and virtualization and installing a more efficient cooling system and finally a 50kW solar array. Overall, the power utilization of the datacenter was reduced 70%. It is important to realize that some energy reduction was achieved by simply reducing the IT load through server virtualization and server room consolidation.

PP 6. Is retreating Arctic sea ice affecting the body condition of bowhead whales?

Matthew L. Druckenmiller (1) and J. Craighead George (2), (1) CIRES Visiting Postdoctoral Fellow, CIRES, University of Colorado Boulder
(2) North Slope Borough Department of Wildlife Management, Barrow, AK

Recent studies suggest that Arctic summer sea ice retreat may drive increased phytoplankton blooms in the Arctic Ocean, which may in turn promote greater zooplankton production. Zooplankton provides an important food source to bowhead whales (Balaena mysticetus), which are migratory ice-associated baleen whales that spend summer in Arctic waters, including the eastern Beaufort Sea. Thus, do summer sea ice conditions affect the health of bowhead whales by influencing food availability? Alaska's North Slope Borough Department of Wildlife Management has collected body-condition measurements (girth, length, and thicknesses of blubber and hypodermis) from bowhead whales of the Western Arctic Stock harvested by Inupiat subsistence hunters since the early 1970's. In this study we investigate relationships between summertime ice severity and bowhead whale body condition from 1979 to 2011. We examine monthly averaged sea ice concentration from SMMR and SSM/I passive microwave data for the summer months of June through September within different feeding areas in the Beaufort Sea. Whale age, sex, and pregnancy status are considered. Preliminary analysis suggests that the body condition of juvenile whales may be more responsive to variability in ice conditions than that of adults. Additional investigations may include analysis of (1) satellite derived ocean color using Chl-a as an indicator for phytoplankton biomass, and (2) a time- and regionally-weighted sea ice severity index that not only considers ice conditions of the previous summer but rather ice concentration over a preceding three-year period across the whale's entire migratory habitat of the Bering, Chukchi and Beaufort Seas.

PP 7. Establishing a Collaborative Effort to Assess the Role of Glaciers and Seasonal Snow Cover in the Hydrology of the Mountains of High Asia

R. Armstrong (1), A. Barrett (1), M.J. Brodzik (1), F. Fetterer (1), S.J.S. Khalsa (1), A. Racoviteanu (2), B. Raup (1), M. Williams (2)
(1) CIRES, (2) INSTAAR

This collaborative project, funded by USAID, will improve our understanding of the water resources of High Asia. While it is generally accepted that a significant component of these water resources comes from the melting of glacier ice and seasonal snow, the actual volume of water available from these two individual sources remains uncertain. The amount, timing, and spatial patterns of snow and ice melt play key roles in providing water for downstream irrigation, hydropower generation, and general consumption. The overall objective of this study is to develop a thorough and systematic assessment of the snow and glacier contribution to the water resources originating across the Himalaya-Karakoram-Hindu Kush, and the Pamir and Tien Shan mountain ranges of Central Asia. Specific project objectives are being accomplished using a suite of satellite remote sensing, reanalysis, and ground-based data as input to specific snow and ice melt models. In addition, we will evaluate the accuracy of the melt model results using innovative isotopic and geochemical analyses to identify and quantify the sources of water (glacier ice melt, seasonal snow melt, rainfall, and ground water) flowing into selected rivers representing the major hydro-climates of the study area. This project will interact with key Asian research groups currently operating across the study region. This will include capacity building to enhance the scientific understanding of the hydrology of the study region among our Asian partners through collaborative field research and technical training. The mountain ranges included in this study are located within the countries of Bhutan, Nepal, India, Pakistan, Afghanistan, Kazakhstan, Uzbekistan, Kyrgyzstan, and Tajikistan, and approximately one-third of the USAID award will be devoted to supporting scientists within these nine partner countries to perform collaborative research with University of Colorado scientists (CIRES and INSTAAR).

PP 8. LiDAR for Snow Depth Mapping

Jeffrey S. Deems (1,2), Thomas H. Painter (3), David C. Finnegan (4)
(1) NSIDC, (2) NOAA Western Water Assessment, (3) NASA Jet Propulsion Laboratory, (4) USACE CRREL

Light Detection and Ranging (LiDAR) is a remote sensing technology that holds tremendous promise for quantifying snow depth in snow hydrology and avalanche applications. In recent years LiDAR has seen a dramatic widening of applications in the natural sciences, resulting in technological improvements and an increase in the availability of both airborne and ground-based sensors. Modern sensors allow recording of multiple returns per pulse or full return-energy waveforms, which allows characterization of vegetation canopies, below-forest terrain, and sub-resolution roughness estimation. Reported vertical accuracies for airborne datasets under typical flight conditions are on the order of 10 cm, with point densities on the order of 50-150 points per square meter in contemporary commercial systems. Ground-based systems typically provide mm-scale range accuracy and cm-scale point spacing (at 500m), with ranges of up to 4000 meters. However many factors in the LiDAR acquisition process, such as laser scan angle, pulse rate, surface reflectance, amplitude, and flight or shot geometry relative to terrain gradients require consideration to achieve specific sampling densities in forested and/or complex terrain. Additionally, laser light interaction with the snow surface has a significant volumetric scattering component, requiring different considerations for surface height error estimation than for other earth surface materials. The penetration depth of the laser pulse at a particular wavelength is dependent primarily on optical grain size, near-surface liquid water content, and the angle of incidence. We use published estimates of penetration depth to estimate radiative transfer errors to depth measurement errors. In this paper, we present a review of LiDAR mapping procedures and error sources, investigate potential errors unique to snow surface remote sensing in the NIR and visible wavelengths, and make recommendations for projects using airborne and ground-based LiDAR for snow depth mapping.

PP 9. Changes in Arctic atmospheric moisture as shown by six reanalyses

Andrew P. Barrett, Mark C. Serreze, Julienne Stroeve, NSIDC-CIRES

We examine recent changes in tropospheric water vapor in the Arctic using output from six reanalyses. Global Climate Models indicate warming will be accompanied by increases tropospheric water vapor. These changes will likely also occur in the Arctic. The Arctic is undergoing considerable changes. In the past decade, there have been substantial increases in tropospheric air temperatures in the Arctic that are larger than those observed for the globe as a whole. This warming is largest in the cold season. September minimum sea ice extent in the Arctic Ocean has declined, with extreme minima occurring in each year since 2002. Increases in moisture transport from lower latitudes, increased temperatures and increased exposure of open water, especially in fall, are all likely to contribute to increased tropospheric water vapor in the Arctic. Atmospheric reanalyses are used widely to study the climate system because they provide temporally complete time series of atmospheric variables with full spatial coverage at standard levels. This is a key advantage over surface and radiosonde stations which have limited spatial coverage at high latitudes. However, inconsistencies can arise in reanalyses because of changes in observing systems. Care must be taken when using renalyses to examine trends. With this caveat in mind, we examine spatial patterns and seasonal changes in Arctic tropospheric water vapor in six reanalyses; MERRA, CFSR, JRA-25, ERA-Interim, ERA-40 and NCEP/NCAR. Data from reanalyses are also compared with profiles of tropospheric water vapor from Arctic radiosonde stations. Clear differences exist between reanalyses. All reanalyses have trouble recreating near-surface profiles of water vapor observed in radiosonde.

PP 10. Simulation of ICESat-2 micro-pulse laser measurements over polar ice/snow surfaces of different geophysical parameters

Mahsa S.Moussavi (1), Waleed Abdalati (2), Ted Scambos (3)

(1)CIRES, ESOC, (2)CIRES, ESOC, (3)NSIDC

The ATLAS instrument on-board NASA's ICESat-2 mission will utilize a rather new technology in altimetry with main science objectives of measuring ice sheet elevation changes, sea ice thickness and vegetation biomass. The instrument will be a multi-beam, micro-pulse photon counting lidar operating at green wavelength, that is expected to provide enhanced measurement capabilities as compared to its predecessor, the original ICESat mission. However, there are some uncertainties about the data quality, as photon-counting altimetry from orbit has not been carried out before. This gives rise to a need for a comprehensive study to investigate the effects of different geophysical parameters (surface slope, roughness, reflectivity, ..) on the ICESat-2 signal and the impact it will have on the elevation retrieval along with elevation change recovery. In this poster, the methodology to simulate micro-pulse measurements over different polar snow/ice surfaces with respect to the ATLAS instrument parameters is described. Preliminary results of the Monte-Carlo simulation along with an outline for future work are also presented.

PP 11. Global Policy Implications of Thawing Permafrost

Kevin Schaefer (1), Tingjun Zhang (1), Lori Bruhwiler (2), Andrew P. Barrett (1), Zhuxiao Li (1)

(1) National Snow and Ice Data Center, 449 UCB, University of Colorado, Boulder, CO 80309-0449; Phone: 303-492-8869, Fax: 303-492-2468, Email: kevin.schaefer@nsidc.org, (2) NOAA Earth System Research Laboratory, 325 Broadway, Boulder, CO 80305

Global treaties to reduce fossil fuel emissions should include a 15% allocation for permafrost carbon emissions or we will overshoot our target CO2 concentration and end up with a warmer climate than planned. Arctic permafrost currently contains 1466 Gt of carbon frozen since the last ice age, roughly double the amount of carbon in the atmosphere. We estimate 190±64 Gt of this carbon will thaw out, decay, and end up in the atmosphere by 2200, potentially increasing atmospheric CO2 concentrations by 87±29 ppm. A carbon release of this magnitude is equal to 15% of the total allowed emissions to hit a target CO2 concentration of 700 ppm. Global targets for fossil fuel emissions must be reduced an additional 15% to account for the release of carbon from thawing permafrost. Current treaty negotiations do not include a 15% allocation for permafrost carbon emissions. We present the scientific basis for our results and summarize our successes and failures in trying to influence international treaty negotiations to reduce fossil fuel emissions.

PP 12. Algorithm Development for Analysis of Multi-Beam Photon-Counting Laser Altimeter Data as a Means to Maximize Expected Science Return From the ICESat-2 Mission

Ute C Herzfeld (1,2), Brian McDonald (2), Bruce F Wallin (1,6), Stephen P Palm (3), Alexander Marshak (4), Thorsten Markus (5), Thomas Neumann (5), Phillip Chen (1,2), Matt Goo (1,2), (1) CIRES, (2) ECEE, (3) NASA Goddard Space Flight Center Science Systems and Applications Inc., (4) NASA Goddard Space Flight Center Climate and Radiation Branch, (5) NASA Goddard Space Flight Center Cryospheric Sciences Branch, (6) New Mexico Tech.

The Ice, Cloud and Land Elevation Satellite-II (ICESat-2) mission has been selected by NASA as a Decadal Survey mission, to be launched in 2016, citing the urgent need to observe the rapidly changing cryosphere. Mission objectives are to measure land ice elevation, sea ice freeboard/thickness and changes in these variables as well as canopy height with an accuracy that will allow prediction of future environmental changes and estimation of sea-level rise. Two innovative components will characterize the ICESat-2 lidar: (1) Collection of elevation data by a multi-beam system and (2) application of micropulse lidar (photon counting) technology. A micro-pulse photon-counting altimeter yields clouds of discrete points, which result from returns of individual photons, and hence new data analysis techniques are required for elevation determination and association of returned points to reflectors of interest including land and sea ice surfaces, ground, tree canopy, water, clouds and blowing snow. In this paper, we present results from algorithm development and analysis of aircraft observations using micro-pulse photon altimeter systems designed or considered as predecessors of ICESat-2 instrumentation, including MABEL and SIGMA aircraft data. GLAS data analyses will be included to illustrate capabilities and challenges of laser altimetry.

PP 13. Bering Glacier Surge 2011 - Observation, Analysis and Parameterization

Brian McDonald (1,2), Ute C. Herzfeld(1,2), Maciej Stachura (3), Alexander Weltmann (1), Robert Grifin Hale (1), William Alex Yearsley (1), Sean O'Grady (1), (1) CIRES, (2) ECEE, (3) CU AES

Bering Glacier, the largest and longest glacier in North America, in summer 2011showed definite signs of a surge, which is a sudden acceleration of the glacier to 100 times or more of its normal velocity and an event that happens only every 25-years in a quasi-cyclic and unpredictable time pattern. Heavy crevassing indicative of sudden deformation, horizontal and vertical displacement of ice and sudden changes in the englacial hydrologic system are components of a surge. Understanding rapid glacier movement is an essential component in understanding changes in the cryosphere and in the Arctic system, and this event provides a rare opportunity for research on exemplary processes of ice acceleration. Funded through an NSF RAPID project, our group collected systematic aerial observations of the Bering-Bagley Glacier System in September 2011, including high-resolution laser altimetry, video and photographic image data and GPS data, which are complemented by satellite data. A second observation campaign is planned for early summer 2012. Objectives of the project are to observe, document and analyze the current surge of Bering Glacier and derive parameters that capture deformation characteristics during surge stages and provide information that may facilitate mechanical modeling of fast glacier movement. Results from the Bering Glacier surge are expected to transfer to (other) Arctic areas or other forms of glacial acceleration, e.g. to some of the processes that occur along the margin of the Greenland ice sheet.

PK 1. High Elevation Lakes of the Western US: Are we Studying Systems Recovering from Excess Atmospheric Deposition of Acids & Nutrients? James O. Sickman, (1) CIRES Sabbatical Fellow, (2) Associate Professor of Hydrology, University of California, Riverside

Instrumental records and monitoring of high elevation lakes in the western United States began in the early 1980s. Much effort has be devoted to detecting chamges in these aquatic ecosystems resulting from atmospheric deposition of acids and nutrients. However, there is growing evidence that thresholds for atmospheric pollutants were crossed much earlier in the 20th Century and that some of the subsequent hydrochemical and ecological changes observed in these lakes may be the result of recovery from earlier atmospheric forcing. We examine responses of high elevation lakes to atmospheric deposition on annual to century timescales using data from a 29-year study of Emerald Lake (Sequoia National Park) and paleolimnological analyses of other high elevation lakes incorporating diatom species analyses and geochemical proxies for fossil-fuel burning. At Emerald Lake, we have observed multiple transitions between nitrogen and phosphorus limitation of phytoplankton, the earliest of which occurred in the beginning of the 1980s and may be the result of reduction in N deposition due to the Clean Air Act. Critical loads analyses incorporating diatom species in lake sediments suggest that thresholds for N deposition were crossed in the period of 1950-1980 in the Rocky Mountains and likely much earlier, 1900-1920, in the Sierra Nevada. Diatom species composition is strongly controlled by acid neutralizing capacity (ANC) in the Sierra Nevada and we have observed a pronounced decline and recovery of ANC over the period of 1920-1980 in some Sierra Nevada lakes that coincides with the abundance of spheroidal carbonaceous particles (i.e., a diagnostic tracer of fossil fuel combustion) preserved in lake sediments; these patterns appear to be driven by increased emissions of oxidized N and S in the mid-20th Century and reductions in acid precursor levels caused by the Clean Air Act in the 1970s. Thus, when interpreting observational records from western high elevation lakes, researchers must consider the possibility that changes in ecology and hydrochemistry may have occurred many decades earlier in the 20th Century. Furthermore, detection of climate forcing of chemistry and aquatic ecosystems in western montane regions is made more difficult by human impacts on atmospheric deposition of acids and nutrients during the past 150 years.

PK 2. Pentachlorophenol hydroxylase Why is it such a poor catalyst and how could it do better?

Klara Hlouchova (1), Johannes Rudolph (2), Shelley Copley (1),

(1) CIRES, (2) Department of Chemistry and Biochemistry, University of Colorado Boulder

Pentachlorophenol (PCP) is a pesticide that has been seriously contaminating our environment as a result of its extensive use initiated in the1930s. The soil bacterium Sphingobium chlorophenolicum has been shown to have recently assembled a novel metabolic pathway to degrade this highly toxic pesticide. However, the pathway is inefficient and the bacterium is unable to tolerate high concentrations of PCP. The first, particularly interesting and rate-determining step in this pathway (see Fig. 1) is catalyzed by PCP hydroxylase (PcpB), a flavin monooxygenase that converts PCP to tetrachlorobenzoquinone (TCBQ). The product of PcpB reaction has been questioned by some researchers who argue that PcpB converts PCP to TCHQ rather than TCBQ. Here we address the substrate/product identification and catalytic limitations of the PcpB. We confirm that the product of the PCP reaction is TCBQ. We show that the downstream metabolite TCHQ is also accepted in the active site of PcpB as a substrate, forming TCBQ and reversing the flow of the pathway. In addition to its poor ability to hydroxylate PCP, PCP hydroxylase exhibits 'uncoupling' during the reaction, as described earlier for related flavin monooxygenases. As a result, an excess of O2 and NADPH, the reaction co-substrates, are consumed, and toxic H2O2 is produced.

PK 3. Accelerating Education in Interdisciplinary Geographic Science and Technology in India: Proposal to the Obama-Singh 21st Century Knowledge Initiative.

Dr. John J. Kineman, Wessman Research Group

Prior research in India focused on developing ecological niche modeling methods and a high-quality geographic database, collaborating with scientists and students at three institutions in India. The Obama-Singh 21st Century Knowledge Initiative, announced last year, affords an excellent opportunity to advance this work and build long-term capacity in India and scholarly exchange with the University of Colorado via CIRES, the Graduate School, and the Office of International Education. India needs improved capacity for conducting geographical analysis to predict and manage problems of ecosystem response to environmental change. Enhancing this expertise at the graduate level will demonstrate the practical value of geospatial technology and interdisciplinary science education to meet current environmental research and management challenges. Advances in Geographic Information Systems and related geospatial modeling software provide the key enabling technologies. Our objective is to provide a critical threshold of training that will build interest among academicians in interdisciplinary landscape science and geospatial technology demonstrated at three institutions in southern India, via collaborative multi-level training and case-study involvement. We will install necessary software at existing facilities and provide individualized training and educational exchanges that will integrate with each institution's existing programs. Methods will be evaluated for long-term application. The main benefit will be to produce experts who will enhance available capacity and train others with relatively little outside assistance, and attract students. The project will stimulate and leverage the production of partners and leaders to creatively solve environment-ecosystem problems that especially threaten developing, highly populated, biodiversity rich, and climatically vulnerable regions such as India, but that also have global implications. Scholars inside and outside of India will benefit from exposure to the problems and capabilities of this region, brought into global education contexts.

PK 4. Resistance and resilience mediate disturbance interactions: A synthesis and modeling exercise.

Brian Buma (1), Carol Wessman (2), CIRES, EBIO

Interactions between disturbances may lead to unexpected results with dramatic implications for landscape structure, composition, and functioning. Compounding disturbance events may exceed ecosystem resilience, pushing it into alternate stable regimes. Seemingly complex, disturbance interactions may be conceptualized as mediated through temporary changes in two fundamental mechanisms: Resistance and resilience. Interactions altering resistance mechanisms increase/decrease the likelihood, severity, and spatial extent of future disturbances. Interactions mediated through resilience mechanisms increase/decrease the ability of the ecosystem to reorganize following subsequent disturbances. These interactions may be time-based (e.g. a second disturbance occurs before recovery from the first) or legacy-based (where disturbance legacies, such as dead materials or alterations to the landscape, alter the characteristics of the second disturbance). While the mechanisms are disturbance and ecosystem specific, the general conceptual framework is applicable to all cases. A synthesis of current studies is presented alongside a spatially-explicit, generalized modeling study (neutral landscape) illustrating how disturbance interactions (both time-based and legacy-based), when mediated through these fundamental properties, can drive alternate landscape configurations. Inclusion of legacy-based interactions creates quantitatively different outcomes. Results indicate that disturbance-driven alterations to resistance and resilience are important drivers of landscape heterogeneity and change in many landscapes.

PK 5. Effects of fish introductions on lakes at high elevations in the Colorado Rockies: Seasonal variability in biomass and production of macroinvertebrates

Thomas M. Detmer (1), James H. McCutchan, Jr. (2), and William M. Lewis, Jr. (3) (1) CIRES Center for Limnology

Previous studies of the effects of fish introductions on lakes at high elevations have demonstrated a decrease in macroinvertebrate biomass during the middle of the growing season. Little is known, however, about how fish introductions influence macroinvertebrate communities during the early and late parts of the growing season or how they change macroinvertebrate production over the entire growing season. We compared macroinvertebrate production and biomass during the early, middle, and late growing season in five lakes with and without fish in Rocky Mountain National Park, Colorado. We found differences in biomass between lakes with fish and lakes without fish during each seasons; the magnitude of differences increased over the course of the growing season. We did not find differences in production between lakes with and without fish; the lakes are homeostatic with respect to macroinvertebrate production, despite biomass differences. This is possible because fish reduce the average body size of macroinvertebrates; smaller body size of macroinvertebrates leads to a higher ratio of production to biomass.

PK 6. Assessing the benefits of green infrastructure: The dynamics of landscape decision, built morphology, and ecosystem services

Carol Wessman(1), Brian Muller(2), Mahda Bagher(2), Brian Buma(1), Travis Flohr(2), Mehdi Heris(2), (1) CIRES and EBIO, (2) CU Planning and Design

Urban natural landscapes provide services that may address a variety of environmental and urban planning needs, including improvement of hydrological systems, disaster risk mitigation, mitigation of climate change effects, amelioration of heat islands and carbon sequestration. Green infrastructure is considered a strategy for adapting to climate change and environmental stresses, however its benefits have not been evaluated systematically as an integrated analysis of landscape morphologies and ecosystem services. We are exploring the drivers and benefits of green infrastructure investment at local and regional scales using remote sensing and spatial data in an emerging mega-region, the Colorado Front Range, which extends across two states from Pueblo, Colorado to Laramie, Wyoming. We focus on two outcomes of landscape decisions: urban phenology and the thermal landscape. This stage of the project has two components. First, we characterize both the built and un-built components of landscape morphologies at sample sites (using high detail data) and across the region (using moderate resolution data). Second, we evaluate patterns of phenology (temporal variation in MODIS NDVI), thermal effects (ASTER), and land use/land cover within the framework of these morphologies. These results support green infrastructure policy as an adaptive strategy to conditions of climate change and resource scarcity.

PK 7. Ice Analysis and Seal Identification with Image Analysis

Betsy Weatherhead (1), Ute Herzfeld (1), Lance Bradbury (1), Jim Maslanik (1), U. Colorado at Boulder

Images of sea ice taken from aircraft can give detailed information on sea ice characteristics over a broad area that can not be retrieved from satellite or finite area studies. Techniques are being developed to analyze these images to supply fundamental physical characteristics of ice and to help identify seals on ice. The techniques rely on state-of-the art image analysis algorithms for both the ice characteristics and the seal identification. The techniques are currently being applied to over 70,000 images from several different countries. Application of these techniques allows for objective analysis of images that has previously been unattainable. Merging of results across the Arctic can offer new insights into Arctic sea ice, seal populations and potential changes. Experts in ice analysis, unmanned aircraft and computer science are joining with international and national colleagues to produce open source tools to aid in both counting seals and understanding the changing Arctic sea ice.

YL 1. Project EXTREMES (Exploration, Teaching and Research for Excellence in Middle and Elementary Science)

Leigh Cooper, Project EXTREMES, CIRES, NSF, EBIO, Computer Science, BVSD

The outdoors provides an excellent stimulus for sparking student interest in the sciences. Through personal exploration of extreme environments our students are not only able to make observations about ecosystems but also become engaged in the dynamic processes of nature. Project EXTREMES (Exploration, Teaching and Research for Excellence in Middle and Elementary Science) traveled with our fifth grade students to the University of Colorado Mountain Research Station (CU MRS) in the Front Range of the Colorado Rockies during the Fall 2011 to learn about high elevation environments. The MRS station offers our socioeconomically diverse students a chance to explore a local ecosystem that otherwise might be inaccessible to them. Through multiple experiential, hands on, and observational activities students discover the effects of mountain pine beetle on lodgepole pines and forest ecosystem processes. Because most of our students were aware of mountain pine beetles due to their high level of publicity, the students were very interested to learn about the changes to Colorado forests caused by mountain pine beetle infestations. The activities taught included lessons on 1) Tree identification; 2) Tree coring; 3) Mountain pine beetle life cycles, and 4) The distribution of tree mortality from mountain pine beetle. Teachers and Fellows have drawn on these common field experiences to expand and develop unique lessons back in the middle school student's classroom. Project EXTREMES is a collaboration among the Boulder Valley School District (BVSD), the University of Colorado's Cooperative Institute for Research in Environmental Science (CIRES), and the Departments of Ecology and Evolutionary Biology and Computer Sciences.

YL 2. Inspiring Climate Education Excellence(ICEE): Developing Elearning professional development modules - secondary science teachers

Emily Kellagher, Susan Buhr, Susan Lynds, CIRES,

Inspiring Climate Education Excellence (ICEE) is a NASA-funded project to develop content knowledge and knowledge of effective teaching strategies in climate education among secondary science teachers. ICEE resources are aligned with the Essential Principles of Climate Science. Building upon a needs assessment and face to face workshop, ICEE resources include iTunesU videos, an ICEE 101 resource site with videos and peer-reviewed learning activities, and a moderated online forum. Self-directed modules and an online course are being developed around concepts and topics in which teachers express the most interest and need for instruction. ICEE resources include attention to effective teaching strategies, such as awareness of student misconceptions, strategies for forestalling controversy and advice from master teachers on implementation and curriculum development. The resources are being developed in partnership with GLOBE, and the National Science Digital Library (NSDL) and are informed by the work of the Climate Literacy and Energy Awareness Network (CLEAN) project. ICEE will help to meet the professional development needs of teachers, including those participating in the GLOBE Student Climate Research Campaign.
http://cires.colorado.edu/education/k12/
http://www.iceeonline.org

YL 3. Addressing climate & energy misconceptions – teaching tools offered by the Climate Literacy & Energy Awareness Network (CLEAN)

Anne U. Gold (1), Tamara Shapiro Ledley (2), Karin Kirk (3), Marian Grogan (2), Susan M. Buhr (1), Cathryn A. Manduca (3), Sean Fox (3), Frank Niepold (4), Cynthia Howell (5), Susan E. Lynds (1)
(1) CIRES, (2) TERC, Cambridge, MA, (3) Science Education Resource Center (SERC), Carleton, MI, (4) NOAA, Climate Program Office

Despite a prevalence of peer-reviewed scientific research and high-level reports by intergovernmental agencies (e.g., IPCC) that document changes in our climate and consequences for human societies, the public discourse regards these topics as controversial and sensitive. The chasm between scientific-based understanding of climate systems and public understanding can most easily be addressed via high quality, science-based education on these topics. Well-trained and confident educators and communicators are required to provide this education. However, climate science and energy awareness are complex topics that are rapidly evolving and have a great potential for controversy. Furthermore, the interdisciplinary nature of climate science further increases the difficulty for teachers to stay abreast of the science and the policy. Research has shown that students and educators alike hold misconceptions about the climate system in general and the causes and effects of climate change in particular. The NSF-funded CLEAN Pathway (http://cleanet.org) as part of the National Science Digital Library (http://www.nsdl.org) strives to address these needs and help educators address misconceptions by providing high quality learning resources and professional development opportunities to support educators of grade levels 6 through 16. The materials focus on teaching climate science and energy use. The scope and framework of the CLEAN Pathway is defined by the Essential Principles of Climate Science (CCSP, 2009) and the Energy Literacy Principles. Following this literacy-based approach, CLEAN helps with developing mental models to address misconceptions around climate science and energy awareness through a number of different avenues. These are: 1) Professional development opportunities for educators–interactive webinars for secondary teachers and virtual workshops for college faculty, 2) A collection of scientifically and pedagogically reviewed, high-quality learning resources on climate and energy topics, 3) Detailed information on effective approaches for teaching climate and energy science for a range of grade levels, and 4) A community support forum (http://iceeonline.org, coordinated by a partner project - Inspiring Climate Education Excellence, ICEE), where educators can exchange information and share advice regarding climate and energy education. In this presentation we focus on our experience coordinating professional development opportunities as well as the "Teaching about Climate and Energy" web pages that are offered through the CLEAN Pathway to show-case how misconceptions can be addressed by educators when teaching or learning about climate and energy topics. Providing educators with a robust foundation of topical knowledge, guiding them through common misconceptions and providing them with a collection of well-vetted learning resources is the approach offered by CLEAN to address student misconceptions of climate and energy topics.

YL 4. The Role of Photography in the Study of Climate Change

Natasha Vizcarra, Allaina Wallace, National Snow & Ice Data Center

Often a photograph of parts of the Earth--a landslide, an underwater reef, or the tongue of a glacier—is just what a scientist needs to strengthen a theory or to crush it. In today's digital world where more people are taking and publishing photographs, how are scientists using photography to understand how the Earth's climate is changing? This poster examines examples from the past, such as the National Snow and Ice Data Center's archive of old and recent glacier photographs. It also explores how scientists use photography now, through such sites as Flickr and Google Earth, and the photographic methods they use, such as 360-degree-panoramas and time-lapse photography.

YL 5. Partnering with the CIRES Education and Outreach Group on Broader Impacts

Susan Buhr (1), Jessica Feld (1), Anne Gold (1), Emily Kellagher (1), Susan Lynds (1), Amanda Morton (1), David Oonk (1), Lesley Smith (1), (1)CIRES

CIRES Education and Outreach group partners with CIRES and NOAA researchers on education components for research projects, known to funding agencies as "broader impacts", or "integrating research and education". A high-quality response to the broader impacts review criterion of NSF programs can make the difference in a competitive funding environment. CIRES EO staff work at no-cost to proposers to develop these components, with the proposed activities then implemented with funding through the successful grant request. This poster details the process of working with CIRES EO during the proposal stage and outlines the capabilities CIRES EO can bring to your project. Examples from existing broader impacts and research/education integration projects are described, including examples from NSF, NASA and NOAA research projects. These examples include after-school programs, classroom kits, student-scientist programs, curriculum development, teacher professional development, videos, project evaluation and more. For more about CIRES EO projects and how to work with CIRES EO see http://cires.colorado.edu/education/outreach/ or contact Susan Buhr at susan.buhr@colorado.edu.

YL 6. The National Ocean Sciences Bowl (NOSB): More Than Just A Competition

Emily Kellagher (1), Amanda Morton (2), (1)CIRES, (2)Consortium for Ocean Leadership, (3)NOSB

From its inauguration in 1998, the National Ocean Sciences Bowl (NOSB) has provided an educational forum for students to excel in math and science and to receive national recognition for their talents. CIRES Education Outreach has hosted a regional competition (The Trout Bowl) for 14 years impacting over 1,000 student contacts since inception, the program has a proven track record for generating student interest and excitement about science and the oceans and offers young people an exceptional opportunity to explore marine science, both as an in-depth area of study and as a possible career path. Enhancements over the years have expanded NOSB from simply a seasonal academic competition into a complex learning community. NOSB has also focused on expanding outreach to diverse audiences. The Trout Bowl teams have come from Colorado, South Dakota, Wyoming, Kansas, Nebraska, and New Mexico to compete.

RD 1. Global Model Study of Isocyanic Acid (HNCO)

Paul J. Young(1,2), Louisa K. Emmons(3), Jean-Francois Lamarque(3), James M. Roberts(2), Christine Wiedinmyer(3), Patrick Veres(4) and John J. Orlando(3) , (1) CIRES, (2) NOAA ESRL, (3) NCAR, (4) Max Planck Institute for Chemistry, Mainz, Germany

A new measurement technique (negative-ion proton-transfer chemical ionization mass spectrometry) has been used to identify the occurrence of isocyanic acid (HNCO) in biomass burning emissions, as well as over urban areas. It has been estimated that levels of HNCO > 1 ppbv may be of concern for human health, as exposure to the cyanate ion (NCO-) has been associated with several deleterious effects, including disease of the kidneys and coronary arteries. The main HNCO sources are thought to be protein pyrolysis (e.g. biomass burning); the photochemical breakdown of amides; and leakage from SCR (selective catalytic reduction) technology in newer diesel engines. Here, we will present our initial results from a global chemical transport modeling study to examine the potential distribution of HNCO. We will highlight potential hotspot regions, as well as consider the sensitivity of the results to different parameterizations of the physical properties of HNCO

RD 2. Organic Aerosol Formation and Processing in the Los Angeles Basin: Role of Gasoline vs. Diesel Emissions

R. Bahreini (1,2), A.M. Middlebrook (2), J. de Gouw (1,2), C. Warneke (1,2), M.K. Trainer (2), S.S. Brown (2), W.P. Dube (1,2), J.S. Holloway (1,2), A.E. Perring (1,2), J.P. Schwarz (1,2), J.R. Spackman (1,2), H. Stark (1,2,3), N.L. Wagner (1,2), D.D. Parrish (2), (1) CIRES, (2) NOAA ESRL CSD, (3) Now also at Aerodyne Research, Inc.

During the CalNex-2010 field project in May-June 2010, the NOAA WP-3D aircraft performed flights up- and down-wind of metropolitan, industrial, agricultural and animal feeding sites in central-southern California. Here airborne data on organic aerosol (OA) properties as measured by a compact time-of-flight aerosol mass spectrometer along with measurements of trace gases affecting secondary production of aerosols in the Los Angeles Basin are presented. The analysis presented indicates that the ratio of organic aerosol to carbon monoxide (OA/CO) is significantly higher than the previously observed ratios of primary OA/CO downwind of urban areas, indicating that even on short time scales of transport within the basin, there is significant production of secondary organic aerosol (SOA). The increase in the ratio of OA/CO is also accompanied by an increase in the fraction of oxygenated species of OA, providing evidence for production of more oxidized SOA as air masses are photochemically processed. Despite a smaller contribution from Diesel vehicles to traffic on weekends, analysis of the weekend vs. weekday data indicates that similar values of delta(OA)/delta(CO)are observed on the weekends compared to weekdays, for air masses with similar degrees of photochemical processing. This indicates that emissions of gas phase organic species from Diesel vehicles are not significant for OA production in the LA Basin. Our calculated steady-state concentrations of hydroxyl radical (OH) indicate that OH concentrations at midday are substantially higher on weekends compared to weekdays, indicating faster chemical processing of air masses during a fixed length of time on the weekends compared to weekdays.

RD 3. Potential Aerosol Mass (PAM) flow-through reactor measurements of SOA formation from BEACHON-RoMBAS

Brett B. Palm (1,2), Amber M. Ortega (1,3), Pedro Campuzano-Jost (1,2), Douglas A. Day (1,2), Thomas Karl (4), Lisa Kaser (5), Werner Jud (5), Armin Hansel (5), Juliane L. Fry (1,6), Steven S. Brown (7), Kyle Zarzana (1,2), William Dube (1,7), Nick Wagner (1,7), Danielle Draper (6), William H. Brune (8), and Jose L. Jimenez (1,2)

(1) CIRES, (2) Department of Chemistry and Biochemistry, University of Colorado, (3) Department of Atmospheric and Oceanic Science, University of Colorado, (4) NCAR, (5) Institute of Ion Physics and Applied Physics, University of Innsbruck, Austria, (6) Department of Chemistry and Environmental Studies, Reed College, (7) Chemical Sciences Division, NOAA, (8) Department of Meteorology, Pennsylvania State University

A Potential Aerosol Mass (PAM) photooxidation reactor (Kang et al., ACP 2007, 2010) was used in conjunction with an Aerodyne High Resolution Time-of-Flight Aerosol Mass Spectrometer (DeCarlo et al. Anal. Chem. 2006; HR-ToF-AMS) to characterize biogenic secondary organic aerosol formation during the July-August 2011 BEACHON-RoMBAS field campaign at the U.S. Forest Service Manitou Forest Observatory, Colorado. The PAM reactor uses mercury lamps to create OH concentrations up to 10,000 times ambient levels. High oxidant concentrations accelerate the photooxidation of volatile organic compounds and inorganic gases, which then partition into the aerosol phase. PAM photochemical processing can represent up to approximately 20 days of equivalent atmospheric aging in the span of 4 minutes of residence time in the reactor, and PAM-processed aerosols have shown similar aging signatures as well as sulfate and SOA yields when compared to aging ambient aerosols (Kang et al., ACP 2010; Lambe et al., ACP 2011). The reactor was also injected with O3 or N2O5 in the absence of lights to investigate oxidation by O3 or NO3, oxidants that are expected to have increased importance at locations dominated by biogenic emissions. Presented here is the analysis of PAM processed aerosols using an HR-ToF-AMS, a Proton Transfer Reaction Time of Flight Mass Spectrometer (PTR-TOF-MS), and an NO3/N2O5 instrument. Preliminary results show that PAM photooxidation enhances SOA at intermediate OH exposure (1-10 equivalent days) but results in net loss of OA at very long OH exposure (10-20 equivalent days). PAM oxidation also results in a Van Krevelen diagram (H/C vs. O/C) slope similar to ambient oxidation. Oxidation with NO3 is shown to result in significant SOA production, and both OH and N2O5/NO3 oxidation cause production of NH4NO3 at low nighttime temperatures.

RD 4. Real-time gas and particle-phase organic acids measurement at a forest site using chemical ionization high-resolution time-of-flight mass spectrometry during BEACHON-RoMBAS

R.L.N. Yatavelli (1), H. Stark (1,2), J.R. Kimmel (2,3), M.J. Cubison(3), D.A. Day(1), J.T. Jayne(2), J. A. Thornton(4), D.R. Worsnop(2), J.L. Jimenez(1)
(1) Department of Chemistry and Biochemistry and CIRES, University of Colorado, Boulder, CO, (2) Aerodyne Research Inc., Billerica, MA, (3) TOFWERK AG., Thun, Switzerland, (4) Department of Atmospheric Sciences, University of Washington, Seattle, WA

We present measurement of organic acids in gas and aerosol particles conducted in a ponderosa pine forest during July and August 2011 as part of the Bio-hydro-atmosphere interactions of Energy, Aerosols, Carbon, H2O, Organics & Nitrogen - Rocky Mountain Biogenic Aerosol Study (BEACHON-RoMBAS; http://tinyurl.com/BEACHON-RoMBAS). The measurement technique is based on chemical ionization, high-resolution time-of-flight mass spectrometry and utilizes a Micro-Orifice Volatilization Impactor [MOVI-CI-HR-ToFMS; Yatavelli et al., AS&T, 2010] to collect sub-micron aerosol particles while simultaneously measuring the gas-phase composition. The collected particles are subsequently analyzed by temperature-programmed thermal desorption. The reagent ion chosen for this campaign is the acetate anion (CH3C(O)O-, m/z 59), which reacts selectively via proton transfer with compounds that are stronger gas-phase acids than acetic acid [Veres et al., IJMS, 2008]. Preliminary results show substantial particle-phase concentrations of biogenic oxidation products such as hydroxy-glutaric acid, pinic acid, pinonic acid, and hydroxy-pinonic acid along with numerous lower and higher molecular weight organic acids. Correlations of the organic acid concentrations with meteorological, gas and aerosol parameters measured by other instrumentation are investigated in order to understand the formation, transformation, and partitioning of gas and particle-phase organic acids in a forested environment dominated by terpenes.

RD 5. The signature of aqSOA: Aerosol modification by secondary organic aerosol formation in the aqueous phase

Barbara Ervens (1,2), Annmarie Carlton (3),
(1) CIRES, (2) NOAA/ESRL CSD, (3) Dept. of Environmental Sciences, Rutgers University, NJ

Organics comprise a large fraction of atmospheric particulate matter. The major fraction of this organic aerosol mass is formed by physical or chemical processes in the atmosphere (secondary organic aerosol, SOA). Traditional approaches describe SOA formation by condensation of low-volatility or semivolatile gas phase species on preexisting aerosol particles. The formation of secondary organic aerosol formation in cloud and aerosol water (aqSOA) has attracted great attention over the past years. While it has been recognized that aqSOA formation might significantly contribute to the total SOA budget in humid and cloudy regions, the modification of specific aerosol properties, such as size distribution ('droplet mode'), oxygenation state (O/C ratio), light-absorbing properties and vertical distribution has not been explored. We apply different models in order to predict typical 'signatures of aqSOA' due to organic mass addition in clouds and aqueous aerosol. (i) A parcel model allows implementing detailed multiphase chemistry and explicitly tracking the modification of aerosol distributions by addition of newly aqSOA mass within wet aerosol and cloud droplets. Since usually aqSOA compounds are more highly oxidized (higher O/C ratio) and water-soluble than those of traditional (gas)SOA, processed aerosol size distributions exhibit not only a distinct modification in their size distribution but also in their size-resolved hygroscopicity. (ii) While such chemical and microphysical detail is not available in larger scale models, such models give information on the three-dimensional aerosol distribution. Using an air quality model (CMAQ), we show that the vertical profile of aerosol is clearly modified in the presence of clouds if aqSOA formation in included.

RD 6. Addressing Science and Policy Needs with Community Emissions Efforts

Gregory Frost (1), Leonor Tarrasón (2), Claire Granier (1,3,4), Paulette Middleton (5), and the ECCAD and CIERA teams, (1) NOAA/ESRL/CSD and University of Colorado/CIRES, Boulder, CO, USA , (2) Norwegian Institute for Air Research (NILU), Kjeller, Norway, (3) Université Pierre et Marie Curie, CNRS/INSU, LATMOS-IPSL, Paris, France, (4) Max Planck Institute for Meteorology, Hamburg, Germany, (5) Panorama Pathways, Boulder, CO, USA,

We present community-driven emissions efforts within the Global Emissions InitiAtive (GEIA, http://www.geiacenter.org/), a joint IGAC/iLEAPS/AIMES initiative of the International Geosphere-Biosphere Programme. Since 1990, GEIA has served as a forum for the exchange of expertise and information on emissions. GEIA's mission is to (1) quantify anthropogenic emissions and natural exchanges of trace gases and aerosols; and (2) facilitate the use of this information by the research, assessment, and policy communities. GEIA supports a worldwide network of over 1200 developers and users in international scientific projects, providing a solid scientific foundation for atmospheric chemistry research. Moving forward, GEIA is broadening its role to serve the scientific, regulatory, and operational emission communities. GEIA intends to demonstrate the potential for improving emission information by promoting the interoperability of datasets and tools and by making use of near-real-time observations. As a first step toward these goals, two new programs are being linked with GEIA:

- ECCAD (Emissions of chemical Compounds & Compilation of Ancillary Data, http://eccad.sedoo.fr/) is GEIA's new interactive emissions data portal, providing consistent access to emission inventories and ancillary data with easy-to-use tools for analysis and visualization.
- CIERA (Community Initiative for Emissions Research & Applications, http://ciera-air.org/) is a new GEIA community project to develop interoperability in emissions datasets and tools, support evaluations of inventories, communicate emissions information in innovative ways, and connect the emissions development and user communities.

We invite the scientific and policy community to join the GEIA network and build partnerships to improve emissions information.

RD 7. NO3-initiated oxidation of biogenic hydrocarbons: An important nighttime sink of volatile organic compounds and source of secondary organic aerosol

Juliane L. Fry (1), Danielle Draper (1), Steven S. Brown (2), James N. Smith (3), Kyle Zarzana (4), Brett B. Palm (4), Pedro Campuzano-Jost (4), Jose L. Jimenez (4), Lisa Kaser (5), Armin Hansel (5), Bill Brune (6), Peter Edwards (2), John Ortega (3), Paul Winkler (3)
(1) Reed College/CIRES Visiting Fellow, (2) NOAA ESRL, (3) NCAR ACD, (4) University of Colorado, Boulder, (5) University of Innsbruck, Austria, (6) Pennsylvania State University

Nighttime NO3 oxidation of some biogenic hydrocarbons has been shown to produce large mass yields of secondary organic aerosol (SOA). During the BEACHON-RoMBAS field campaign (ponderosa pine forest in the Colorado front range, July – August 2011), we investigated this mechanism by measuring gas/aerosol partitioning of ambient organic nitrates, as well as potential aerosol mass from NO3 oxidation of ambient biogenic hydrocarbons. Thereafter, we conducted follow-up chamber experiments at the NCAR Community Lab, investigating SOA growth rates and mass yields from individual hydrocarbons representative of the ambient mix in a ponderosa pine forest. We observed great diversity in SOA growth among monoterpenes and sesquiterpenes. This paper will present a combination of field, chamber, and model results to guide future thinking on the role of NO3 oxidation in both biogenic hydrocarbon budgets and SOA production.

RD 8. Twenty-five years of ozonesonde measurements at South Pole: An assessment of changing loss rates

Birgit Hassler (1,2), John S. Daniel (2), Bryan J. Johnson (3), Susan Solomon (4), Samuel J. Oltmans (1)
(1) CIRES, (2) NOAA ESRL CSD, (3) NOAA ESRL GMD, (4) MIT

In 2010, 25 years of continuous, year-round ozone soundings at South Pole station, Antarctica, were completed. These measurements provide unique information about ozone depletion in the polar stratosphere at high vertical resolution. We analyzed these ozone soundings to learn more about the onset time of the seasonal ozone depletion, the observed loss rates, and their changes since the measurement series began. During the last 25 years the seasonal onset of ozone loss at South Pole has moved forward significantly. The fastest highest loss rates occur between the end of August and end of September near 50 hPa to 30 hPa. Loss rates at these pressure levels increased from the late 1980s to the late 1990s and have remained roughly stable since then. To estimate a time frame when a reduction in ozone loss rates will be observable outside the range of annual variability at the South Pole, we scale the estimated loss rates to the future projected concentrations of equivalent effective stratospheric chlorine (EESC). We project that ozone loss rates will first be significantly reduced between 2017 and 2021.

RD 9. Importance of Biotic vs Abiotic Controls on VOC Emissions from Ponderosa Pine

Allyson S.D. Eller (1), Peter C. Harley (2), Russell K. Monson (1,3), (1) CIRES, (2) NCAR, (3) University of Arizona

The emissions of VOCs, including monoterpenes (MTs) and 2-methyl-3-buten-2-ol (MBO), from ponderosa pine can be important contributors to the regional production of ozone and secondary organic aerosols in the Western United States. The goal of this study was to better characterize the influences of biotic and abiotic factors on the emissions of these compounds. Using PTR-MS coupled with measurements of photosynthesis and stomatal conductance (gs) we generated light and temperature curves from intact needles of mature ponderosa pine trees and used abscisic acid (ABA) to reduce gs and photosynthesis under constant light and temperature conditions. Stomatal conductance and photosynthesis were almost perfectly correlated during all our measurements, so we were unable to separate their influences. We found that increasing temperature by 10 oC increased emissions of both MTs and MBO by 80-120% even though gs and photosynthesis were reduced by ~50%. Light curves performed at 30 oC showed that gs and photosynthesis were strongly related to MT and MBO emissions although the effect was more pronounced for MBO than MT emissions. In most cases a 60% reduction in gs and photosynthesis was correlated with a ~50% reduction in MBO emissions and a 5-20% reduction in MT emissions. Using ABA we were able to induce stomatal closure while maintaining a constant light and temperature environment and we found that stomatal closure due to ABA resulted in declines in MT and MBO emissions that were similar in magnitude to those seen in the light curves. When compared at the same light and temperature conditions, individuals with lower gs and photosynthesis did not necessarily have lower emissions than those with higher gs and photosynthesis, indicating that gs and photosynthesis may not be good predictors of emissions between individuals, but within each individual the instantaneous changes in gs and photosynthesis did appear to be related to the emissions of VOCs. These data show that plant physiology is an important constraint in regulating the instantaneous emissions of VOCs, but also that the relationships are modified by external temperature, probably through the increased volatility of the VOCs.

RD 10. Influence of Benzene on the Optical Properties of Titan Haze Laboratory Analogs in the Mid-Visible

Y. Heidi Yoon (1), Melissa G. Trainer (2), Margaret A. Tolbert (1,3), (1) CIRES, (2) NASA Goddard, (3) Department of Chemistry, UC-Boulder

The Cassini Ion and Neutral Mass Spectrometer (Waite, Jr., et al., 2007) and the Composite Infrared Spectrometer (Coustenis, A., et al., 2007) have detected benzene in the upper atmosphere and stratosphere of Titan. Photochemical reactions involving benzene in Titan's atmosphere may influence polycyclic aromatic hydrocarbon formation, aerosol formation, and the radiative balance of Titan's atmosphere. We measure the effect of benzene on the optical properties of Titan analog particles in the laboratory. Using cavity ring-down aerosol extinction spectroscopy, we determine the real and imaginary refractive index at 532 nm of particles formed by benzene photolysis and Titan analog particles formed with ppm-levels of benzene. These studies are compared to the previous study by Hasenkopf, et al. (2010) of Titan analog particles formed by methane photolysis.

References:

Coustenis, A., et al.: 'The Composition of Titan's Stratosphere from Cassini/CIRS Mid-Infrared Spectra'. Icarus, Vol. 189, pp. 35-62, 2007.

Hasenkopf, C. A., et al.: 'Optical Properties of Titan and Early Earth Haze Laboratory Analogs in the Mid-Visible'. Icarus, Vol. 207, pp. 903-913, 2010.

Waite, Jr., J. H., et al.: 'The Process of Tholin Formation in Titan's Upper Atmosphere'. Science, Vol. 316, pp. 870-875, 2007.

RD 11. Volatile organic compounds (VOCs) in the South Coast Air Basin (SoCAB): Characterizing the gas-phase chemical evolution of air masses during CalNex 2010

J.B. Gilman (1,2), B.M. Lerner (1,2), W.C. Kuster (1,2), D. Bon (1,2,3), C. Warneke (1,2), E.J. Williams (1,2), J.S. Holloway (1,2), I.B. Pollack (1,2), T.B. Ryerson (1), E.L. Atlas (4), D.R. Blake (5), S.C. Herndon (6), M.S. Zahniser (6), A. Vlasenko (7), S.M. Li (7), S. Alvarez (8), B. Rappenglueck (8), J. Flynn (8), N. Grossberg (8), B. Lefer (8), J.A. de Gouw (1,2)

(1) NOAA ESRL Chemical Sciences Division, (2) CIRES at Univ. of Colorado, Boulder, (3) Now at Colorado Dept. of Public Health and Environ., (4) RSMAS at Univ. of Miami, (5)Dept of Chemistry, Univ. of CA-Irvine, (6) Aerodyne Research, (7) Environ. Canada, (8) University of Houston

Volatile organic compounds (VOCs) are critical components in the photochemical production of ozone (O3) and secondary organic aerosol (SOA). During the CalNex 2010 field campaign, an extensive set of VOCs were measured at the Pasadena ground site, and aboard the NOAA WP-3D aircraft and the WHOI Research Vessel Atlantis. The measurements from each platform provide a unique perspective into the emissions, transport, and atmospheric processing of VOCs within the South Coast Air Basin (SoCAB). The chemical evolution of air masses as a function of the time of day is investigated in order to determine the relative impacts of primary emissions vs. secondary VOC products on OH reactivity and potential SOA formation. The reactivity of VOCs with the hydroxyl radical (•OH) at the Pasadena site was dominated by the light hydrocarbons, isoprene, and oxygenated VOCs including aldehydes (secondary products) and alcohols (primary anthropogenic emissions). Toluene and benzaldehyde, both of which are associated with primary anthropogenic emissions, are the predominant VOC precursors to the potential formation of SOA.

RD 12. Depositional ice nucleation on monocarboxylic acids: effect of the O:C ratio

Gregory Schill and Margaret Tolbert
CIRES and Department of Chemistry and Biochemistry, University of Colorado, Boulder, CO, USA

Heterogeneous ice nucleation by atmospheric particles has been identified as a potential pathway for cold cloud formation; however, the ice nucleation efficiency of organic particles is poorly constrained due to the complexity and mutability of atmospheric organic matter. This study focuses on systematic experiments to unveil general trends in organic ice nucleation efficacy. Specifically, the heterogeneous ice nucleation efficiency of a series of thin C3-C6 monocarboxylic acid films between 180 and 200 K has been investigated using a Knudsen cell flow reactor. At each temperature, the critical ice saturation ratio for depositional nucleation was found to be strongly dependent on the chemical nature of the film. For the organic acids used in this study, increasing the O:C ratio lowered the ice supersaturation required for the onset of heterogeneous nucleation (37 ± 4% from O:C 0.33 to 0.67 across all temperatures). This could be the result of an increase in surface hydrophilicity, which allows the film to better adsorb a metastable, ice-like layer of water that serves as a template for the new phase of ice. These ice nucleation results are in excellent agreement with ice nucleation on both laboratory generated α-pinene secondary organic aerosol as well as on predominantly organic particles collected in Mexico City.

RD 13. Winter Ozone Production: Uintah Basin, Utah

Russ Schnell(1), Samuel Oltmans(2), Ryan Neeley(2) and Thomas Mefford(2), (1)NOAA Global Monitoring Division, (2)CIRES

Rapid, high concentration, diurnal photochemical ozone production occurs in the Uintah Basin, Utah in the coldest portion of the winter when there is snow on the ground. In a typical event, ozone concentration may increase from 40 ppb at sunrise to 120-140 ppb following solar noon. The precursors for the ozone formation appear to be coming from associated oil and gas fields. In the absence of snow there is limited excess ozone production.

RD 14. Absorption Cross Sections of Ozone and Hydrogen Peroxide Between 350 nm and 470 nm

Jessica L. Axson (1)(2), Steve S. Brown (3), Greg Frost (2)(3), Tara F. Kahan (3), Veronica Vaida (1)(2), Rebecca A. Washenfelder (2)(3), and Cora J. Young (2)(3), (1) Department of Chemistry and Biochemistry, University of Colorado, Campus Box 215, Boulder, CO 80309, USA
(2) Cooperative Institute for Research in Environmental Sciences, 216 UCB, University of Colorado, Boulder, CO 80309, USA
(3)Chemical Sciences Division, National Oceanic and Atmospheric Administration, 325 Broadway, Boulder, CO 80305, USA

The absorption of sunlight by small molecules plays an important role in atmospheric composition. Even very weak absorptions can result in photochemical transformations. However, spectroscopic techniques do not always have the sensitivity required to resolve small cross sections. Incoherent broadband cavity-enhanced absorption spectroscopy (IBBCEAS) is a relatively new technique which offers high sensitivity over a wide range of wavelengths. We have constructed an IBBCEAS and used it to measure absorption cross sections of two atmospherically important molecules – ozone and hydrogen peroxide – in spectral regions where measurements have previously been poor or nonexistent. These measurements will reduce uncertainty in several areas of atmospheric chemistry, including interpreting satellite retrieval data and predicting the concentrations of important atmospheric species.

RD 15. Long term variations in springtime Arctic boundary layer ozone depletion events at Barrow, Alaska (1973-2012)

Samuel J. Oltmans (1,2), Joyce M. Harris (2), Laura C. Patrick (1,2), Bryan J. Johnson(2), (1)CIRES, University of Colorado, Boulder, Colorado
(2)NOAA/ESRL, Global Monitoring Division, Boulder, Colorado

Since the discovery in the early 1980s of strong boundary layer ozone depletion in the spring in the Arctic, and its association with the activation of bromine emitted from the ocean, there has been extensive research and modeling aimed at understanding this phenomena. At Barrow, Alaska at the NOAA Observatory where this depletion was first noted there is now a forty year record of surface ozone measurements. Depletion events (hourly ozone mixing ratios <10 ppb) that may last several hours or days are associated with air flow off the Arctic Ocean to the site at Barrow, which is just a few kilometers from the coast. The long term surface ozone measurements at Barrow reveal that in March there has been a dramatic increase in the frequency of the depletion events (numbers of hours with ozone <10 ppb). This change is most pronounced in the second half of the record beginning in the early 1990s. Although April is the month with the greatest frequency of depletion events a similar change has not occurred during April. The likely cause of the increase in March is the changing character of Arctic sea ice. Although overall ice extent has diminished somewhat in March, the dramatic change has been the large reduction in multi-year ice and its replacement with annual (first year) ice. It has been shown that first year ice conditions are more advantageous for producing ozone depletion because of a greater number and extent of fissures in the ice that allow for the accumulation of brine on the ice surface and the subsequent activation of bromine. This significant change in the occurrence of boundary layer ozone events in March may signal a change in atmospheric chemistry in the Arctic that is related to climate change in this sensitive region.

RD 16. Evaluation of turbulence of marine stratocumulus in large-eddy simulations against ship-borne data

Takanobu Yamaguchi (1)(2), Alan Brewer (2), Graham Feingold (2), (1) CIRES (2) NOAA ESRL

The VOCALS field experiment yielded a rich data set on cloudy boundary layer dynamics and the opportunity to evaluate numerical models against observations. In this presentation, turbulence statistics computed with the Advanced Research WRF model are evaluated against those measured by a high resolution Doppler lidar on board the R. H. Brown. Clouds and turbulence are inextricably linked. However, this linkage is missing at the initial model time. In order to compare with the observed turbulence, it is crucial to establish a turbulent field that is balanced with the initial cloud field. We utilize a nudging technique to maintain the horizontal mean profiles of the horizontal wind components, potential temperature, total water (vapor+cloud water) as well as the total number concentration (CCN and droplet), while turbulence is allowed to freely develop. This produces the required adjustment of turbulence and cloud for subsequent simulation. In order to examine the ability of the model to represent turbulence in the cloudy marine boundary layer and identify how to improve it, simulations are performed for a variety of grid spacings for domains O(5-50 km). The experiments address the resolution and domain-size requirement for simulation of mesoscale organization as well as the requirements to capture observed turbulence.

RD 17. A revised look at the oceanic sink for atmospheric carbon tetrachloride (CCl4)

James H. Butler (1), Shari A. Yvon-Lewis (2,6), Jurgen M. Lobert (3,6), Daniel B. King (3,6), Stephen A. Montzka (1,6), James W. Elkins (1), Bradley D. Hall (1), Valentin Koropalov (5), John L. Bullister (7)

(1) NOAA Earth System Research Laboratory, Global Monitoring Division, Boulder, CO, USA; (2) Texas A&M University, Department of Oceanography, College Station, TX, USA; (3) Entegris Inc., Franklin, MA, USA; (4) Chemistry Department, Drexel University, Philadelphia, PA, USA; (5) Roshydromet, Moscow, Russia; (6) CIRES, University of Colorado, Boulder, CO, USA; (7) NOAA Pacific Marine and Environmental Laboratory, Seattle, WA, USA

Extensive negative saturation anomalies for carbon tetrachloride (CCl4) from 16 cruises in the Pacific, Atlantic, and Southern Oceans from 1987 through 2010 confirm that atmospheric CCl4 is consumed in large amounts by the ocean. Data support findings previously reported from four research cruises, all in the Pacific Ocean [JH Butler et al, EOS 78 (46):F105, 1997; SA Yvon-Lewis and JH Butler JGR 107 (D20):4414, 2002], with only slight quantitative change. All seasons in both hemispheres are captured in this record and some cruises are repeat transects separated by over a decade. Nearly continuous, in situ measurements were made by gas chromatography with electron capture and/or mass spectrometer detection on air and surface water samples. Surface water was equilibrated with a continuous flow equilibrator. Grab samples of air were collected to confirm in situ measurements with independent instruments on land and, on some cruises, supporting grab samples of surface water were analyzed on board ship. Net CCl4 saturation anomalies, corrected for physical effects associated with radiative heat flux, mixing, and air injection, were commonly on the order of -5% to -10%. The atmospheric flux required to sustain these anomalies still implies that the ocean accounts for about 1/4-1/3 of the total sink of atmospheric CCl4. Although CCl4 hydrolyzes in seawater, currently published hydrolysis rates for this gas cannot support such large saturation anomalies and inferred losses, given our current understanding of air-sea exchange rates. Explanation of the measured, surface-water undersaturations requires higher hydrolysis rates, additional sink mechanisms, such as biological consumption in surface waters or at depth,lower rates of air-sea exchange, or some combination of these processes.

RD 18. Shorter-lived trace-gases: opportunities for mitigating ozone depletion and climate change

S. Montzka (1,2), G. Dutton (2), B. Miller (2), C. Siso (2), D. Mondeel (2), T. Conway (1), E. Dlugokencky (1), B. Hall (1), D. Nance (2), J. Elkins (1), and J. Butler (1), (1) National Oceanic and Atmospheric Administration, Boulder, CO, (2) Cooperative Institute for Research in Environmental Sciences

The depletion of stratospheric ozone is caused primarily by chemicals having lifetimes of 30 to 100 years. It might come as a surprise, then, that only a few years after nations across the globe limited production of these chemicals via the Montreal Protocol on Substances that Deplete the Ozone Layer the atmospheric concentration of ozone-depleting halogen began decreasing. The key to this rapid turnaround was restrictions on the production of shorter-lived, ozone-depleting chemicals, specifically methyl chloroform and methyl bromide. Controls on shorter-lived gases, however, have limits; the decline in ozone-depleting halogen concentration has been sustained over nearly 2 decades because long-lived gases were also controlled in the Montreal Protocol. A parallel situation exists for greenhouse gases. Most radiative forcing is contributed by human-induced changes in carbon dioxide concentration. Furthermore, CO2 behaves as a long-lived gas: the global atmospheric concentration of CO2 is elevated for decades to millennia after an emission input. The trace gas with the next-largest contribution to radiative forcing, however, is methane. Methane is thought to have an atmospheric lifetime of ~10 years, and this timescale is set by the global mean hydroxyl radical concentration. Other non-CO2 greenhouse gases (N2O, CFCs, HCFCs, HFCs) also contribute to atmospheric radiative forcing and many have lifetimes shorter than CO2. Given this, reductions in emissions of these non-CO2 gases have the potential to slow the increase in radiative forcing on shorter timescales than could be achieved by reductions in CO2 emissions alone. In this presentation the factors influencing these timescales will be discussed, including variability in the global mean hydroxyl radical concentration, as will the limits of reducing emissions of non-CO2 greenhouse gases compared to those of CO2 as a means to slow the ongoing increase in global radiative forcing.

RD 19. The glyoxal budget and its contribution to organic aerosol for Los Angeles, California during CalNex 2010

R. A. Washenfelder (1, 2), C. J. Young (1,2), S. S. Brown (2), W. M. Angevine (1,2), E. L. Atlas (3), D. R. Blake (4), D. M. Bon (1,2), M. J. Cubison (1,5), J. A. de Gouw (1,2), S. Dusanter (6,7,8), J. Flynn (9), J. B. Gilman (1,2), M. Graus (1,2), S. Griffith (6), N. Grossberg (9), P. L. Hayes (1,5), J. L. Jimenez (1,5), W. C. Kuster (1,2), B. L. Lefer (9), I. B. Pollack (1,2), T. B. Ryerson (2), H. Stark (1, 10), P. S. Stevens (6), and M. K. Trainer (2)
(1) Cooperative Institute for Research in Environmental Sciences, University of Colorado, 216 UCB, Boulder, CO 80309, USA
(2) Chemical Sciences Division, Earth System Research Laboratory, National Oceanic and Atmospheric Administration, 325 Broadway, Boulder, CO 80305, USA, (3) Division of Marine and Atmospheric Chemistry, University of Miami, Miami, FL 33149, USA, (4) Department of Chemistry, University of California Irvine, 570 Rowland Hall, Irvine, CA 92697, USA, (5) Department of Chemistry and Biochemistry, University of Colorado Boulder, UCB 215, Boulder, CO 80309, USA. (6) Center for Research in Environmental Science, School of Public and Environmental Affairs, and Department of Chemistry, Indiana University, Bloomington, IN 47405, USA. (7) Univ Lille Nord de France, F-59000 Lille, France. (8) EMDouai, CE, F-59508 Douai, France. (9) Department of Earth and Atmospheric Sciences, University of Houston, Houston, TX 77204, USA
(10) Aerodyne Research, Incorporated, 45 Manning Road, Billerica, MA 01821, USA

Recent laboratory and field studies have indicated that glyoxal is a potentially large contributor to secondary organic aerosol mass. We present in situ glyoxal measurements acquired with a recently developed, high sensitivity spectroscopic instrument during the CalNex 2010 field campaign in Pasadena, California. We use three methods to quantify the production and loss of glyoxal in Los Angeles and its contribution to organic aerosol. First, we calculate the difference between steady-state sources and sinks of glyoxal at the Pasadena site, assuming that the remainder is available for aerosol uptake. Second, we use the Master Chemical Mechanism to construct a two-dimensional model for gas-phase glyoxal chemistry in Los Angeles, assuming that the difference between the modeled and measured glyoxal concentration is available for aerosol uptake. Third, we examine the nighttime loss of glyoxal in the absence of its photochemical sources and sinks. Using these methods we constrain the glyoxal loss to aerosol to be 0 – 5 × 10-5 s-1 during clear days and (1 ± 0.3) × 10-5 s-1 at night. Between 07:00 - 15:00 local time, the diurnally-averaged secondary organic aerosol mass increases from 4.4 µg m-3 to a maximum of 9.3 µg m-3. The constraints on the glyoxal budget from this analysis indicate that it contributes 0 - 0.2 µg m-3 or 0 - 4% of the secondary organic aerosol mass.

RD 20. Comparisons between aircraft, balloon and remote sensing measurements of UT/LS water vapor during the NASA MACPEX mission

A. W. Rollins (1,2), T. D. Thornberry (1,2), R.-S. Gao (2), L. A. Watts (1,2), D. W. Fahey (1,2), E. G. Hall (1,3), A. F. Jordan (1,3), D. F. Hurst (1,3), J. B. Smith (4), M. R. Sargent (4), D. S. Sayres (4), C. Schiller (5), N. Spelten (5), M. Krämer (5)
(1) Cooperative Institute for Research in Environmental Sciences, University of Colorado; (2) NOAA ESRL Chemical Sciences Division; (3) NOAA ESRL

Mixing ratios of water vapor in Earth's upper troposphere and lower stratosphere (UT/LS) reach low values (< 10 ppmv), yet water in this region has a significant impact on Earth's radiation budget. Large discrepancies have repeatedly been observed between multiple high precision measurements of water vapor at the low mixing ratios in the UT/LS, leading to significant uncertainties in the absolute values and trends of lower stratospheric water vapor, and in the microphysical processes leading to dehydration in the tropopause region. During the NASA MACPEX mission a new chemical ionization mass spectrometer (CIMS) instrument was used to quantify water vapor on the NASA WB-57. The NOAA WV-CIMS instrument included a novel calibration system utilizing two independent water vapor standards to accurately determine the measurement background and sensitivity during flight. To our knowledge this was the first UT/LS water vapor measurement to be calibrated in situ using standard additions over the measured range of water vapor mixing ratios. In this work we briefly describe the NOAA WV-CIMS instrument and compare the CIMS measurements from the UT/LS to those made by the Harvard Water Vapor (HWV) and Fast In situ Stratospheric Hygrometer (FISH) instruments also on the WB-57. The mixing ratios reported from the three instruments typically spanned a 20% range, with the largest fractional differences observed at the lowest mixing ratios. We also compare the CIMS measurement to coincident balloon frost point soundings and satellite measurements from MLS on Aura. On average, the frost point instruments measured 0.7 ppmv drier than CIMS at mixing ratios below 10 ppmv. At 121 and 83 hPa the average differences between MLS and CIMS were 0.0 and 0.3 ppmv respectively, with the larger differences occurring at the higher altitudes. Because each instrument has reported uncertainties on the order of ±10%, measurements by all of these instruments typically agreed within the combined instrumental error estimates. However, the remaining systematic differences between the aircraft instruments at low mixing ratios clearly indicate that these differences are likely caused by inaccurate quantification of the in situ instrumental background.

RD 21. Medical Aerosols for Global Health: New Needle-Free Methods of HPV Vaccine Delivery of Dry Powders and Aerosols

Stephen P. Cape (1), David H. McAdams (1,2), Elizabeth Gersch (4), David Chen (1,2), Nisha K. Shah (1,2), Robert L. Garcea (3,4) and Robert E. Sievers (1,2,3). (1)Cooperative Institute for Research in Environmental Sciences, U. of Colorado. (2)Department of Chemistry and Biochemistry, U. of Colorado. (3)Biofrontiers Inst., Jeannie and Jack Thompson Vaccine Center, U. of Colorado
(4)Department of Molecular, Cellular and Developmental Biology, U. of Colorado

Human papilloma virus (HPV) infection is both the most prevalent sexually transmitted disease and the initiating factor for cervical cancer, the second leading cause of cancer deaths in women worldwide (more than 300,000). The new HPV vaccines, Gardasil™ and Cervarix™, are composed of recombinant HPV viral capsid proteins assembled into virus-like particles (VLPs). Although highly efficacious, these vaccines are expensive ($360 initial series), require refrigeration (cold chain), and are now injected rather than inhaled, as we are proposing. Capsid protein subunits (capsomeres) are also excellent HPV immunogens. Our new inhaled HPV vaccine capsomers are very stable, and produce an antibody response in a rat model.

RD 22. Application of a volatility basis set model to secondary organic aerosol simulations across the U.S.

R. Ahmadov (1,2), S. McKeen (1,2), R. Bahreini (1,2), A. Middlebrook (2), J.A. de Gouw (1,2), J.L. Jimenez (1,3), P.L. Hayes (1,3), M. Trainer (2)
(1) Cooperative Institute for Research in Environmental Sciences, University of Colorado at Boulder, Boulder, CO, USA
(2) Earth System Research Laboratory, National Oceanic and Atmospheric Administration, Boulder, CO, USA
(3) Department of Chemistry and Biochemistry, University of Colorado, Boulder, CO, USA

A new secondary organic aerosol (SOA) parameterization based on the volatility basis set is implemented in a regional air quality community based model – WRF-CHEM. Full meteorological and chemistry simulations were carried out for the U.S. for August-September, 2006. Predicted organic aerosol (OA) concentrations are evaluated by using extensive surface and aircraft measurements. The updated model demonstrates a significant improvement in simulating the OA concentrations compared to the standard WRF-CHEM, which predicted very little SOA. The improvement in OA is noticeable in both correlations and model bias. The model with the new SOA scheme is also applied to other regions and case studies. Simulations are carried out for May-June, 2010 time period for California region focusing on Los Angeles basin. The available measurements for meteorological, gas-phase and particle species from the NOAA P3 aircraft and the Caltech supersite in Pasadena provide valuable datasets to evaluate the model. The preliminary evaluations using the CalTech site measurements reveal that much higher model grid resolution is necessary to capture the strong afternoon maximum in diurnal cycle of OA species. In addition, the modeling tool is used to interpret high SOA formation downwind of the Deepwater Horizon (DWH) oil spill disaster in the Gulf of Mexico in May-June, 2010. The results show that the updated WRF-CHEM model is a suitable tool to address OA distribution in the atmosphere from different anthropogenic and biogenic sources across several regions and case studies. The implementation of the new SOA scheme within the MADE aerosol module makes it possible to apply the WRF-CHEM model for air quality applications requiring better OA predictions with reasonable computational cost.

RD 23. BioCORN Study 2011 – Eddy covariance fluxes over energy crop ecosystems

Martin Graus (1, 2), Carsten Warneke (1, 2), Eric J Williams (1, 2), Brian M Lerner (1, 2), Jessica B Gilman (1, 2), Rui Li (1, 2), Allyson SD Eller (1, 3), Christopher Gray (1, 3), Noah Fierer (1, 3), Ray Fall (1, 4), Peter C Harley (5), James M Roberts (2), Christopher Fryrear (6), Mark Collins (6), Karl Whitman (6), Joost De Gouw (1, 2)
(1) CIRES, University of Colorado, Boulder, CO, United States. (2) CSD, NOAA, Boulder, CO, United States.
(3) Department of Ecology and Evolutionary Biology, University of Colorado, Boulder , CO, United States.
(4) Department of Chemistry and Biochemistry, University of Colorado, Boulder, CO, United States.
(5) ACD, NCAR, Boulder, CO, United States. (6) ARDEC, Colorado State University, Fort Collins, CO, United States.

In summer 2011 an eddy covariance system was set up in a corn field at ARDEC (CSU, Ft Collins, CO) to investigate the energy flux and the trace gas exchange of the US' dominant biofuel crop. Besides energy flux, evapotranspiration and CO2 flux a comprehensive suite of volatile organic compounds and inorganic species (O3, NO, NO2, CO) were measured for virtual disjunct eddy covariance (vDEC) analysis and true eddy covariance (EC) fluxes, respectively. VOCs were monitored by PTR-MS and, for the first time, fluxes of formic acid were measured utilizing NI-CIMS data for vDEC analysis. Besides the EC approach leaf level flux measurements and soil flux measurements were performed using a GC-MS system (TACOH) coupled to a modified Li6400 system and to soil chambers, respectively. Ethanol and methanol are amongst the compounds with the largest emissions from corn leaves. DMS is amongst the species found to be emitted by the soil and to a significantly larger extent from the corn leaves with a strong diurnal pattern indicating stomatal control over the DMS flux. This comprehensive dataset of trace gas fluxes over one of the most abundant plant species in the USA will help us better understand the potential influence of agricultural crops on regional air chemistry.
http://esrl.noaa.gov/csd/tropchem/biocorn2011/

RD 24. Decadel Change and Regional Trends of PH Throughout the Southern Ocean

Andrew R. Margolin (1,2), Nicole S. Lovenduski (2,3), Jose-Luis Jimenez (1,4), Cortlandt G. Pierpont (1)
(1) Department of Chemistry and Biochemistry, (2) INSTAAR, (3) ATOC, (4) CIRES

Recent studies show that the Southern Ocean is experiencing changes in its carbon chemistry due to the uptake of anthropogenic carbon dioxide (CO2) from the atmosphere, a process that lowers the pH. These changes have reduced the surface carbonate concentration of the Southern Ocean by more than 10% when compared to preindustrial levels. Here, we use total alkalinity, dissolved inorganic carbon, and the partial pressure or fugacity of CO2 to quantify the change of pH throughout the Southern Ocean. We calculate pH at every location where two of the parameters were measured on over sixty hydrographic cruises, creating an array of new pH data. Profiles of decadal pH change from multiple repeat cruises are used to determine focus regions where pH change is most dramatic for further trend analysis. Using measurements from the 1970's to the present day we examine the vertical and spatial heterogeneity in trend patterns, and comment on the statistical significance of pH trends. Implications of these results will be used to assess carbon-climate model performance.

RD 25. Vertical profiles of HONO during NACHTT 2011: Relative importance of heterogeneous production on aerosol versus the ground surface

C. J. Young (1,2), T. C. VandenBoer (3), N. L. Wagner (1,2), W. P. Dube (1,2), T. P. Riedel (4), R. Bahreini ((1,2), F. Ozturk ((1,2), C. Warneke (1,2), J. de Gouw (1,2), W. C. Keene (5), A. A. P. Pszenny (6), J. A. Thornton (4), D. Wolfe (1), S. S. Brown (1), A. M. Middlebrook (1), and J. M. Roberts (1)

The photolysis of the atmospheric trace gas nitrous acid (HONO) has been implicated as a major source of the OH radical, especially in early morning hours. Chemical interferences and instrumental sensitivity on the order of pptv make quantification of HONO an analytical challenge. Daytime photostationary concentrations on the order of tens to hundreds of pptv have been observed in a variety of environments, indicating unknown or underestimated daytime HONO sources. Accumulation at night has been proposed to occur via heterogeneous reaction of NO2 and H2O and is therefore related to the chemical processes producing halogen species, such as uptake of N2O5 on acidic aerosol where branching of the ClNO2 production mechanism at low aerosol pH yields Cl2 and HONO. The relative significance of ground and aerosol surface in HONO production and the importance of fine aerosol composition in HONO and halogen production have not been investigated via field observations. During the Nitrogen, Aerosol Composition and Halogens on a Tall Tower (NACHTT) experiment in Erie, CO, a Negative Ion – Proton Transfer – Chemical Ionisation Mass Spectrometer (NI-PT-CIMS) was deployed to measure a suite of 9 gaseous inorganic and organic acids, including HCl and HONO. Measurements were made from an instrument carriage continuously traversing the 300 m tower from February to March 2011 at the Boulder Atmospheric Observatory (BAO). Supporting measurements of aerosol composition, surface area, meteorology, and nitrogen oxides and halogens were made simultaneously on this platform. HONO vertical structure showed significant gradients throughout the campaign, with night-time maxima typically near 1 - 1.5 ppbv and a few tens of pptv throughout the day. HCl vertical structure was more complex. The competing surface and aerosol heterogeneous mechanisms of night-time formation, surface flux, and several unique event studies will be presented. In addition, a new mechanism for the night-time loss and daytime recovery of HONO from soil surrogates by flow tube experiments is presented.

RD 26. N2O5 uptake coefficients determined from ambient wintertime measurements

N. L. Wagner (1, 2), T. P. Riedel (3,4), J. M. Roberts (1), J. A. Thornton (3), T. C. VandenBoer (1), W. P. Dubé (1,2), A. M. Middlebrook (1), B. C. Sive (5), R. S. Russo (5), C. A. Brock (1), C. J. Young (1,2), F. Ozturk (1), R. Bahreini (1,2), Y. Zhou (6), R. Swarthout (6), S. S. Brown (1)
(1) NOAA Earth System Research Laboratory, R/CSD7, 325 Broadway, Boulder, CO 80305, USA
(2) Cooperative Institute for Research in Environmental Sciences, University of Colorado, Boulder, CO 80309, USA
(3) Dept of Atmospheric Sciences, University of Washington, Seattle, Washington 98195, USA
(4) Dept. Chemistry, University of Washington, Seattle, Washington 98195, USA. (5) Dept. Chemistry, Appalachian State University Boone, NC 28608
(6) Climate Change Research Center, University of New Hampshire, Durham, NH 03824

Nighttime chemistry accounts for up to half of the NOx removal from the atmosphere and produces atomic chlorine in the early morning through photolysis of ClNO2. NOx is removed through the production and heterogeneous loss of N2O5. The heterogeneous loss of N2O5 typically produces nitric acid which is removed through deposition. However, it has recently been discovered that in the presence of aerosol chloride, the N2O5 uptake produces ClNO2. The rate N2O5 heterogeneous loss has been the subject of several laboratory studies; however, it has rarely been studied using ambient measurements. In this work, N2O5 uptake coefficients are determined from ambient wintertime measurements at the BAO tower in Erie, CO. The uptake coefficients are determined using an iterative box model. These uptake coefficients were found to be anti-correlated with the nitrate fraction of aerosol confirming suppression of uptake by aerosol nitrate. Additionally, a plume of chloride was observed in measurements of aerosol chloride, HCl and ClNO2. The N2O5 uptake coefficient was enhanced in this plume due to the competition between aerosol chloride and nitrate to react with N2O5.

RD 27. Henry's law coefficients and hydrolysis rate coefficients of atmospheric trace gases

Ranajit K Talukdar (1,2)*, Bartlomiej Witkowski (1,2,3), A. R. Ravishankara (2), and James B. Burkholder (2)
(1) CIRES; (2) NOAA, ESRL, CSD; (3) Permanent address: Department of Chemistry, University of Warsaw, Poland.

Solubility coefficients of gases in liquids (Henry's law constant, H) and rate coefficients for the hydrolysis of molecules in the liquid phase (k) of atmospheric trace gases are needed to model and quantify their aqueous-phase processing. We built an experimental apparatus to measure Henry's law solubility coefficients of weakly soluble atmospherically relevant compounds and, in applicable cases, their hydrolysis rate coefficients. The apparatus, shown schematically in Fig 1, consists of a closed-cycle bubble reactor combined with a Fourier transform infrared (FTIR) spectrometer that was used to measure the gas phase concentration of the dissolving gas and products of hydrolysis reaction. Results from experiments with perfluoro-2-methyl-3-pentanone (C2F5C(O)F(CF3)2, PFMP) and perfluoro-2-methyl-3-butanone (CF3C(O)CF(CF3)2, PFMB) will be presented. PFMP is currently being used as a fire suppressant in place of Halons, which have high ozone depletion potentials (ODP); PFMP and PFMB have essentially zero ODPs. The tropospheric photolysis lifetime of PFMP is relatively short, on the order of several weeks; thus, this molecule has a small Global Warming Potential (GWP). However, the hydrolysis of PFMP is known to produce HFC-227ea (CF3CHFCF3), a molecule that has low solubility, an atmospheric lifetime of 38.9 years, and a GWP of 3580 (100 year time horizon). Therefore, the atmospheric aqueous-phase processing of PFMP to produce HFC-227ea, even if only a minor loss pathway, can lead to a very large GWP attributable to its emission. To validate our methodology, the Henry's law solubility constants for SF6, CF3CHF2 (HFC 134a), and C2F5CF(CF3)2 (HFC 227ea), molecules that have well established H values and extremely low hydrolysis rate coefficients, were also measured. The results of these measurements will be presented and atmospheric implications of these findings discussed.
Fig 1. Experimental setup

GR 1. Multi-scale observations of small cloud systems

Allison McComiskey (1,2), Graham Feingold (2), Andrew Vogelmann (3)
(1) CIRES, (2) NOAA Earth System Research Laboratory, (3) Brookhaven National Laboratory

Shallow cumulus dominates cloud feedbacks in general circulation models (GCMs) and also exhibits the greatest amount of inter-model spread. A major challenge for this cloud regime is that the horizontal dimension of a GCM grid cell is large relative to the high frequency variability that governs radiative forcing. Evaluation of these models is often based on means, or sometimes simple distributions of properties retrieved from space; however, simple averaging of sub-grid scale variability may create biases in the representation of individual properties or parameterizations that are not based in physics. Sub-grid distributions of cloud liquid water, cloud fraction, and microphysical properties are essential for representing accurate grid-scale radiative fluxes but raise some questions: To what extent do distributions of cloud characteristics vary under different conditions of aerosol concentrations or environmental variables? What are the factors controlling the various distributions? Do distributions vary as a function of observational approach or scale? To answer these questions, we combine surface, in situ, and satellite observations and analyze radiatively-pertinent characteristics of small clouds and their determining factors, including the larger-scale environmental state, cloud-scale dynamics, and aerosol. The internal consistency of these systems is examined using multivariate distributions of many of these properties.

GR 2. Processing and presentation of high-resolution DART® data for recent significant tsunami events

George Mungov(1,4), Marie C. Eblé(2), Kelly J. Stroker(3)
(1) NOAA National Geophysical Data Center, Boulder, CO, USA. (2) NOAA Center for Tsunami Research, PMEL, Seattle, WA, USA
(3) UNESCO/IOC, JCOMMOPS, Toulouse, France. (4) CIRES, University of Colorado, Boulder, CO, USA

The National Geophysical Data Center (NGDC) is part of the U.S. National Oceanic and Atmospheric Administration (NOAA) Satellite and Information Service. NGDC hosts the long-term archive and management of tsunami data for research and mitigation of tsunami hazards under collaborative development between the National Weather Service, the Pacific Marine Environmental Laboratory, and the National Data Buoy Center. Archive responsibilities include the global historic tsunami event and run-up database, the bottom pressure recorder data collected by the Deep-ocean Assessment and Reporting of Tsunami (DART□) stations, coastal tide-gauge data from US/NOAA operated stations, historic marigrams, and other hazards related data and information. Currently NGDC process and stores in the archive the 15 seconds high-resolution DART® bottom pressure records. The tsunami signal-to-noise ratios in the deep-ocean are such that de-tiding based on a combination of tidal harmonic predictions and carefully constructed filters are necessary to obtain clean tsunami records. The processing includes removing tides using the customized version of the tidal package of Mike Foreman. Additional processing is applied for parts of the records with registered tsunami events where the noise from the intra-gravity waves and components representing larger scaled oceanic processes are removed by band-pass Kaiser-Bessel filters. At the moment all high-resolution records for the period 2002-2010 are processed. For recent significant tsunami events, real-time and archived high-resolution observations are now available through new event pages, including the Tohoku tsunami in March 2011. These pages are integrated with the NOAA Global Historical Tsunami Event Database. Event pages are developed to deliver summaries of the tsunami events, including socio-economic impacts, tsunami travel time maps, raw observations, de-tided residuals, spectra of the tsunami signal compared to the energy of the background noise, and wavelets. These data are essential to tsunami researchers and educators in providing a more complete record of tsunamis and their propagation in the open ocean. They could be accessed under http://ngdc.noaa.gov/hazard/recenttsunamis.shtml. Details of the filtering and tide removal techniques are discussed. Spatial distribution and density of the observations along with some general statistics are presented. Results are presented for the Tohoku event om 11 March 2011 using all recently obtained 15 seconds high-resolution DART observations. http://ngdc.noaa.gov/hazard/recenttsunamis.shtml

GR 3. Decadal Variability in the Background Stratospheric Aerosol Layer

R.R. Neely III(1,2,3), R. Michael Hardesty (1,2), S. Solomon(4), Owen B. Toon (3,5), Jeffrey P. Thayer (6), John E. Barnes(2), Karen Rosenlof(2), E.G. Dutton(2), Michael O'Neill(1). (1) CIRES, (2) NOAA ESRL, (3) CU-ATOC, (4) MIT, (5) LASP, (6) CU-ASEN

Stratospheric aerosol variability is due to a combination of variability in dynamics and sources. It is poorly understood due to limited observations, inherent biases and deficiencies of current observational tools and models. Discussion will include advancements in lidar observations in conjunction with model simulations to improve our understanding of aerosol properties and their role in climate processes. Specifically, the causes of decadal variability of background stratospheric aerosols observed by globally located ground based aerosol lidars will be addressed.

GR 4. Feasibility of US National Wind and Solar Energy Production System

Alexander E. MacDonald (1), Anneliese Alexander (2), Christopher Clack (1), Adam Dunbar (1), Yuanfu Xie (1). (1) NOAA ESRL, (2) CIRES

A study is being done to determine the optimal wind and solar generation system over the conterminous United States using historic weather observations and land-use limitations. Wind and solar generation was obtained from historical weather conditions over a three-year period on a 13-km resolution grid. The locations where wind and solar technologies can be deployed are limited by the amount of available land inside each grid box and the slope of the land. Observed electricity demand for the conterminous U.S. for 2006-2008 was obtained from FERC and grown to 2030 levels to reflect population and GDP growth. Existing nuclear and hydroelectric generation were also included. Then a minimization study was performed to build the most cost-effective wind and solar generation system to meet the remaining electricity demand after nuclear and hydroelectric generation was removed. The minimization examines the impacts on the final system characteristics as the domain size changes.

GR 5. ncISO Facilitating Metadata and Scientific Data Discovery

David Neufeld (1), Ted Habermann (2)

1. CIRES, University of Colorado, Boulder, CO, United States. 2. NGDC, NOAA, Boulder, CO, United States.

Increasing the usability and availability climate and oceanographic datasets for environmental research requires improved metadata and tools to rapidly locate and access relevant information for an area of interest. Because of the distributed nature of most environmental geospatial data, a common approach is to use catalog services that support queries on metadata harvested from remote map and data services. A key component to effectively using these catalog services is the availability of high quality metadata associated with the underlying data sets. In this presentation, we examine the use of ncISO, and Geoportal as open source tools that can be used to document and facilitate access to ocean and climate data available from Thematic Realtime Environmental Distributed Data Services (THREDDS) data services. Many atmospheric and oceanographic spatial data sets are stored in the Network Common Data Format (netCDF) and served through the Unidata THREDDS Data Server (TDS). NetCDF and THREDDS are becoming increasingly accepted in both the scientific and geographic research communities as demonstrated by the recent adoption of netCDF as an Open Geospatial Consortium (OGC) standard. One important source for ocean and atmospheric based data sets is NOAA's Unified Access Framework (UAF) which serves over 3000 gridded data sets from across NOAA and NOAA-affiliated partners. Due to the large number of datasets, browsing the data holdings to locate data is impractical. Working with Unidata, we have created a new service for the TDS called "ncISO", which allows automatic generation of ISO 19115-2 metadata from attributes and variables in TDS datasets. The ncISO metadata records can be harvested by catalog services such as ESSI-labs GI-Cat catalog service, and ESRI's Geoportal which supports query through a number of services, including OpenSearch and Catalog Services for the Web (CSW). ESRI's Geoportal Server provides a number of user friendly search capabilities for end users, and links to data endpoints that can be used immediately in web-based mapping and analysis tools, as well as delivered to desktop applications. http://www.ngdc.noaa.gov/eds/tds/

GR 6. Application of Wave Interferometry to Experimental Investigation of Infragravity Waves off New Zealand

Nikolay Zabotin (1,2), Oleg Godin (2,3), Anne Sheehan (4,2), Zhaohui Yang (4,2), and John Collins (5)

(1) Department of Electrical and Computer Engineering, University of Colorado, (2) CIRES, University of Colorado, (3) NOAA Earth System Research Laboratory, Physical Sciences Division, (4) Department of Geological Sciences, University of Colorado, (5) Woods Hole Oceanographic Institution, Woods Hole, MA

In the course of the Marine Observations of Anisotropy Near Aotearoa (MOANA) Seismic Experiment, bottom pressure sensors (differential pressure gauges), along with broadband ocean bottom seismometers, were deployed off both east and west coasts of the South Island of New Zealand at approximately 100 km spacing and at water depths from 550 m to 4680 m. We use the year-long, continuous records of pressure at 30 locations on the seafloor to study the total energy, spectral structure, coherence, and directivity of infragravity waves (IGWs) in the 0.5–30 mHz frequency range. We have developed a technique that allows one to compensate for wave dispersion in evaluating the cross-correlation function of a random wave field. When applied to the seafloor pressure data, the technique drastically reduces the signal averaging times necessary for emergence of deterministic features and allows for accurate passive measurements of IGW travel times and directivity. The reduction in the averaging time makes it possible to study dynamics on the IGW field, including seasonal variations of the directionality, and helps to constrain possible IGW generation mechanisms.

GR 7. Long term changes in the upper stratospheric ozone at Syowa, Antarctica

Koji Miyagawa (1), Irina Petropavlovskikh(2), Robert D. Evans (3), C. Long(4), J. Wild (4), G. Manney (5)and W. Daffer (5)
(1)Japan Meteorological Agency, Japan; (2) CIRES; (3)NOAA ERSL; (4)NOAA Climate Prediction Center; (5) NASA JPL and New Mexico Institute of Mining and Technology

Analyses of stratospheric ozone data recorded by Dobson Umkehr measurements since 1977 at the Syowa (69.0S, 39.6E), Antarctica station show a significant decrease in ozone above 4 hPa during the 1980s and 1990s. Ozone values over Syowa remain low since 2001. The time series of upper stratospheric ozone from the homogenized NOAA (/2) SBUV V8 overpass data (+/-4 degrees, 24 hours) are in qualitative agreement with Syowa station data. Ozone recovery during the austral spring over Syowa station appears to be slower than predicted by use the Equivalent Effective Stratospheric Chlorine (EESC) curve. The long-term changes in station's equivalent latitude are derived from MERRA analysis at ~ 3 hPa and ~50hPa. These data are used to attribute some of the upper and middle stratospheric ozone changes to the changes in vortex position relative to station location. In addition, high correlation of the Southern Hemisphere Annular Mode (SAM) with polar upper stratospheric ozone during years of maximum solar activity points toward strong relation between the strength of the Brewer-Dobson circulation and the Polar stratospheric ozone recovery. Detection of stratospheric ozone recovery in the Antarctic region requires careful consideration of counteracting contributions from chemical and dynamical processes.

GR 8. Lightning NOx Parameterization for Synoptic Meteorological-scale Predictions with Convective Parameterization in WRF-Chem

John Wong (1), David Noone (1), Mary Barth (2)

Lightning NOx (LNOx) is an important precursor to tropospheric ozone production and monsoonal upper tropospheric ozone enhancement. This presentation showcases the results from a preliminary implementation of a LNOx parameterization designed for convective-parameterized synoptic meteorological-scale predictions. The implementation uses the Price and Rind (1992) method based on cloud top height to produce a flash density. Comparison against Boccippio et al (2000) multiyear climatology shows confidence in reproducing the proper geographical distribution. Regional comparison against National Lightning Detection Network (NLDN) data also shows confidence of using a constant tuning parameter to produce a flash density similar to that observed. Finally, the predicted flash density is converted into NO production with a constant emission per flash and single Gaussian vertical distribution.

GR 9. Diurnal variations of meteoric Fe layers in the mesosphere and lower thermosphere at McMurdo (77.8°S, 166.7°E), Antarctica

Zhibin Yu1, Xinzhao Chu1, Wentao Huang1, Weichun Fong1, and Zhangjun Wang1. 1Cooperative Institute for Research in Environmental Sciences & Department of Aerospace Engineering Sciences, University of Colorado at Boulder, USA

As one of the main metal species in the mesosphere and lower thermosphere, neutral Fe layers provide an excellent tracer for studying atmospheric dynamics and chemistry. Unfortunately, most Fe measurements were made in the night, except a few reports from the Antarctic and Arctic. So far studies of the diurnal variations of Fe layers are very rare. This situation poses interesting questions like how Fe layers vary through a diurnal cycle, whether such variations change with seasons, and what mechanisms contribute to the diurnal variations. To help address this issue, we report the diurnal variations of Fe densities, based on our lidar observations made at McMurdo, Antarctica. The data were collected with an Fe Boltzmann lidar since late December 2010 through austral autumn, winter and spring in 2011, covering the states of polar days under full sunlight, alternations between day and night, and polar nights under total darkness. By taking composite days, we obtain 24-h Fe coverage for every month, allowing relatively detailed study of the diurnal variations. Our preliminary analyses show an interesting phenomenon that the bottom boundary of Fe layers extends downward from ~80 km to ~75 km or lower when switching from night to day. This phenomenon is obvious in continuous (straight) 24-h data as well as in composite 24-h data during March and April when the sunlight conditions have day and night switches. The results indicate that photochemistry, rather than wave dynamics, may play an essential role in determining the Fe layer bottom. No obvious diurnal variations are observed in polar summer and mid-winter; however, the layer bottom altitude descends for several kilometers from polar day to polar night. These likely reflect the influences of temperatures, waves, mesospheric clouds and aurora activities.

GR 10. Impact of Atmospheric Tides on Ionosphere-Thermosphere System

T.-W. Fang(1), T. J. Fuller-Rowell(1), R. A. Akmaev(2), and F. Wu(1)
1 CIRES, University of Colorado, Boulder, Colorado, USA . 2 Space Weather Prediction Center, NOAA, Boulder, CO, USA

The Coupled Thermosphere Ionosphere Plasmasphere with self-consistent Electrodynamics (CTIPe) model is a nonlinear, coupled thermosphere-ionosphere-plasmasphere code that includes a self-consistent electrodynamics scheme for the computation of neutral wind induced dynamo electric fields. The model consists of a global thermosphere, a high-latitude ionosphere, a mid- and low-latitude ionosphere/plasmasphere and an electrodynamical calculation of the global dynamo electric field. The diurnal and semidiurnal propagating tidal modes are imposed at 80 km altitude with a prescribed amplitude and phase. The Whole Atmosphere Model (WAM) is an extension of the operational weather prediction Global Forecast System (GFS) general circulation model (GCM) to the top of the atmosphere. The model is being built to study and potentially develop a capability to predict the effects of lower atmosphere dynamics and variability on the upper atmosphere and ionosphere. Since atmospheric waves can be important sources in reproducing ionospheric variability and thermospheric phenomena, we implement WAM parameters at the lower boundary of CTIPe. The geopotential height, neutral temperature, zonal and meridional wind which were prescribed by Hough mode at 80 km in CTIPe are replaced by the WAM outputs between 80 and ~100 km. We compare the tidal modes reproduced in CTIPe and WAM thermosphere to validate the wave propagation scheme in CTIPe and to understand their impact on ionospheric electrodynamics. Several thermospheric phenomena such as midnight temperature maximum (MTM) and midnight density maximum (MDM) and influences of planetary waves in ionosphere and thermosphere are also studied using CTIPe with the new boundary condition.

GR 11. Diurnal and Seasonal Variations of Temperatures from Lower to Upper Atmosphere at McMurdo, Antarctica from 2010 to 2011

Weichun Fong (1), Xinzhao Chu (1), Zhibin Yu (1), Cao Chen (1), Wentao Huang (1). (1) CIRES

Temperature is one of the fundamental parameters for atmospheric science studies. Many phenomena, such as polar mesospheric clouds, polar stratospheric clouds, and metallic layer chemistry at MLT region, are dominated by temperature. Also, temperature is a key tracer for tidal and gravity waves. A ground-based Fe Boltzmann temperature lidar has been installed at McMurdo and started data collection since December 2010. McMurdo (77.83□S, 166.66□E), near south magnetic pole and close to the Trans-Antarctic Mountain Ridge, is a scientifically critical location for polar atmospheric study. Over 1000 hours of data have been retrieved so far, providing long-duration continuous observations that cannot be achieved by satellites, not to mention high latitude and diurnal coverage for satellites are usually poor. With full-diurnal coverage and year-round lidar measurements of temperatures, we establish the morphology of atmospheric thermal structure for McMurdo. The diurnal and seasonal variations of the thermal structure from 30 to 105 km are characterized, which will help understand metal layer variations and PMC formation, and provides ground-truth observations for satellite measurements. The amplitude and phase of 24-hour tide and the first few harmonics are investigated as well. The tide is believed to have small amplitude in polar winter. However, in the MLT region, a coherent wave structure with period between 4 and 6 hours appears in the monthly composite temperature in June, which might provide a clue for studies of tidal and gravity wave interaction. Finally, we compare winter data with existed satellite measurements, such as MLS and SABER, and atmospheric models, such as TIME-GCM and WACCM.

GR 12. Quantifying Digital Elevation Model (DEM) Uncertainty Introduced by Interpolative Gridding

Christopher Amante (1,2), Barry Eakins (1,2)
(1) CIRES (2) NOAA National Geophysical Data Center (NGDC)

Digital elevation models (DEMs) are representations of the Earth's solid surface and are the framework for modeling numerous processes including tsunami, storm surge, and sea-level rise. Deviations from the actual seabed or land surface constitute errors in DEMs. DEM errors originate from both the source elevation measurements (e.g., multibeam sonar, lidar) and the interpolative gridding technique (e.g., spline, natural neighbor, inverse distance weighting) used to estimate elevations in areas with no source measurements. Previous research found that interpolation errors are as significant as the measurement errors and should be considered when generating and using DEMs. Numerous studies also indicate that interpolation errors are positively correlated with terrain complexity and increasing distance to known measurements. The magnitude of interpolation errors is often unknown and the lack of knowledge about these errors represents the uncertainty introduced by the interpolative gridding process. We have developed a computer program that utilizes a split-sample methodology to quantify interpolation errors. The program omits a percentage of the xyz points, applies a gridding algorithm, and quantifies the interpolation errors as the differences between the interpolated elevations and the omitted elevations. A method for quantifying DEM uncertainty introduced by interpolative gridding from the range of interpolation errors is described. In addition, regression methods are used to model the relationship between interpolation uncertainty, distance to known measurements, and terrain complexity.

GR 13. Lidar and radar investigation of gravity wave characteristics, propagation and dissipation from the stratosphere to the lower thermosphere over McMurdo, Antarctica

Cao Chen (1), Xinzhao Chu (1), Weichun Fong (1), Zhibin Yu (1), Adrian J. McDonald (2) and Xian Lu (3)
(1) CIRES, (2) Department of Physics and Astronomy, University of Canterbury, Christchurch, NZ, (3) Department of Physical Sciences, Embry-Riddle Aeronautical University, Daytona Beach, FL, USA

In the middle atmosphere, dissipating gravity wave is one of the major forcing in driving the mean meridional circulations, which greatly affects the thermal structure and constituent transport in this region. Gravity waves also play a crucial role in the coupling process from the lower to the upper atmosphere. Therefore, in order to constrain gravity wave parameterizations in general circulation models, long-duration, large-altitude-range and high resolution measurements of gravity waves are essential to provide real observations. In particular, the long-standing 'cold pole' problems in many models can be attributed in large part to missing wave drag which can be estimated based on the gravity wave measurements around polar regions. However, at high latitudes, such measurements are rare in Antarctica. Simultaneous lidar and radar observations at McMurdo (77.8°S, 166.7°E) provide such an opportunity to study gravity waves in details. Besides, located just east to a vigorous gravity wave source, the Trans-Antarctic Mountain (ridge), McMurdo has been highlighted as a gravity wave 'hotspot'. In this paper, we perform a combined study of Fe Boltzmann lidar and MF radar observations of gravity waves events in the polar winter. We use Fe and Rayleigh temperature lidar data collected from early June to late July to extract the gravity wave perturbations. For each dataset, one or two dominant wave modes are identified from stratosphere to lower thermosphere (~30 km to ~110 km). The wave properties, such as apparent period, vertical wavelength, and phase speed, are characterized. Our preliminary analysis indicates dissipation of gravity waves, some in stratosphere and some even in the mesosphere and lower thermosphere. We will further characterize the wave dissipation via investigating vertical wavenumber power spectra. Hodograph analysis of MF radar wind data measured at the same location will be used to study characteristics of horizontal propagation directions and intrinsic properties of these waves.

GR 14. Observed Ocean Spectra from Argo Profiling Floats

Katherine McCaffrey (1,2), Baylor Fox-Kemper (1,2)
(1) University of Colorado, Department of Atmospheric and Oceanic Sciences. (2) Cooperative Institute for Research in Environmental Sciences

The spectral characteristics of turbulence and eddies in the ocean are examined using ARGO profiling float data. Many theories predict the spectral slopes associated with the statistics of ocean macro-turbulence, but there are few observations at depth to guide these discussions. Here, a method developed for estimating the structure function of atmospheric macro-turbulence using rawinsondes is adapted to estimate the structure function and corresponding spectral slope of oceanic macro-turbulence using data collected by ARGO profiling floats. Horizontal structure functions over a range of depths and latitude bands, as well as in eddy-rich and eddy-poor regions will be shown. The structure function evaluated at pressure levels differs from that evaluated along potential density surfaces, consistent with the internal wave spectrum. In pressure coordinates below 45m at scales larger than 100km, results follow the Batchelor (1959) theory and smaller scales follow a steeper slope. The potential density coordinates results are consistent with the Batchelor theory for passive tracers at large scales over all depths. The spectral slope's dependence on depth, and the presence of eddies will also be discussed.

GR 15. Ozone depletion in filaments of the Arctic Polar Vortex observed during the first Global Hawk UAS science mission

James W. Elkins (1), Eric J. Hintsa (1,2), Geoffrey S. Dutton (1,2), Bradley D. Hall (1), Fred L. Moore (1,2), Ru-shan Gao (1), Samuel J. Oltmans (1,2), Bryan Johnson (1), Eric A. Ray (1,2), David W. Fahey (1) , and Paul A. Newman (3) plus GloPac, HIPPO, and MLS teams.
(1) NOAA ESRL, Boulder, CO 80305 USA; (2) CIRES, University of Colorado, Boulder, CO 80309 USA; (3) NASA GSFC, Greenbelt, MD 20771 USA

One of the important potential uses of the NASA Global Hawk Unmanned Aircraft System (UAS) in scientific research is to study stratospheric ozone depletion in polar regions. Manned flights involve remote and hazardous duty, which pose great risks to pilots, crew, and scientists. Arctic ozone depletion observed in the spring of 2010 by satellites, manned aircraft campaigns, ground-base stations was less severe than that observed this year (2011). The Global Hawk UAS flight on 23 April 2010 was the first to observe ozone-depleted air with a UAS platform. Temperatures in the polar vortex were cold enough for Type II Polar Stratospheric Clouds (PSC) to form for a short period (days) at 50 hPa in 2010, and cold temperatures existed for almost 2 months for Type I PSC formation. Based on the NOAA Global Monitoring Division's Unmanned aircraft systems Chromatograph for Atmospheric Trace Species (UCATS) ozone versus nitrous oxide tracer correlation plot (below), there is 21% less ozone in air from a polar filament sampled on 7 April 2010 compared to the Arctic air sampled later on 23 April 2010. The NOAA Chemical Science Division UAS Fast Ozone Instrument showed a similar pattern with respect to N2O. Age-of-air values derived from on board SF6 observetions were about 5 years in the filament versus about 3 years outside the filament in the subsequent polar flight. The Global Hawk UAS flights were part of the Global Hawk Pacific Experiment (GloPac), which demonstrated flights up to 28.6 hr duration, altitudes as high as 19.8 km and a maximum range of 9200 nm while carrying a payload of in situ and remote instrumentation for atmospheric chemical and aerosol tracers. This first science mission of the NASA Global Hawk UAS demonstrated its huge potential for stratospheric ozone research over remote and hazardous polar areas.

GR 16. Three Decades of Continuous Monitoring of Long-lived Halocarbons

Geoff Dutton (1), Brad Hall (2), J. David Nance (1), Debra J. Modeel (1), James W. Elkins (2)
(1) CIRES, (2) NOAA ESRL

In the mid-1970s, the National Oceanic and Atmospheric Administration's (NOAA) Geophysical Monitoring for Climate Change (GMCC) program made a commitment to measure and monitor trace gases including carbon dioxide, methane, nitrous oxide (N2O) and chlorofluorocarbons (CFCs). Over the next three decades GMCC grew into a division of NOAA/ESRL, and many trace gas measurement programs evolved into separate projects with different instrumentation. Multiple measurements of the same gases at identical locations (e.g., using both in situ instruments and grab samples) can sometimes lead to confusion when determining what measurement to use for analysis. We present a statistical method developed to combine measurements from independent NOAA programs to construct continuous long-term global records for the following ozone-depleting substances: CFC-11, CFC-12, CFC- 113, methyl chloroform (CH3CCl3) and CCl4. The combining technique takes advantage of co-located measurements and accounts for systematic differences between measurement programs. We also use two different statistical approaches to characterize uncertainties in hemispheric and global means. The combined data sets and uncertainties can be used in global growth rate and top down emission estimates of these important gases.

GR 17. A Comparison of Solar and Lunar Position Algorithms

Allen Jordan (1,2), Emiel Hall (1,2), Jim Wendell (2), Ellsworth Dutton (2). (1) CIRES, (2) NOAA ESRL

This poster will give information about various solar and lunar position calculation algorithms, showing comparisons of their output. Resulting accuracy, runtime/efficiency of calculation, and platform portability (microcontroller, etc) will be examined over a large input range. These algorithms are useful in many applications, particularly solar and lunar tracking for the NOAA Solar Radiation group's instrumentation.

GR 18. Simultaneous and Common-Volume Lidar Observations of the Mesospheric Fe and Na Layers at Boulder (40°N, 105°W)

Wentao Huang(1), Xinzhao Chu(1), Zhangjun Wang(1), Weichun Fong(1),
Zhibin Yu(1), John A. Smith(1), Brendan Roberts(1). 1. CIRES, Univ. of Colorado at Boulder, Boulder, CO 80309

The rich features of the mesospheric metal layers are produced by the complicated chemical and dynamical processes in the Upper Mesosphere/Lower Thermosphere region. Current chemical models with parameterized inputs are able to reproduce some large-scale structures but challenged in small-scale features. Simultaneous and common-volume observation of multiple species is an important method to help reveal the determining mechanisms in small scales and validate the models. Such observations of Fe and Na layers are relatively rare, despite several reports based on one or a few nights of data, and one extensive study at Wuhan (30°N), China. In summer and fall 2010, we made over 16 nights of such observations at Boulder (40°N, 105°W) with two resonance lidars: an Fe Boltzmann temperature lidar and a 3-frequency Na Doppler lidar. The data shows the primary characteristics of Fe vs. Na layers as reported in mid-latitude, e.g., higher Fe density and column abundance, lower Fe peak and centroid altitude, larger density gradient at the bottom of Fe layer etc. Their altitudes of lower boundaries are similar and closely follow each other through the night, while the upper boundary of Na layer normally extends to higher altitude. Moreover, we introduced the method using the relative density perturbations in analyzing the simultaneous measurements. Although this method reveals generally correlated density fluctuations in the main layers as well as in the sporadic layers, there are noticeable differences of the amplitude and phase in a few cases. On 11 August 2010, we also caught meteor trails of Perseids meteor shower, which may have increased the column abundance of both Fe and Na layers.

GR 19. Improving our understanding of ozone depleting substances (ODS) in the upper atmosphere

J. D. Nance (1,2), J. W. Elkins (2), F. L. Moore (1,2), G. S. Dutton (1,2), E. J. Hinsta (1,2), B. D. Hall (2), D. J. Mondeel (1,2), B. J. Miller (1,2), C Siso (1,2), and S. A. Montzka (2). (1) CIRES, University of Colorado, Box 216 UCB, Boulder, CO 80309 USA.
(2) NOAA/ESRL/GMD, 325 Broadway, Boulder, CO 80305 USA

The Montreal Protocol on Substances that Deplete the Ozone Layer and its subsequent amendments has been successful in decreasing the total equivalent chlorine of man-made halocarbons in the atmosphere by ~13% since its peak in 1994-5. The National Oceanic and Atmospheric Administration's Earth System Research Laboratory (NOAA/ESRL) maintains a global, ground-based in situ and flask sampling network for the measurement and analysis of halocarbons and other atmospheric trace gases. Measurements of nitrous oxide and chlorofluorocarbons -11 and -12 started in 1977. The purpose of this work is to study atmospheric trace gases that affect climate change, stratospheric ozone depletion, and air quality from observations at NOAA-affiliated sites. The analysis of flask samples and in situ data is conducted at the Global Monitoring Division (GMD) in Boulder, Colorado, USA. Through collaborations with the National Aeronautics and Space Administration (NASA) and the National Science Foundation (NSF), NOAA/ESRL also operates a number of in situ and flask sampling systems from manned and unmanned aircraft up to 21 km, and balloon platforms up to 32 km . We measure over 40 trace gases in the atmosphere including nitrous oxide (N2O), chlorofluorocarbons (CFCs), hydrochlorofluorocarbons (HCFCs), hydrofluorocarbons (HFCs), methyl halides, numerous halocarbons, sulfur gases (COS, SF6, CS2), and selected hydrocarbons. This presentation will highlight our recent observations of halocarbons and other trace gases from the NSF and NOAA sponsored HIAPER Pole-to-Pole Observations airborne campaign over NDACC and NOAA stations from 2009 to 2011, and the NASA and NOAA sponsored Unmanned Aircraft Systems Missions. For more information see http://www.esrl.noaa.gov/gmd/hats. Our data are available via anonymous ftp at ftp://ftp.cmdl.noaa.gov/hats.

GR 20. Studying the 'cold pole' problem in WACCM and comparisons to lidar temperature morphology

Bo Tan(1)(2), Han-Li Liu(2), and Xinzhao Chu(1)
(1) CIRES & Aerospace, University of Colorado at Boulder, 216 UCB, Boulder, CO, USA
(2)High Altitude Observatory, National Center for Atmospheric Research, Boulder, CO, USA

The 'cold pole' problem refers to the cold bias of polar stratosphere temperature, especially in the south, in most general circulation models (GCMs) during the winter and spring, when compared to observations. Accompanying the cold pole is the warm bias in the lower mesosphere and strong jet in the stratosphere. It is a long-standing problem, most likely caused by the lack of wave forcing in the southern stratosphere. In this study, a newly implemented gravity wave scheme with inertial waves added to the original mesoscale waves provides additional wave forcing in the stratosphere. With this new scheme, WACCM simulation results show much improved agreement with the temperature and wind climatology obtained from lidar and ERA-40, respectively.

GR 21. Experimental Validation of a New Balloon-Borne Supercooled Liquid Sensor

Emrys Hall (1,2), Allen Jordan (1,2), Dave Serke (3), Frank McDonough (3), John Bognar (4), Spencer Abdo (4), Kirstin Baker (4), Tom Seitel (4), Randolph Ware (5), Marta Nelson (5), Andrew Reehorst (6)
(1) NOAA ESRL Global Monitoring Division, Boulder, Co. (2) Cooperative Institute for Research in Environmental Sciences, University of Colorado
(3) NCAR Research Applications Laboratory, Boulder, Co. (4) Anasphere Inc, Bozeman, Mt. (5) Radiometrics Corporation, Boulder, Co
(6) NASA Glenn Research Center, Cleveland, Oh

An improved version of the ATEK Corporation vibrating wire sensor, used to measure supercooled cloud liquid water content (LWC), has been developed by Anasphere, Inc. This updated sensor reduces the weight of the instrument while improving performance when compared to the preceding balloon-borne sensor that was developed in the 1980's by Hill and Woffinden. Results from recent laboratory testing show that data collected from the Anasphere sensor compares well to data reported during similar icing tunnel testing in 1989 at Eglin Air Force Base with the ATEK Corporation instrument. These two icing tunnel datasets were used to develop algorithms to calculate the LWC measured from the vibrating wire frequency. Balloon-borne test flights were performed from Boulder, Colorado during February and March of 2102 providing comparisons to integrated liquid water and profiles of liquid water content derived from a collocated multichannel profiling radiometer built and operated by Radiometrics Corporation. Inter-comparison data such as these are invaluable for calibration, verification, and validation of remote-sensing instruments. The data gathered from this sensor is important in the detection of icing hazards to aircraft and for truthing of microphysical output from numerical models.

The disposable Anasphere sensor interfaces with an InterMet Systems iMet radiosonde measuring pressure, temperature, humidity, windspeed, and winddirection. All flight data can be seen in real time.

GR 22. Determining constraints on aerosol parameter retrievals from direct and diffuse irradiances from 300 to 1050 nm

P. Kiedron (1), K. Lantz (1), P. Disterhoft (1), J. Michalsky (2). (1) CIRES , (2) NOAA GMD

In radiative transfer models the scattering and absorbing properties of aerosols are usually defined by three parameters: aerosol optical depth (AOD), singles scattering albedo (SSA) and the asymmetry parameter (AP). These parameters are wavelength dependent, i.e., AOD(λ), SSA(λ), AP(λ). These functions are "bland", i.e., they and their low order derivatives are monotonic. On the other hand, the surface albedo SA(λ) is not a "bland" function of wavelength. AOD is retrieved from direct normal irradiance (Idir) so it is unaffected by SA(λ), however, in the first order approximation, mathematically Idif depends on the SSA(λ)*SA(λ). Since SSA(λ) is physically independent of SA(λ), one can check the retrieved SSA(λ) for the presence of SA(λ) spectral imprint in its wavelength dependence. Furthermore, during a stable day with AOD approximately constant, one may postulate that the two remaining parameters are also time independent. While the magnitude of SA depends on sun zenith angle (α) the spectral component is relatively unaffected by α. Therefore testing the retrieved ssa(α) for systematic dependence on sun zenith angle α determines the region of validity - in terms of angle α - of the retrieval procedure. Data from rotating shadowband spectroradiometer (RSS) at the Atmospheric Radiation Measurement (ARM) site near Billings, Oklahoma, are used to study the robustness and validity of the retrieving algorithm.

GR 23. Comparison of Continuous Surface Ozone Measurements from Two Arctic Observatories

L. Patrick1, S.J. Oltmans1, I. Petropavlovskikh 1. 1Cooperative Institute for Research in Environmental Science, Boulder, USA

The Hydrometeorological Observatory of Tiksi and NOAA's Barrow, Alaska Observatory are equipped with Thermo Scientific Model 49 Ozone Analyzers and have been continuously measuring surface ozone levels since October 2010. The two observatories are in the Arctic Circle at similar latitudes of 71.6oN and 71.3oN, respectively. Their locations provide a unique opportunity for measurement comparison due to minimization of solar zenith angle differences. Instrumentation at the site, data collection and quality assurance are discussed. General seasonal trends are presented and we quantify mean surface ozone levels. Both stations show surface ozone depletion events during 2011, likely due to high bromine originating in nearby ice leads. The events were investigated using back trajectories from the Hybrid Single Particle Lagrangian Integrated Trajectory (HYSPLIT) Model. At both observatories, back trajectories during depletion events indicate winds passed over the ice leads prior to reaching the stations. However, due to differences of seasonal ice lead longevity at the two sites, the depletion events were found in different months. In addition to study conclusions, recommendations for further study are also discussed.

GR 24. Global Trends in Sulfur Hexafluoride

Brad Hall (1), Geoff Dutton (2), Debbie Mondeel (2, presenter), David Nance (2), Dale Hurst (2), Matt Rigby (3), Fred Moore (2), James Butler (1), James Elkins (1). (1) NOAA ESRL, (2) CIRES, (3) Massachusetts Institute of Technology

Sulfur hexafluoride (SF6) is a potent greenhouse gas and useful atmospheric tracer. NOAA SF6 measurements from two ESRL/GMD programs (flask and in situ) were combined to produce global and hemispheric mean records. These data were used to examine changes in the growth rate of SF6 and corresponding SF6 emissions. Global emissions and mixing ratios from 2000-2008 are consistent with recently published work. Interannual variability of the SF6 growth rate show some features that appear to be transport-related. A transport model was run with constant emissions to examine a recent decline in the growth rate. A 10% decline in SF6 emissions in 2008-2009 is suggested, corresponding with a decrease in world economic output. This decline was short-lived, as the global SF6 growth rate has recently increased to near its 2007-2008 maximum value of 0.29 ppt yr-1.

GR 25. Enhancing natural hazards data discovery with visual media

Heather L. McCullough (1), Evan McQuinn (2), Jesse Varner (2). 1) NOAA National Geophysical Data Center, (2) CIRES

Photographs and other visual media provide valuable pre- and post-event data for natural hazards. Scientific research, mitigation, and forecasting rely on visual data for post-analysis, inundation mapping and historic records. Instrumental data only reveal a portion of the whole story; photographs explicitly illustrate the physical and societal impacts from the event. Visual data is rapidly increasing as the availability of portable high resolution cameras and video recorders becomes more attainable. Incorporating these data into archives ensures a more complete historical account of events. Integrating natural hazards data, such as tsunami, earthquake and volcanic eruption events, socio-economic information, and tsunami deposits and runups along with images and photographs enhances event comprehension. Global historic databases at NOAA's National Geophysical Data Center (NGDC) consolidate these data, providing the user with easy access to a network of information. NGDC's Natural Hazards Image Database (ngdc.noaa.gov/hazardimages) was recently improved to provide a more efficient and dynamic user interface. Built on the Grails web framework, the site utilizes a number of JavaScript interface components to make browsing hazard images more intuitive and interactive. It uses the Google Maps API and Keyhole Markup Language (KML) to provide geographic context to the images and events. Descriptive tags, or keywords, have been applied to each image, enabling easier navigation and discovery. This combination of features creates a simple and effective way to enhance our understanding of hazard events using imagery.

GR 26. Trace Gas Distributions Observed During the HIPPO Project

Eric J. Hintsa (1,2), Fred L. Moore (1,2), Geoff S. Dutton (1,2), Brad D. Hall (1), J. David Nance (1,2), and James W. Elkins (1)
(1) NOAA/ESRL/GMD, (2) University of Colorado/CIRES

The goal of the HIAPER Pole-to-Pole Observations (HIPPO) of Carbon Cycle and Greenhouse Gases project is to measure a large set of trace gases and black carbon aerosols as a function of altitude and latitude in different seasons in order to better understand their sources, sinks, and atmospheric transport, and to use these measurements to compare with a variety of chemical transport models. This should ultimately lead to improvements in the models. The NSF/NCAR Gulfstream V (GV) aircraft (formerly known as HIAPER) was equipped with a suite of instruments for carbon cycle and greenhouse gases, ozone and a few other reactive gases, aerosols, and meteorological parameters, and flew a set of five transects in 2009-2011 from Colorado, to Anchorage, AK, to near the north pole, then south to Christchurch, NZ, toward the edge of Antarctica, and back to the northern hemisphere high latitudes, with intermediate stops at different locations in the Pacific Ocean. On each leg of the journey, the GV carried out a series of profiles from the marine (or continental) boundary layer to the stratosphere, generating a set of altitude/latitude slices of the atmosphere in different seasons (January 2009, March-April 2010, June-July 2011, August-September 2011, and October-November 2009). In this poster, results are shown that were obtained from the UCATS instrument and other sensors on board the GV. UCATS (the UAS Chromatograph for Atmospheric Trace Species) was configured to measure N2O, SF6, H2, CH4, CO, water, and ozone during HIPPO. The focus here is on the distribution of molecular hydrogen (H2) and related trace species.

GR 27. Sub-grid scale processes of the marine boundary layer cloud-aerosol system

Jan Kazil(1,2), Graham Feingold(2,1). (1) CIRES (2) NOAA ESRL

Climate simulations resolve cloud-aerosol interactions and their role for Earth's climate on spatial scales of 1-3° (~100-300 km). With increasing computing power, the resolution of climate simulations will continue to increase. However, the processes that govern marine boundary layer clouds, an important element of the climate system, take place on spatial scales of 10s of meters. Before reaching this resolution, climate simulations will rely on subgrid scale parameterizations of these processes, and on the insight from highly resolved, local simulations. We give an overview of the marine boundary layer processes that take place below the resolved scale of a climate model, using a new large eddy simulation model with detailed coupling between aerosol, cloud, chemical, and surface processes. The simulations reveal a rich network of interactions between marine boundary layer clouds, dynamics, ocean emissions, gas phase chemistry, and aerosol processes, which is currently not represented in climate simulations. The insights gained from these simulations can be used to improve representation of the marine boundary layer in climate models.

GR 28. An Information Management System for the U.S. Extended Continental Shelf Project

Jennifer Henderson(1), Elliot Lim(1), Evan McQuinn(1), Jesse Varner(1), Barry Eakins(1), John LaRocque(2), Anna Milan(2), Robin Warnken(2), and Susan McLean(2). (1)Cooperative Institute for Research in Environmental Sciences (CIRES), at University of Colorado at Boulder. (2)NOAA/NESDIS/ National Geophysical Data Center, Boulder, Colorado.

The United States Extended Continental Shelf (ECS) Project is a multi-year, multi-agency collaboration co-chaired by the State Department, NOAA, and the Department of Interior, involving several U.S federal agencies and academic institutions whose mission is to establish the full extent of the U.S. continental shelf beyond 200 nautical miles consistent with international law. The process to determine the outer limits of the ECS requires the collection and analysis of data that describe the depth, shape, and geophysical characteristics of the seafloor and sub-seafloor, as well as the thickness of the underlying sediments. The specific types of data that need to be collected include bathymetric data, seismic profiles, magnetic and gravity data, and other geophysical data. In 2007 the U.S. ECS Task Force designated NOAA's National Geophysical Data Center (NGDC) as the Data Management lead for the U.S. ECS Project and as the data stewards and archival location for all data related to this project. NGDC is responsible for establishing and maintaining a central repository of data and metadata that is accessible, robust, and effective in supporting ECS regional analyses. Over the past two years, NGDC and CIRES staff have been constructing and populating this "Information Management System" (IMS), linking it where appropriate with other existing databases, and working with other partner agencies in developing standards and protocols for data and metadata as part of the overall system for preserving the critical analyses and decisions made in support of the U.S. ECS determination. The geospatial database includes primary data, derivative data and products, associated metadata, and regional analyses from the various ECS regions of interest. Web applications, including interactive map services (built using ESRI's ArcGIS Server and the corresponding JavaScript API) aid in locating data and products. The interactive maps will show the spatial coverage of selected marine geophysical surveys from a variety of federal government and academic sources, and will include tools for identifying surveys and for querying the database.

GR 29. Stochastic Weather Generator Based Ensemble Streamflow Forecasting

Nina Caraway (1), Balaji Rajagopalan (1),(3), Andy Wood (2), Kevin Werner (2)
(1) Civil, Environmental, and Architectural Engineering, University of Colorado, Boulder, CO; (2) Colorado Basin River Forecast Center, Salt Lake City, UT; (3) CIRES, University of Colorado, Boulder

Efficient water resources management owes considerably to skillful basin wide streamflow forecasts at various time scales; the skillful projection of the streamflow probability density function (PDF) is especially of interest. Currently, forecasting centers such as the Colorado Basin River Forecasting Center (CBRFC) implement methods based on observed data, such as Ensemble Streamflow Prediction (ESP). ESP is created from historical daily weather sequences and a physically based watershed model. However, the number of ensembles is restricted to the number of years of historical data. Presently, the CBRFC maintains a 30 year calibration period. Furthermore, if seasonal forecast information is included through a use of a subset of these years, the ensemble size decreases substantially, further degrading the resolution of the estimated PDF. To improve on this, we propose a stochastic weather generator based approach coupled to the hydrologic modeling system. The weather generator uses a Markov Chain to simulate the precipitation state of a day (wet or dry) and a K-nearest neighbor (K-NN) resampling approach to simulate the daily weather vector. This weather generator can also produce daily weather sequences conditioned on seasonal categorical climate forecasts. However, k-NN resampling can only be performed on a single time series, which proves troublesome for multisite generation. A K-means clustering analysis was implemented to organize available weather time series into correlated groupings. Each cluster was combined by an elevation-weighted average to produce a synthetic time series for the k-NN weather generator. From this, daily weather sequences can be produced on a basin-wide scale and can then be driven through the hydrologic model to produce an ensemble forecast of streamflow. The San Juan River Basin was chosen for testing as it contains complex terrain and ENSO climate signals. Preliminary results will demonstrate the weather generator's ability to capture historic variability across multiple locations in the basin. Results will also include the pairing of the weather generator with CBRFC's new Community Hydrologic Prediction System (CHPS).

GR 30. Global Stokes Drift and Climate Wave Modeling

Adrean Webb, Baylor Fox-Kemper. CIRES

The Stokes drift is an important vector component that appears often in ocean surface wave dynamics, such as Langmuir turbulence. Inclusion of this unresolved turbulence via a wave model in climate models has the potential to correct a well-known, mixed-layer bias in the Southern Ocean. However, recent research has found that simplified Stokes drift estimates between different wave models vary drastically and is in contrast to the generally good agreement found among calculations of wave height. In addition, these estimates tend to overestimate the full Stokes drift by 33%, illustrating a need for a coupled wave model in climate studies. Progress on developing a prototype climate wave model using radial basis functions is also presented. This novel method uses an unstructured node layout and removes numerical singularities.

GR 31. Extreme Events: Pacemakers of Adaptation?

William R. Travis. CIRES, Center for Science and Technology Policy Research

Simulations of selected climate-sensitive adaptation decisions in agriculture and flood control show that extreme events can, as proposed in the literature, evoke adaption sooner than an underlying climate trend alone would, but also that extremes can, in the words of Schneider et al., trip "false starts leading to maladaptation." A decision analysis model of a farm undergoing droughts superimposed on a gradual climate change, and of an urban drainage system experiencing an underlying change in rainfall intensity, are used to test for adaptive efficiency occasioned by the timing and intensity of extremes forced into the simulation. Results indicate that larger variability tends to mask climate trends and thus actually slow adaptation, while extreme events can indeed trip early adaptation, with sub-optimal outcomes.

GR 32. NGDC's first foray into CLASS: the transition of data archive and stewardship into an external archival facility

Francine Coloma (1), Robert Prentice (1), and Peter Elespuru (1). (1) CIRES

The NOAA National Environmental Satellite, Data and Information Service (NESDIS) office operates three National Data Centers: the National Climatic Data Center (NCDC), the National Geophysical Data Center (NGDC), and the National Oceanographic Data Center (NODC). Each Data Center acquires, archives, and stewards data according to its mission. NOAA is considering transitioning Data Center holdings into an external archival facility, the NOAA-wide enterprise infrastructure called the Comprehensive Large Array-data Stewardship System (CLASS). As its first offering, NGDC has selected to transition its holdings of the National Geodetic Survey's (NGS) Continuously Operating Reference Stations (CORS) data set into CLASS. CIRES staff at NGDC took the lead in many aspects of this effort in coordination with NOAA, such as defining and implementing the interface between a data center and the external archival facility. The most important aspect of this project was to initiate a process of providing data stewardship while using an external archiving facility, a groundbreaking effort for NOAA's data centers. As of October 7, 2011 forward-looking CORS data has been successfully loaded operationally and continuously into the CLASS system. CIRES staff continue to assist in the enhancement and evolution of this NOAA Data Center transition into the CLASS environment.

GR 33. A real-time model of the equatorial ionospheric eastward electric field driven by ACE solar wind data.

Manoj Nair, Stefan Maus. CIRES and NOAA NGDC

A significant portion of the short-period variability of the equatorial ionospheric electric field (EEF) can be explained by prompt penetration (PP) of the inter-planetary electric field (IEF). By combining a climatological model with a PP model driven by solar wind measurements, one can thus predict the EEF in real time. Manoj et al. (2008) proposed a transfer-function-based model to predict EEF variations due to prompt penetration of the IEF. This model is driven by the solar-wind electric field data from the ACE satellite and is limited to the day-time. The model could account for around 30% of the variability found in the JULIA radar measurements EEF. We propose two improvements to our model: 1) We estimate a transfer function tensor between the interplanetary electric field vector and the equatorial electric field. Previously we considered only the dawn-dusk (Ey) component of the IEF vector. 2) We introduce local-time and seasonal dependencies to our model by correlating the EEF data derived from the Jicamarca ISR with the IEF data. In general, PP is maximally efficient for the variations in the IEF with 2- hour periodicity. The magnitude of penetration of IEF Ez to EEF is an order of magnitude smaller than that of IEF Ey. The diurnal curve of the correlation between IEF and EEF shows the well-known reversals of polarity at dawn and dusk. In addition, the correlation reduces at local noon, owing to the increased conductivity of the ionosphere. The paper discusses the implications of these results in predicting the EEF. Finally, we implemented the model as a real-time estimator of the prompt penetration electric field, driven by the ACE solar-wind data. The model is available at http://geomag.org/models/PPEFM/RealtimeEF.html.

GR 34. Student Training and Atmospheric Research (STAR) Na Doppler LIDAR at Boulder, Colorado

John A. Smith, Weichun Fong, Brendan Roberts, Wentao Huang, Xinzhao Chu. CIRES

We present a Na wind and temperature (Doppler) lidar developed by graduate students at the University of Colorado at Boulder-the "Student Training and Atmospheric Research" (STAR) lidar. Although based on a classical dye-laser transmitter, the performance far exceeds that of existing Na lidars with similar power-aperture products, yielding very high resolution temperature, wind and Na density measurements in the mesosphere and lower thermosphere. Such superb performance results from innovative approaches to high optical efficiency in the lidar receiver and detection systems. Significant gains in signal were achieved by detailed ray tracing of the receiver and telescope optics. Observations of temperature, vertical wind and Na density are shown to demonstrate the first high-resolution measurements by the STAR lidar at Boulder (40N, 105 W), Colorado. We also demonstrate a technique for characterizing PMT nonlinearity and pulse pileup effects using equipment familiar in resonance-fluorescence lidars. The approaches presented here are applicable to existing Na lidars as well as other resonance fluorescence lidars for significantly improving their performance and enabling new science studies such as high-frequency wave dynamics and eddy flux measurements.

GR 35. Climate adaptation barriers and opportunities in the United States: A focus on policy and decision making at the sub-national scale

Lisa Dilling. CSTPR/CIRES and Environmental Studies Program

As reported in the Fourth Assessment Report of the IPCC, even within countries with a high level of economic activity such as the United States, adaptive capacity is not necessarily commensurate with wealth and access to technology, and governance and social factors can be equally important influences on adaptive capacity. The same review indicated that adaptation activities are not evenly distributed within a region, and that public policy plays an important role in facilitating climate adaptation. Furthermore, recent research has suggested that despite calls for adaptation and the presence of planning efforts, adaptation actions on the ground are limited. Research has also demonstrated that many adaptation actions are taken in the context of other priorities, or motivated by other goals than reducing vulnerability to climate change. This paper focuses on two questions: what factors motivate communities to build adaptive capacity or take adaptive actions, and what role does information play in those decisions? These questions were studied for various aspects of climate-related decision making at the local policy level using a combination of interviews, document analysis, and survey research. Results are presented here from empirical studies of climate-related decision making at the local level in the areas of public lands management, hazard management and water supply management in several localities in the United States. This study specifically highlights the barriers and opportunities in decision making within local-scale governance processes for these areas. Preliminary results indicate that while opportunities to initiate or catalyze adaptation activities may come from many different sources, barriers such as lack of resources, competing priorities, uncertainty about the actions needed, and lack of relevant information can be powerful disincentives.

GR 36. The ionospheric gravity and diamagnetic current systems

P. Alken (1), S. Maus (1), A. D. Richmond (2), A. Maute (2)
(1) CIRES. (2) NCAR.

Large scale currents in the ionosphere are driven by a variety of sources, including neutral winds, gravity, and plasma pressure gradients. While the stronger day-time wind-driven currents have been extensively studied, gravity and diamagnetic currents in the ionosphere have received very little attention, but can have substantial effects even during the night. With the availability of a new generation of magnetic field models based on high-accuracy satellite magnetic measurements, it becomes increasingly important to account for these smaller current systems. In this work, we use the stand-alone NCAR TIEGCM electrodynamics solver along with empirical density, wind and temperature inputs, to model the global current systems caused by gravity and diamagnetism in the F-region ionosphere and calculate their magnetic perturbations. These results allow us for the first time to visualize the global structure of these currents and quantify their magnetic perturbations. We find a significantly higher gravity-driven current during the night than one would expect from the lower conductivity. We also find some discrepancies between the diamagnetic perturbation and a theoretical prediction which could indicate interesting physical effects not accounted for by the theory. These results will allow geomagnetic field modelers to account for these important current systems and create more accurate models. This work will also be crucial in analyzing ionospheric magnetic field measurements from the upcoming Swarm satellite mission.

GR 37. Anomaly analysis of recent summer heat waves

Emily C. Gill (1), Emily P. Wilson(1), Thomas Chase(1). (1)CIRES

Extreme warm, localized, temperatures (heat waves) appear to be increasing globally. Specifically, the 2010 Russian heat wave has been a controversial extreme climate event, initially dubbed as a result of natural atmospheric processes. This initial hypothesis has been refuted as new statistical methods revealed an 80% likelihood that it was caused by climate change. Under the supervision of Dr. Thomas N. Chase, research in regards to possible environmental factors causing temperature anomalies was conducted specifically looking into variables like soil moisture, specific humidity, long-wave surface incident and vegetation index. This study investigates trends in spatial and temporal variability and possible correlations between these factors and temperature. Recent findings show a strong connection between increased long-wave surface incident anomalies and increased specific humidity anomalies in the past 10 years. These findings provide more information regarding the recent increase of average temperature.

GR 38. NOAA Mobile Laboratory's Unique Contribution to the Uintah Basin Study

Jonathan Kofler(1), Gabrielle Pétron(1), Bill Dubé(1), Peter Edwards(1), Steven S Brown(1), Felix Geiger(2), Carsten Warneke(1), Laura Patrick(1), Sara Crepinsek(1), Benjamin R Miller(1), Pat Lang(1), Tim Newberger(1), Jack Higgs(4), Colm Sweeny(1), Doug Guenther(1), Anna Karion(1), Sonja Wolter(1), James Salzman(3), Jonathan Williams(4), Mark Slovak(5), Allen Jordan(1), Pieter Tans(3), Russ Schnell(3)
(1) CIRES, (2) Karlsruhe Institute of Technology, (3) NOAA ESRL,(4) Science and Technology Corporation (5) Idaho National Laboratory

A van capable of continuous real time measurement of CH4, CO2, CO, Water Vapor, Ozone, NO, NO2, VOCs (including aromatics) and other trace gases was driven in the oil and gas fields of the Uintah basin in northeastern Utah. Compressor stations, processing plants, oil and gas well heads, separators, condensate tanks, evaporation pond disposal facilities, holding tanks, hydraulic fracturing sites, gas pipeline and more were studied using the van. The mobile measurements provide powerful tool to get to the source of emissions and reveal the unique chemical signature of each of the stages and components of oil and gas production as well as overall basin and background gas concentrations. In addition to a suite of gas analyzers, the van includes a meteorological system, GPS tracking, flask sampling system, and a battery power system. Aspects of the vans hardware, sampling methods and operations are discussed along with a few highlights of the measurements.

GR 39. Hurricane Wake Restratification Mechanisms

Haney, S. R. (1,2), Fox-Kemper, B. (1,2), Bachman, S. (1,2), Cooper, B. (1,2), Kupper, S. (1,2), McCaffrey, K. L. (1,2), Stevenson, S. (1,2,3), Van Roekel, L. P. (1,2,4), Webb, A. (2,5), Ferrari, R. (6).
(1) Dept. of Atmospheric and Oceanic Science, University of Colorado, Boulder; (2) CIRES, Boulder, CO, (3) University of Hawaii, Honolulu, HI, (4) Northland College, Ashland, WI, (5) Dept. of Applied Mathematics, University of Colorado, Boulder, (6) MIT Dept. of Earth, Atmospheric, and Planetary Sciences, Cambridge, Massachusetts

As a hurricane passes over the ocean, the intense cyclonic winds draw cold water up from the deep ocean, and make the surface mixed layer much deeper than normal. The result after the hurricane passes is a deep, cold wake which restratifies over time. We analyze the restratification of the cold wakes of Hurricanes Frances, Katrina, and Igor, based on scalings for different processes that can restore the hurricane wake to near the pre-hurricane conditions. The scalings are derived from model results and well-known parameterizations of air-sea heat fluxes, Ekman buoyancy fluxes, and mixed layer eddies. To obtain realistic scalings, we used satellite observations for temperatures inside the wakes, and climatological data from drifters for temperatures outside the wake and to calculate mixed layer depths. We find that the dominant mechanism for restoration of the surface is the Ekman transport of warmer water adjacent to the cold wake, while submesoscale eddy bolus fluxes have the dominant subsurface effect. The resulting restratification timescales will be compared to approximate restratification times inferred from satellite SST data.

GR 40. The TropSat Observatory for Mesoscale Convective System Processes in the Global Maritime Tropics

David G. Long, Brigham Young University, Ernesto Rodriguez, Jet Propulsion Laboratory , Ralph F. Miliff, Visiting Fellow, CIRES , Robert Gaston, Jet Propulsion Laboratory
Brigham Young University, Jet Propulsion Laborator, Visiting Fellow, CIRES

TropSat is an earth-observing satellite mission concept with a minimum science goal of detecting and characterizing mesoscale convective system (MCS) as they occur successively for individual systems in all tropical ocean basins. Tropical MCS are fundamental drivers of global weather and climate. Their accurate characterization is the key to understanding and modelling the sub-grid scale processes critical to the evolution of large-scale air-sea dynamics; i.e. including tropical cyclogenesis, monsoons, the Madden-Julian Oscillation, and the El Nino-Southern Oscillation. MCS processes are now, or will soon be, within the resolution limits of the most sophisticated global general circulation models. However, MCS processes across the MCS life-cycle, are poorly represented in these models. TropSat observations will finally offer the observational basis necessary to understand and parameterize MCS initiation and life cycles for each tropical basin, setting the stage for major advances in global modelling. The TropSat instrument concept is a spacecraft integrated active and passive microwave sensor with channels and polarizations carefully selected to optimize simultaneous detection of the MCS environmental signals. TropSat will provide high spatial resolution measurements of surface winds, rain rate, total column moisture, and layer-averaged temperatures (i.e. SST and upper-level atmospheric temperature). Broad swath design and an unique low-inclination orbit focus temporal resolution (approximately two-hourly) on the global maritime tropics. The principal geophysical targets for TropSat are the processes of organization, evolution and senescence that characterize the MCS life-cycle stages.

OG 1. TRACING THE GEOMORPHIC SIGNATURE OF LATERAL FAULTING IN NEW ZEALAND'S MARLBOROUGH HILL COUNTRY

Alison R. Duvall (1), Gregory E. Tucker (1), (1) CIRES

Strike-slip faults occur commonly in all types of tectonic settings and, when active, count among the most dangerous geologic features on Earth. Despite this importance, characterizing in detail their rate of motion, seismic hazard, and evolution over a range of timescales remains a challenge in earth science. One promising and under-exploited tool to decode information about fault motion is quantitative analysis of the local terrain surrounding the fault. However, most past work of this kind has focused almost exclusively on vertical rather than horizontal motion in orogenic systems. We seek to develop a new framework for applying landscape analysis to constrain seismic hazards associated with major continental strike-slip fault zones. Research of this kind will move the scientific community toward a comprehensive and quantitative understanding of the geomorphic response to lateral crustal motion, which we currently lack. A suite of parallel strike-slip faults known as the Marlborough Fault System (MFS), South Island, New Zealand offers an excellent natural experiment to investigate this problem. From north to south, fault initiation ages as well as cumulative fault displacement are proposed to decrease whereas slip rate increases over four fold, providing snapshots of different stages of fault evolution. Comparison of landscape morphometrics and short-term river erosion rates from across the landscape will be used to identify variability in landscape morphology between regions of variable slip rate and fault age. The surficial response to different strike-slip scenarios will also be explored using computer simulations of the region's evolving landscape. Preliminary observations of planform and river longitudinal profiles derived from digital elevation data highlight zones of strong disequilibrium within tributaries that drain to active fault strands and suggest that river capture related to fault activity may be a regular process in strike-slip fault zones. Thus, systematic variability in fluvial knickpoint location, drainage area, and incision rates along different faults or fault segments may be expected and could act as a useful indicator of tectonic activity.

OG 2. Passive Tomography using a Dense Array of Single-Channel Seismic Recorders with applications to the Bighorn Mountains, Wyoming

Colin T. O'Rourke (1), Anne F. Sheehan (1), Joshua C. Stachnik (1,3), Lindsay L. Worthington (2) and the BASE Seismic Team

(1) CIRES, University of Colorado; (2) Texas A&M University

The Bighorn Arch Seismic Experiment (BASE) was a large NSF-funded project aimed at seismically imaging the Bighorn Mountain range in northern Wyoming. Part of this project involved installing lines of single channel "Texan"-style dataloggers (Reftek 125A) with 4.5Hz geophones. Typically only used for active source crustal imaging, we are now using these instruments to measure teleseismic arrivals and image deep structure. While deployed and running in continuous mode for a two week time period, these 834 instruments managed to record a total of 45 pickable teleseismic events with magnitudes ranging from 4.1 to 7.0 at ranges up to 105 degrees, yielding over 13,000 P wave first arrival picks. We use the fast-marching-method tomography package FMTOMO published by Nicholas Rawlinson1 to create a preliminary 3D seismic velocity model of the crust and upper mantle below the Bighorns. From this inversion we are able to infer geologic structure, at least to a first order. Future studies will involve combining this passive source dataset with active-source shots detonated along the main E-W and N-S lines of the array, picks from regional earthquakes, and arrival times from abundant mine blasts in the region. This joint inversion will help constrain the crust, which will allow for more detailed study of the upper mantle and Moho. We believe that the use of Texan-style instruments in passive recording mode represents a viable option for future seismic studies, and hope that the results presented here can serve as examples of the types of data these small instruments can produce.

OG 3. Buoyancy sources in the Western U.S.

Will Levandowski (1), Craig Jones (1), Weisen Shen (2), Mike Ritzwoller (2). (1) CIRES, (2) CIEI, Dept. of Physics, CU

. The heterogeneous geologic history of the western U.S. invites a broad spectrum of possible ways of supporting modern, widely varied topography ranging from orogen-scale thermal support to highly variable combinations of crustal buoyancy, mantle temperature, lithospheric composition, and convective effects. We explore the need for diverse means of support in two areas: the Sierra Nevada region with P-wave tomography and the Utah-Colorado-Kansas region spanning several provinces imaged with ambient noise tomography. Expected topography is initially calculated from crustal densities derived from seismic wavespeeds combined with mantle densities inferred from wavespeeds assuming a chemically homogeneous but thermally varying mantle. This expected topography has internal uncertainties of a few hundred meters and compares well with observed topography in broad terms, but substantial deviations reflect the presence of melt and compositional variations. Predicted topography is too high in the Cascade backarc, the eastern Basin and Range, and in much of the Southern Rocky Mountains. This difference we attribute to the presence of melt of less than 0.5% of total volume, which lowers wavespeed with little effect on density. Reducing the density anomaly to account for melt can reconcile this discrepancy. Conversely, parts of the Wyoming craton and Great Plains have predicted topography lower than observed, a discrepancy most plausibly related to iron depletion of the Archean and early Proterozoic mantle lithosphere. No results to date require sublithospheric loads and probably preclude variations in topography from such loads exceeding ~0.5 - 1 km in each region.

OG 4. Constraining Mantle Anisotropy under the South Island of New Zealand

Daniel W. Zietlow(1), Anne F. Sheehan(1), Zhaohui Yang(1), Joshua C. Stachnik(1,4), John Collins(2), and Martha K. Savage(3)
(1) CIRES and Department of Geological Sciences, University of Colorado, Boulder, CO 80309, USA. (2) Department of Geosciences, Woods Hole Oceanographic Institute, Woods Hole, MA 02543, USA. (3) Institute of Geophysics, Victoria University of Wellington, Wellington 6012, New Zealand
(4) now at Geophysical Institute, University of Alaska, Fairbanks, AK 99775, USA

Due to its well-understood tectonic history, New Zealand is an ideal location to investigate strain at depth through seismic anisotropy studies; however, previous investigations have resulted in conflicting interpretations. Central regions of the South Island, as well as its northern end, exhibit fast axis orientations nearly parallel to the Alpine Fault with magnitudes ranging between one and two seconds, independent of distance from the fault. The nearly fault-parallel splitting directions were considered to either represent lithospheric shearing or asthenospheric flow. In order to discriminate between these two proposed mechanisms for anisotropic generation, it is necessary to expand the current array of seismic stations. We report on investigations of shear-wave splitting measurements of waveforms obtained from ocean bottom seismometers (OBS) deployed off the South Island with approximately 100 km spacing. Despite obvious disadvantages of installing seismometers on the ocean floor, the installation of the OBS allowed us to study the extent of anisotropy across a distance approximately five times greater than the width of the South Island. Preliminary results reveal one event with clear SKS phases and another with SKKS phases on a number of stations. While a few of these yield null splitting results, fast orientations off the east coast tend to be near perpendicular to the Alpine fault, whereas the east coast exhibits fast orientations more parallel to the fault. If similar splitting measurements are made for more events, these results suggest that asthenospheric flow cannot account for the generation of anisotropy in the mantle under the South Island.

OG 5. Reducing the Uncertainty in the Estimation of Deformation across the Rio Grande Rift Region

James Choe1, R. Steven Nerem1,3, Anne Sheehan2,3, Henry Berglund4, Mark H. Murray5. 1Department of Aerospace Engineering Sciences, University of Colorado, Boulder CO 80309. 2Department of Geological Sciences, University of Colorado, Boulder CO 80309
3Cooperative Institute for Research in Environmental Sciences, Boulder CO 80309. 4UNAVCO, Boulder, Colorado 80301
5Department of Earth & Environmental Science, New Mexico Tech, Socorro, NM 87801

We analyze over 5 years of continuous GPS measurements from 25 GPS sites across the Rio Grande Rift (RGR) region in New Mexico and Colorado. Plate Boundary Observatory (PBO) GPS sites in adjoining eastern Colorado Plateau and western Great Plains are also included in the analysis. Surface velocities for each GPS sites are computed by GIPSY/OASIS in a North America fixed reference frame and are used to derive strain-rate deformation in the RGR region. The time series from the first 5 years are also examined to assess RGR site stability. An attempt is made to estimate the surface loading correction due to hydrology from Gravity Recovery and Climate Experiment (GRACE) measurements over the same time period. This correction is applied on the vertical time series to better model annual displacement on the surface velocity estimation and to reduce the uncertainty in the strain-rate estimation.

OG 6. Controls on the evolution of the Himalayan thrust belt

Delores M. Robinson, CIRES

In the Himalayan thrust belt of far western Nepal, forward modeling reconstructions and data derived from the thrust belt and the foreland basin ties the erosional unroofing and associated deposition to the kinematics and age of fault motion. The deformation in the thrust belt is reproduced by using a forward propagating, linked fold-thrust belt-foreland basin system. The magnitude of erosion is estimated at each time step as well as the load the fold-thrust belt places on the Indian plate. The reconstructions reveal that the units which supply the sediment to the foreland basin changes through time: 25 to 13 Ma-erosion of Tethyan Himalaya; ~12 Ma-first exposure of the Greater Himalaya (GH); ~11 Ma-first exposure of Lesser Himalaya (LH). Exposure of the GH and LH rock is associated with the formation of a ramp that cuts through 7 km of footwall LH stratigraphy and translates >7 km of LH stratigraphy over the ramp. An increase in structural relief focuses erosion over the region of the ramp and facilitates exposure of GH and Proterozoic LH rocks. As the LH ramp propagates southward, more LH thrust sheets are incorporated into the duplex. Although uniquely dating thrust events is challenging, this reconstruction allows us to associate steps in the reconstruction with an age of deposition or exhumation. What emerges is a tempo of deformation that varies with time with periods of rapid shortening during the propagation of the Main Central thrust and development of the LH duplex (~25-30 mm/yr). Both early (after the emplacement of the Ramgarh thrust) and late stages of duplex development are marked by windows of slow shortening (~13-14 mm/yr). Although long term and modern (geodetic) rates of deformation agree at ~20 mm/yr, rates of shortening through time have varied from 4-33 mm/yr.

OG 7. Estimated Shallow Crustal Shear Velocity Structure Off the South Island, New Zealand from Seafloor Compliance Measurements

Justin S. Ball (1), Anne F. Sheehan (2)

Ocean surface gravity wave energy at sufficiently long periods can propagate to the seafloor producing a time-varying pressure load. The transfer function between applied pressure and resulting displacement fields measured at the seafloor is known as the seafloor compliance and depends strongly on the shear structure beneath the measurement site. The Marine Observations of Anisotropy Near Aotearoa (MOANA) experiment in 2009-2010 deployed 30 broadband ocean bottom seismometers (OBS) with collocated differential pressure gauges (DPGs) off the South Island of New Zealand with the goal of using regional anisotropy measurements to quantify the strain field at depth and elucidate the mantle rheology. Teleseismic methods of resolving anisotropy such as receiver function analysis and shear-wave splitting depend on high signal-to-noise ratios that are difficult to achieve at OBS sites due largely to the effects of low-velocity sediments. Methods of removing sediment effects from teleseismic data typically require accurate estimates of sediment column velocities, to which seafloor compliance is sensitive. Preliminary compliance curves were calculated from pressure and acceleration power spectra at periods between 33-500s and normalized by the coherence between pressure and vertical acceleration signals to suppress non-infragravity noise sources. The resulting compliance values range from 10^-10 - 10^-8 Pa^-1 and are sensitive to changes in basement shear modulus at depths that increase with forcing period. Data uncertainties increase with depth to approximately 5% at 7km. 1D forward velocity models with a depth range of 100-7000m are used to calculate synthetic compliance curves and the best-fitting model for each station is presented. The use of these models for the removal of sediment-converted S-phases from teleseismic receiver functions is demonstrated. Additionally, time-varying compliance observations at one station corresponding with anomalous long-period pressure signals are interpreted as possible gas migration events.

BL 1. Ground-based GPS Observation of SED-associated Irregularities Over CONUS

Yang-Yi Sun1,2,3 , Tomoko Matsuo1,2, Eduardo A. Araujo-Pradere1,2, and Jann-Yenq Liu3
1Cooperative Institute for Research in Environmental Sciences, University of Colorado at Boulder, Boulder, Colorado, USA.
2Space Weather Prediction Center, National Oceanic and Atmospheric Administration, Boulder, Colorado, USA.
3Institute of Space Science, National Central University, Chung-Li, Taiwan

In this study, we construct the total electron content (TEC) map over the continental of United States (CONUS) from ground-based GPS TEC data, using the nonstationary wavelet-based estimate error covariance with the Kalman filter update formulas, to study the relationship between the SED-associated irregularities and TEC gradients during the intense geomagnetic storms of March 31, 2001 and October 30, 2003. Our results show that large-scale TEC gradients and SAPS play an important role in the formation of irregularities at the boundary between the SED and the mid-latitude low TEC region. Small-scale TEC gradients are related to the formation of SED-associated irregularities in the low TEC region.

BL 2. Evaluation of the differential Doppler velocity approach for sizing particles in ice clouds

Sergey Matrosov, CIRES

Measurements from ground-based collocated Ka- and W-band vertically pointing Doppler radars were used to evaluate the differential Doppler velocity (DDV) approach to retrieve a size parameter of the aggregate particle distributions in ice clouds. This approach was compared to a more traditional method based on the dual-frequency reflectivity ratio (DFR) using case study observations in different clouds. Due to measurement errors and other uncertainties, meaningful DDV based retrievals were generally available for the size slope parameter interval of 9 cm-1< Λ < 25 cm-1. The DFR were generally available for particle populations with Λ up to about 45 cm-1. Expected retrieval errors in the Λ interval between 10 cm-1 and 25 cm-1 were about 30-40% for the DFR-based estimates and about a factor of 2 larger for the DDV method. Comparisons of the DDV- and DFR- inferred values of Λ when both retrievals were available revealed their general consistency with a relative standard deviation between results being within retrieval uncertainties. While the DFR approach appears to be more accurate, it requires a 0 dB constraint near cloud tops, which mitigates uncertainties in absolute radar calibrations and differing attenuation paths. The DDV approach generally does not require such a constraint if radar beams are perfectly aligned in vertical (which might not be exactly a case during some observations). Given this, DDV measurements may potentially allow ice particle sizing in situations when DFR constraining is not effective or available (e.g., in precipitating clouds and in clouds with substantial amounts of supercooled water).

BL 3. Identifying Multiple Peaks in W-band Radar Doppler Spectra during Drizzle Events in VOCALS 2008

Christopher R. Williams (1, 2), Chris Fairall (2), and Ken Moran (1, 2), (1) CIRES, (2) NOAA ESRL PSD

During the VOCALS 2008 cruise, a NOAA W-band (94 GHz) radar was mounted on a stabilized platform and pointed vertically to observe the marine boundary layer cloud structure. Occasionally during drizzle events, while the reflectivity was consistent with time and height, the estimated spectrum width had large values. Examination of the Doppler velocity power spectra reveled that many of the spectra with large spectrum widths actually contained multiple peaked spectra. These multiple peak spectrum invalidates the assumption that drizzle can be modeled as a single peaked spectrum of droplets described by three parameters (e.g., intensity, mode, and spread). The observed multiple peaked spectra suggest that multiple physical processes are generating different sized drizzle droplets that are being observed within the same radar pulse volume. To identify and study the origin of the different sized drizzle droplets, a multiple peak picking routine was developed that identifies multiple peaks in each spectrum. The spectrum moments (reflectivity, mean velocity, and spectrum width) are estimated for each peak. Time-height cross-sections of Doppler velocity spectra show evolution of drizzle droplet distributions with time and height. This work was presented in Poster number OS43A-1520 at the December 2011 AGU Fall Meeting.

BL 4. WRIT: Web Based Renanalyses Intercomparison Tools

Catherine A. Smith and Gilbert P. Compo, CIRES and NOAA/ESRL PSD

We have developed the first two of a set of web based tools to examine and compare re-analysis datasets.These datasets include the National Center for Environmental Prediction/National Center for Atmospheric Research Reanalysis (NCEP/NCAR R1), National Center for Environmental Prediction/Department of Energy Reanalysis (NCEP/NCAR R2) , NCEP Climate Forecast System Reanalysis (CFSR), NASA Modern Era Retrospective-Analysis (MERRA), the 20th Century Reanalysis and the ECMWQF Reanalysis (ERA-Interim). The webpages are developed with HTML/Perl and use NCL to read and plot the data. For some datasets, OPeNDAP is used to read remote files. The first tool plots monthly maps and cross-sections of the datasets for mean fields, anomalies, and climatologies. Users can also plot the differences between reanalyses for each type of plot. The time series plotting tool extracts and plots monthly means and anomalies from the reanalysis datasets. It also plots differences between them and calculates statistics such as correlation. The WRIT can be expanded to include new variables and datasets as well as different timescales and other functionality.

BL 5. The automated detection and analysis of short-term changes in coronal dimmings

Larisza Krista (1), Alysha Reinard (2)
(1 & 2) CIRES, NOAA/SWPC

We present a new approach to the detection of coronal dimming regions. The Coronal Hole Evolution (CHEVOL; Krista 2011) algorithm was adapted to study the temporal evolution of dimming region properties using either SDO/AIA and HMI or SOHO/EIT and MDI data. The algorithm was found successful in locating dimming regions with relatively low intensities and clear boundaries. The area, location and magnetic properties of dimming regions were determined at high temporal cadence from the time of their appearance to the time of their disappearance. As a result, we were able to study the properties and spatial evolution of the dimming regions. Four dimming regions were analysed, including a recurring dimming near the same active region. The recurring dimming appeared to be formed in a very similar way first expanding then shrinking and stabilizing as a coronal hole. The repeated similar behavior may indicate a quasi-steady magnetic configuration. With an extended dimming list, the method will be used to study the magnetic field reconfiguration caused by reconnection and to relate dimming region properties to those of CME's.

BL 6. Physical Modeling of Neutral Winds in the Thermosphere: Initial Results

Mariangel Fedrizzi(1,2), Timothy J. Fuller-Rowell(1,2), Mihail Codrescu(2), Mark Conde(3), Kazuo Shiokawa(4)
(1)University of Colorado/CIRES, (2)NOAA/Space Weather Prediction Center, (3)University of Alaska Fairbanks/Geophysical Institute,
(4)Nagoya University/Solar-Terrestrial Environment Laboratory

Thermospheric winds are one of the main sources of variability in the thermosphere-ionosphere (T-I) system. Neutral winds in the thermosphere have been studied extensively using ground-based, in situ and remote sensing satellite data, leading to a reasonably complete understanding of their climatology and to a development of detailed empirical and numerical general circulation models. The validation of the dynamics of the best available physics-based models, however, has been far from comprehensive. The challenge for the future is to quantitatively characterize the thermospheric dynamics and the global circulation. This step requires detailed analysis of observations on the dynamics itself and its impact on the T-I system, guided by numerical models. This work presents initial comparisons of thermospheric neutral winds obtained from a self-consistent physics-based coupled model of the thermosphere, ionosphere, plasmasphere and electrodynamics (CTIPe) with Fabry-Perot Interferometer observations. This study aims to quantitatively assess the capabilities and limitations of the model, and advance the understanding of the T-I system dynamics on different spatial and temporal scales.

BL 7. Auroral Forms that Extend Equatorward from the Persistent Midday Aurora during Geomagnetically Quiet Periods

J. V. Rodriguez (1), H. C. Carlson, Jr. (2), R. A. Heelis (3)
(1) CIRES and NOAA NGDC, (2) USTAR Space Weather Center, Utah State University, (3) William B. Hanson Center for Space Sciences, University of Texas at Dallas

Auroral forms ('crewcuts') that extend equatorward from the persistent midday aurora have been characterized based on a survey of Svalbard 630.0-nm all-sky images from eight December solstice seasons. The 630.0-nm forms are directly related to a mix of precipitating magnetosheath and plasma sheet electrons embedded in a population of boundary layer ions, as observed by NOAA 6. The associated midday aurora lies at the equatorward edge of poleward velocity-dispersed cusp 'ion plumes' observed by DMSP F7 at 10 magnetic local time. In this survey, crewcuts are found to occur for $Kp \leq 3$. Distinct in many salient ways (including dynamics, orientation and associated IMF polarity) from the poleward-moving auroral forms (PMAFs) associated with transient dayside merging, crewcuts represent a solar wind-magnetosphere interaction that is more characteristic of quiet geomagnetic conditions. Crewcuts are most likely to be observed when IMF Bx and By (GSM) are dominant. Considering these observations in the context of magnetic merging topologies, we suggest crewcuts observed at Svalbard are most likely to lie at the foot of overdraped field lines recently opened by patchy, quasi-steady merging in the southern hemisphere.

BL 8. The effects of 3D error covariance and background model bias for an ionospheric data assimilation model

C. Y. Lin (1,2,3), T. Matsuo (1,2), E. A. Araujo-Pradere (1,2), and J. Y. Liu (3)
(1) Cooperative Institute for Research in Environmental Sciences, University of Colorado, Boulder, Colorado, USA;
(2) Space Weather Prediction Center, National Oceanic and Atmospheric Administration, Boulder, Colorado, USA;
(3) Institute of Space Science, National Central University, Jhongli, TAIWAN

NOAA/SWPC data assimilation model for the ionosphere is based on the Gauss-Markov Kalman filter with the International Reference Ionosphere (IRI) as the background model, with the electron density profiles described in terms of a handful of Empirical Orthogonal Functions (EOF). To obtain assimilative analyses over the Northern America, EOF coefficients at a given longitude-latitude grid location are inferred from ground-based GPS total electron content (TEC) data by using a Kalman filter. The model has been proved to have an accuracy of about 2 TECu (1016 #/cm2) on average over CONUS, when used for ground-based GPS data. However, we have found that the model is not suited to assimilate FORMOSAT-3/COSMIC (F-3/C) GPS occultation TEC data. Due to the fact that occultation observation paths pass through large longitude latitude areas at different altitudes, the original EOF-based method with 2D background error covariance cannot be applied to occultation data. To overcome the limitation of the EOF-based method, we used the 3D background error covariance to assimilate both space-based F-3/C occultation data and ground-based GPS observation data. Moreover, we have found that IRI shows regional biases with respect to F-3/C occultation TEC and ground-based GPS observation TEC. The bias correction is also an important issue to increase the accuracy of the assimilation result. We characterize regional IRI background model biases, by comparing simulated synthetic TEC to the two sets of GPS data: F-3/C occultation and ground-based GPS data.

BL 9. New ways of discretizing global climate models

Shan Sun (1,2) and Rainer Bleck (1,2,3). (1) CIRES, (2) NOAA ESRL, (3) NASA GISS

A 3-dimensional global ocean circulation model, named iHYCOM, is under development at NOAA's Earth System Research Laboratory. The model is destined to become the oceanic counterpart of the finite-volume, flow- following, icosahedral atmospheric model FIM (http://fim.noaa.gov). FIM uses an icosahedral horizontal grid and a hybrid-isentropic vertical coordinate. Preliminary results from the ocean model alone and the coupled model will be discussed. Numerical merits of new ways of discretizing equations will be assessed by comparing iHYCOM and the standard HYCOM, both are forced with the same CORE forcings. Several performance measures indicate that running HYCOM on an icosahedral mesh is feasible. This paves the way for efficient coupling to an icosahedral atmospheric model without the need for an interpolating flux coupler.

BL 10. High-resolution modeling approaches to understanding changes in extreme precipitation projections

Kelly Mahoney(1), Michael Alexander(2), Jamie Scott(1), Joe Barsugli(1)
(1) CIRES, (2) NOAA ESRL

One of the challenges inherent to understanding the effect of global climate change on precipitation extremes is the mismatch of scale. Climate models simulate large-scale patterns of long-term change, while weather models generally diagnose small-scale weather phenomena such as extreme rainfall. Therefore, understanding the potential effects of global-scale changes on local-scale weather requires new research approaches to connect questions and processes across weather and climate scales. This study represents one such integrated approach by investigating projected changes in warm-season extreme precipitation events using a dynamical downscaling framework that sequentially interfaces climate- and weather-scale data. Focusing on the Colorado Front Range, global simulations are first downscaled to a medium/regional-scale resolution; the resulting simulations are then further downscaled using a high-resolution weather model. The high-resolution model is able to explicitly simulate intense thunderstorms using 1.3-km grid spacing, thus resolving the small-scale physical processes that generate extreme precipitation. Physical process explanations are sought for projected changes in rainfall amount, hail occurrence, and flood risk. Past and future extreme event simulations are compared with respect to environmental drivers such as low-level instability (e.g., CAPE), large-scale forcing, and vertical temperature and moisture profiles. The events are also examined for systematic differences in storm-scale processes such as updraft strength, hail production and hail melting, dry air entrainment, and downdraft formation. Qualitative and quantitative consistency (or the lack thereof) across global, regional, and local-scale simulations is also explored.

BL 11. Adapting to Climate Change on the Shoshone National Forest: a science-management collaboration to develop planning and management tools

Janine Rice (1, 2), Linda Joyce (2), Bryan Armel (3), and Jeff Lukas (1). (1) CIRES Western Water Assessment, University of Colorado
(2) USDA Forest Service, Rocky Mountain Research Station. (3) USDA Forest Service, Shoshone National Forest

Climate change introduces a significant challenge for natural resource managers and decision makers. In response to that challenge in the western United States, the CIRES Western Water Assessment at the University of Colorado, the USFS Rocky Mountain Research Station and the Shoshone National Forest collaborated in a science-management partnership to develop reference materials and decision-support tools to aid resource managers as they incorporate climate-change considerations into management and planning. Initial discussions with the Forest identified the need for an assessment of what was currently known about the potential climate change effects on the Shoshone National Forest. Accordingly, the first component of this project was a synthesis report that identified past and current climate changes as well as the potential for climate change to affect natural disturbances and many ecosystem services produced in the Shoshone National Forest. This report is now being used as a resource in the Shoshone's forest planning process. Resource managers also identified the need for education on climate change and to provide an opportunity for staff to discuss current scientific findings on climate change and resource management. A "Natural Resources and Climate Change Workshop" held in April 2011 engaged Shoshone National Forest staff, other public land and private land resource managers, and scientists from USGS, the University of Wyoming, the State of Wyoming, as well as CIRES Western Water Assessment and the USFS Rocky Mountain Research Station. The workshop included presentations and discussions on climate change, water resources, snowpack and glacial change, Yellowstone cutthroat trout, species and ecosystem modeling for climate change, and the potential effects of climate change on public land, migration, recreation and tourism. The third component of the project was the development of a vulnerability assessment to identify potential vulnerabilities of the Shoshone National Forest to climate change. Here the Forest staff identified water availability, the Yellowstone cutthroat trout, and vegetation as key resources to consider in the assessment. The vulnerability assessment builds on the current literature on climate impacts as well as the data specific to the Shoshone National Forest. Results from this assessment have already been used to assist the Forest in directions for monitoring, and an evaluation of potential locations for restoration projects for Yellowstone cutthroat trout habitat. This science-management partnership also facilitated the Shoshone National Forest's effort to meet individual elements of the USFS Climate Change scorecard, a reporting mechanism that is part of the USFS Roadmap for Climate Change.

BL 12. Turbulence profiles and cloud-surface coupling in Arctic stratiform clouds

Matthew D Shupe (1), P. Ola G Persson (1), Amy Solomon (1), Ian Brooks(2), Guylaine Canut (2)
(1) CIRES / NOAA ESRL, (2) University of Leeds, UK

Stratiform clouds play a key role in Arctic climate through their high frequency of occurrence, persistence, variability of phase composition, and impacts on radiation and hydrology. Many of the key mechanisms that characterize these clouds are poorly understood due to complexities associated with a three-phase water system that is sensitive to aerosol properties and intricately tied to the atmospheric structure. Observations suggest that these clouds are at times thermodynamically coupled to the surface while at other times they are decoupled by an intervening stable layer. In this study we examine the coupling state of mixed-phase stratiform clouds during the fall and spring transition seasons at Barrow, Alaska. Characteristic signatures of the coupling state can be derived from ground-based remote sensors such as Doppler cloud radar. For example, radar-derived turbulent dissipation rates that are quasi-constant in height from the cloud layer down to the surface suggest that both the cloud and surface contribute to the turbulence affecting the cloud layer. On the other hand, a decrease in dissipation rates below the cloud suggest that the cloud itself is primarily responsible for generating its own turbulence without much influence from the surface. Retrievals of the dissipation rate are first evaluated using independent measures from aircraft and tethered-balloon systems, demonstrating that the radar-estimates are able to reasonably represent the dissipation rates and their vertical distribution. We then explore the impact that the coupling state has on a number of cloud properties such as depth, height, microphysical properties, and temporal variability. For example, it is generally found that surface-coupled clouds tend to have larger liquid water paths and stronger vertical motions than those that are decoupled. Overall, the cloud-surface coupling state can have significant impacts on the cloud structure and lifetime as it controls the balance of heat, moisture, and aerosols to the cloud from below and above.

BL 13. Inventory of NGDC high-resolution coastal tide gauge datasets for tsunami mitigation

Erica L. Harris, George Mungov. CIRES, NOAA NGDC

High-resolution coastal water level observations are a critical component for the accurate detection of tsunami event generation, propagation and inundation necessary for validation of tsunami warning models. Although automated coastal tide gauge records extend back to the late 1800s, they were often incapable of detecting tsunami event characteristics due to low sampling frequencies. Following the devastating December 2004 Indian Ocean tsunami, the U.S. National Oceanic and Atmospheric Administration (NOAA) /National Ocean Service (NOS) began a system-wide upgrade of tide gauge instrumentation for its 196 long-term U.S. water level stations to enable collection and dissemination of 1-minute water level sample data. This increase in sampling frequency provides adequate resolution for even small amplitude tsunamis. Post-collection programmatic processing, archiving and distribution of this data is then provided by NOAA's National Geophysical Data Center (NGDC). To clearly isolate tsunami waves from records dominated by local tides and coastal effects, NGDC is applying the following steps to all data:

- Data verification and quality control with identification and removal of gaps, spikes, data shifts and long-term trends
- Tidal harmonic analysis to identify the suite of tidal constituents present in the irregularly sampled data and long records
- Analysis for effects of stochastic influences (i.e. storm surge and river discharge)
- Residual time series analysis for investigation of events and processes previously unrecognized

Described here are the extent of available data at NGDC as a coverage of U.S. coasts and available periods. Also, discussed are the processing steps necessary to extract the local tsunami signal and illustration of the importance in applying this technique to support the ongoing effort to increase our understanding and forecasting capability of future tsunami events.

BL 14. Remote Sensing of the Mountain Snowpack: Integration of Observations and Models to Support Water Resource Management and Ecosystem Science

Noah Molotch (1,2), Jeff Deems (2), Bin Guan (3), Leann Lestak (4), Dominik Schneider (1), Michael Durand (5), Thomas Painter (3), and Jeff Dozier (6)
(1) Geography/INSTAAR, University of Colorado, (2) WWA/CIRES, (3) Jet Propulsion Laboratory - CAL TECH, (4) Institute of Arctic and Alpine Research
(5) Earth Sciences, The Ohio State University (
6) Donald Bren School of Environmental Science and Management, University of California, Santa Barbara

The impacts of climate change on water sustainability in mountainous regions is inherently linked to changes in mountain snow accumulation and snowmelt timing which sustains agricultural and municipal water demands for 60 million people in the U.S. and one billion people globally. Hence, accurate estimates of the volume of snowpack water storage are critical for supporting water resource planning and management. While snow extent is one of the earliest observed land surface variables from space, hydrologic applications of these data have been limited as the variable of interest for water management is snow water equivalent (SWE) which is not remotely observable at the fine-scale resolution needed in the mountains. Since the early 1980's, several works have illustrated the connection between runoff volume and snow cover depletion patterns as observed from satellite. In this regard, we present a series of experiments which illustrate that patterns of snow cover depletion can be coupled to spatially distributed snowmelt models to reconstruct the spatial distribution of SWE. In this regard, we present a proof-of-concept for a global product, providing daily estimates of snow water equivalent at 500-m scale for the observation record of the Moderate Resolution Imaging Spectroradiometer (MODIS). Estimates of the reconstructed SWE are validated against observed SWE from extensive snow surveys across the Sierra Nevada and Rocky Mountains with adequate spatial sampling, and compared to the operational Snow Data Assimilation System (SNODAS) SWE product produced by the U.S. National Weather Service. Snow survey SWE is underestimated by 4.6% and 36.4%, respectively, in reconstructed and SNODAS SWE, averaged over 17 surveys from sites of varying physiography. Corresponding root-mean-square errors are 0.20 m and 0.25 m, respectively, or 2.2 and 2.6 mean standard deviation of the snow survey SWE. Comparison between reconstructed and snow sensor SWE suggests that the current snow sensor network in the U.S. inadequately represents the domain SWE due to undersampling of the mid-lower and upper elevations. Correlation with full natural flow is better with reconstructed SWE than with ground-based snow sensors, or with SNODAS SWE on average; particularly late in the snowmelt season after snow stations report zero values but snow persists at higher elevations. These results indicate that inclusion of remotely sensed snow cover depletion patterns dramatically improves estimates of snow distribution in mountainous regions. Example applications for improving water resource management and understanding ecosystem response to water availability will be shown.

BL 15. Enhancing short term wind energy forecasting for improved utility operations: The Wind Forecast Improvement Project (WFIP)

Irina V. Djalalova (1), Laura Bianco (1), and James. M. Wilczak (2)

It is widely recognized within the wind energy and electric utility operations communities that current skill levels of wind energy forecasting are adding increased costs to the integration of wind energy onto the U.S. electrical grid. To address this, the U.S. Department of Energy has implemented a joint research program with NOAA and private industry to improve wind energy forecasts. The key elements of this program are a one-year deployment of extensive meteorological observing systems in two regions with significant wind energy production; assimilation of these observations into hourly-updated NOAA High-Resolution Rapid Refresh (HRRR) Model, run nationwide at 3 km resolution; and evaluation of the benefits of these improved wind forecasts on electrical utility operations. We will describe early results from the one-year field program, which began in July 2011. In particular we will describe the regions selected; the instrumentation deployed; the data quality control procedures; and a preliminary analysis of ESRL model forecast skill versus the NWS operational Rapid Refresh/RUC models.

BL 16. Low-frequency variability of and impact of climate change on Southern California's Santa Ana winds

Mimi Hughes (1); Dan Cayan (2); Alex Hall (3). (1) CIRES; (2) Scripps Institution of Oceanography (3) UCLA

The low frequency variability of and impact of climate change on Southern California's Santa Ana winds are investigated within surface observational data from the last half-century and a downscaled regional climate change experiment. A dynamical framework used to diagnose the forcing causing these strong offshore surface winds is presented. This framework relates the occurrence of Santa Ana winds to two mechanisms: a synoptic scale pressure gradient and a local temperature gradient. When a large-scale pressure anomaly causes offshore geostrophic winds roughly perpendicular to the region's mountain ranges this may in turn cause surface flow as the offshore momentum is transferred to the surface. However, many days have strong Santa Ana wind conditions without proportionately large synoptic forcing, due to local thermodynamic forcing that also causes strong offshore surface flow: a large temperature gradient between the cold desert surface and the warm ocean air at the same altitude creates an offshore pressure gradient at that altitude, in turn causing katabatic-like offshore flow in a thin layer near the surface. The contribution of 'synoptic' and 'local thermodynamic' mechanisms can be quantified using a bivariate linear regression model. We use this bivariate regression model to investigate the low frequency variability of three groups of Santa Ana wind events - synoptically forced, locally forced, and dually-forced events - using a network of surface meteorological stations from the mid-20th century to the present. The low frequency variability of each of the three types is compared with large-scale climate indices (e.g., the Southern Oscillation Index) to determine relationships between this local phenomena and large-scale climate measures. In addition, trends in both Santa Ana occurrence and the associated meteorological conditions over the last halfcentury are identified and explained. Following the observational analysis, the frequency and character of Southern California's Santa Ana wind events are investigated within a 12-km-resolution downscaling of late-20th and mid-21st century time periods of the National Center for Atmospheric Research Community Climate System Model global climate change scenario run. The number of Santa Ana days per winter season is approximately 20% fewer in the mid-21st century compared to the late-20th century. Since the only systematic and sustained difference between these two periods is the level of anthropogenic forcing, this effect is anthropogenic in origin. In both time periods, Santa Ana winds are partly katabatically-driven by a temperature difference between the cold wintertime air pooling in the desert against coastal mountains and the adjacent warm air over the ocean. However, this katabatic mechanism is significantly weaker during the mid-21st century time period. This occurs because of the well-documented differential warming associated with transient climate change, with more warming in the desert interior than over the ocean. Thus the mechanism responsible for the decrease in Santa Ana frequency originates from a well-known aspect of the climate response to increasing greenhouse gases, but cannot be understood or simulated without mesoscale atmospheric dynamics. In addition to the change in Santa Ana frequency, we investigate changes during Santa Anas in two other meteorological variables known to be relevant to fire weather conditions -- relative humidity and temperature. We find a decrease in the relative humidity and an increase in temperature. Both these changes would favor fire. A fire behavior model accounting for changes in wind, temperature, and relative humidity simultaneously is necessary to draw firm conclusions about future fire risk and growth associated with Santa Ana events.

BL 17. ENSO Diversity in the NCAR-CCSM4 Model

Antonietta Capotondi. (1) CIRES (2) NOAA ESRL PSD1

El Niño-Southern Oscillation (ENSO) is a fundamental component of the climate system due to its profound impact upon the global climate. Over the last few years extensive literature has developed to describe a type of El Niño in which the maximum sea surface temperature (SST) anomalies are located in the central equatorial Pacific rather than in the eastern Pacific, as in the canonical event. This central equatorial Pacific warming has been referred to as "Central Pacific El Niño" (CP- El Niño), "warm-pool El Niño", "dateline El Niño", and "El Niño Modoki" in an attempt to distinguish it from the classical Eastern Pacific (EP) El Niño. However, it is not clear whether there is a clear dichotomy between eastern vs. central Pacific warming events, or whether the location of maximum warming ranges over a continuum of longitudes resulting in events that could be defined as "central", "central-eastern" or "eastern". Different locations of maximum warming can lead to different patterns of extra-tropical teleconnections. In particular, the dominance of CP- vs. EP- El Niño over decadal long periods seems to produce a decadal modulation of the influence of ENSO upon temperature and precipitation over the United States. Central Pacific warming appears also to influence North Atlantic tropical cyclones, and may be linked to Antarctic warming. In this study we use the recently-released NCAR-CCSM4, a state-of-the-art climate model whose representation of ENSO has a large degree of realism, to characterize ENSO diversity, dynamical processes associated with different ENSO "flavors", and the dependency of the teleconnection patterns upon the longitude of maximum warming. We first validate some aspects of ENSO diversity in the model against the Simple Ocean Data Assimilation (SODA) product, as well as other SST data sets. We then use 500 years of model output to examine the teleconnection patterns associated with different ENSO flavors. The much longer duration of the model time series, relative to the observational record, allows a characterization of ENSO diversity with a higher degree of statistical significance.

BL 18. Global speleothem oxygen isotope measurements since the Last Glacial Maximum

Anju Shah (1), Carrie Morrill (1), Ed Gille (1), Wendy Gross (2), Dave Anderson (2), Bruce Bauer (2), Rodney Buckner (2), Mike Hartman (1)
(1) CIRES, (2) NOAA NCDC

Oxygen isotope measurements from cave deposits provide some of the highest-resolution and best-dated information about past fluctuations in temperature and precipitation. Over the past decade, a relatively dense network of sites has been measured spanning the time period from the Last Glacial Maximum to present. These sites yield data that address key scientific questions surrounding climate sensitivity to greenhouse gas concentrations, non-linear responses and thresholds in the climate system, and the skill of state-of-the-art climate models in reproducing states different from the present one. This compilation of speleothem oxygen isotope records includes quality-controlled values from sixty cores spanning part or all of the last deglaciation and Holocene, provided on a common age scale (calendar years before present, where present = 1950 A.D.) and with common measurement units (per mil PDB). The main data file is in comma-separated values format and first gives metadata information for each of the sixty cores (i.e., site name, core name, latitude, longitude, principal investigator, journal citation). Also provided in these metadata are the FTP locations (URLs) for machine-readable text files for each core, which give more complete information about site-specific metadata, dating methods and all raw data.

BL 19. Evaluation of the impact of radar reflectivity data assimilation on RR and HRRR reflectivity and precipitation forecasts

Patrick Hofmann (1), Steve Weygandt (2), Ming Hu (1), Stan Benjamin (2), Haidao Lin (3), Curtis Alexander (1), David Dowell (2)
(1) CIRES, (2) NOAA ESRL, (3) CIRA

The Rapid Refresh (RR) mesoscale analysis and prediction system assimilates national mosaic radar reflectivity data via a diabatic digital filter initialization procedure. This procedure, initially developed and applied within the Rapid Update Cycle (RUC) system, is key for improvements of both short-range RR convective forecasts and the High Resolution Rapid Refresh (which runs as a nest within the RR). In order to quantify the impact of the radar data assimilation, as well as other model configuration changes, we have developed a comprehensive reflectivity and precipitation verification package. This package, which runs in real-time on all RR and HRRR parallel cycles and has been applied to various retrospective test cases, is crucial for quickly evaluating possible improvements. The multi-scale verification package first maps native precipitation and reflectivity fields to several coarser grid resolutions (facilitating "neighborhood verification"), then computes standard verification scores and creates plots of hits, misses, and false alarms for several thresholds on each resolution grid. The verification data are then loaded into a database and a web interface that allows many statistical measures (CSI, bias, RMS, coverage area, etc.) to be displayed and overlaid with a wide variety of user input stratification specifications. The verification system allows isolation of patterns to model errors (diurnal, lead time, etc.), quickly giving feedback on changes made to the various real-time and retrospective forecast cycles. In this poster, we will report on the application of this system to quantify the impact of the RR reflectivity data assimilation on the RR and HRRR forecasts of reflectivity and precipitation. In addition to evaluating real-time runs (parallel RR at EMC, ESRL primary and development RRs, and ESRL primary and developmental HRRRs), we have evaluated several retrospective runs. Key issues we are examining with regard to the radar data assimilation are 1) documenting the impact for the DFI-radar assimilation in both the RR and the HRRR as a function of forecast length and time-of-day, 2) quantifying the sensitivity of the impact to the strength of the latent heating based temperature tendency. In particular, we are conducting experiments to see if we can improve forecast skill by adding stability and convective life-cycle dependencies to the latent heating specification. We will also present the results and subsequent changes made to the radar assimilation algorithm.

BL 20. A climatology of short-range weather forecasts from the High Resolution Rapid Refresh model

Eric James (1), Curtis Alexander (1), Brian Jamison (2), Stan Benjamin (3), Steve Weygandt (3)
(1) CIRES, (2) CIRA, (3) NOAA ESRL

The High Resolution Rapid Refresh (HRRR) model is being run hourly in real-time at the Global System Division (GSD) of the Earth System Research Laboratory (ESRL). The model is run out to fifteen forecast hours over a domain covering the entire conterminous United States (CONUS) at a spatial resolution of three kilometers, allowing the use of explicit convection. Initial and boundary conditions are obtained from the 13-km Rapid Refresh (RAP). In order to learn more about the systematic biases in the HRRR, we have initiated a long-term effort to map the temporal and spatial error patterns for an extensive history of HRRR forecasts. To facilitate this study, we established a real-time archive of two-dimensional HRRR forecast grids starting in late January 2012. In this presentation, we will stratify HRRR forecasts by time of day and lead time in order to discern the model's skill in representing the diurnal cycle of boundary layer structures and moist convection. We will also group forecasts by synoptic weather regimes and by sub-regions of the model domain. Forecasts of low-level winds and cloudiness will be evaluated in the context of the HRRR's utility for use in renewable energy applications. Evaluation of HRRR convective forecasts in regional and diurnal perspectives will be presented and ultimately used to calibrate time-lagged ensemble forecasts of convection. We will provide a description of HRRR time-lagged ensemble convective forecasts and their use as an estimate of thunderstorm likelihood for aviation and severe-weather applications.

BL 21. A Conditional Skill Mask for Improved Seasonal Predictions

Kathy Pegion(1,2), Arun Kumar (3). (1) CIRES. (2) NOAA/ESRL/PSD. (3) NOAA/NWS/NCEP/CPC

In Spring 2011, the Missouri and Ohio river valleys experienced precipitation greater than 200% of normal during the season, while much of Texas and New Mexico received only 25% of normal precipitation. The National Centers for Environmental Prediction (NCEP), Climate Forecast System (CFS) model successfully forecasted many aspects of the U.S. temperature and precipitation anomaly pattern during this time. However, the official NCEP/Climate Prediction Center (CPC) outlooks did not include the CFS precipitation forecast because the model was not considered to be skillful in these regions based on an average of historical forecast skill. Is it possible to know ahead of time when forecast skill would be higher than average and use that information to make better seasonal predictions? For seasonal predictions, higher skill is likely related to the phase and amplitude of the El Nino Southern Oscillation (ENSO). This project investigates the potential for improving the skill of seasonal temperature and precipitation forecasts for the continental United States by constructing and applying a skill mask that is conditional on a commonly used index of ENSO, thereby enabling the forecaster to use the CFS during times when the forecast is expected to be more skillful.

BL 22. Diagnosing a daily index of tornado variability with global reanalysis

Philip Pegion (1) and Martin Hoerling (2). (1) CIRES, 2(2) NOAA/ESRL/PSD

The recent record setting tornado outbreaks in April 2011 has spurred a lot of discussion and debate of the causes of this record setting month. Global warming and the decaying La Niña were both common causes suggested as the reason behind such a destructive tornado season. Due to the inhomogeneity of the observed tornado record, there are few published studies that relate climate variability to occurrences of tornados. We employ a method developed by Harold Brooks and co-authors in 2003 that discriminates tornadic and severe weather soundings from everyday convection to circumvent the problems with the observed tornado record. We will show how this index, derived from the CFS-R, realistically reproduces the observed variability in tornadoes, and the relative impacts of different modes of climate variability on tornadoes over the United States. This analysis will provide a baseline that will be expanded to climate model simulations of the 20th Century and future projections.

BL 23. Implementation of Space Environmental Anomalies Expert System Real Time

Jonathan Darnel (1), Janet Green (2), William Denig (2). (1) CIRES, (2) NOAA

The National Geophysical Data Center (NGDC) has implemented the Space Environmental Anomalies Expert System Real Time (SEAESRT) system within NOAA. Originally developed by The Aerospace Corporation, the algorithms with comprise the SEAESRT system provide near-real-time estimates of the likelihood of spacecraft anomalies for satellites in geostationary orbit. Spacecraft anomalies are strongly correlated with the local radiation environment and the general level of geomagnetic activity. SEAESRT uses space weather data available from NOAA's Geostationary Operational Environmental Satellite (GOES) at a particular local time along with other ancillary real-time data and calculates a set of hazard quotients associated with the geostationary environment at all local times. NGDC is validating the SEAESRT results before making SEAESRT available for implementation in operations. We present here initial results and a demonstration of the utility of SEAESRT.

BL 24. Doppler Lidar Study of Wind Flow Characteristics in the Wake of Operating Wind Turbine

Pichugina Y.L.(1, 2), R. M. Banta (2), W. A. Brewer (2), J.K. Lundquist (3), N. D. Kelley (4), R. M. Hardesty (2),
Andrew Clifton (4), R. J. Alvarez (2), M. L. Aitken (3), J. D. Mirocha (5), S. P. Sandberg (2), and A. M. Weickmann (1, 2)
(1) Cooperative Institute for Research in Environmental Sciences (CIRES), Boulder, CO, U.S.A.
(2) Earth System Research Laboratory (ESRL), NOAA, Boulder, CO, U.S.A. (3) University of Colorado (CU), Boulder, CO, U.S.A.
(4) National Renewable Energy Laboratory (NREL), Golden, CO, U.S.A. (5)Lawrence Livermore National Laboratory (LLNL), Livermore, CA, U.S.A

Velocity deficits and enhanced turbulence generated by the blade rotation are two major wake effects that could extend to distances of several rotor diameters behind a wind turbine. Accounting for wakes is an important issue in the optimization of siting turbines in the wind farm, operational strategies to reduce wake effects, and improved design of wind turbines. We used NOAA's High-Resolution Doppler Lidar (HRDL) to obtain simultaneous measurements of vertical and horizontal wind flow features both upwind and downwind of a Siemens 2.3 MW research wind turbine during the Turbine Wake and Inflow Characterization Study (TWICS) at the NREL National Wind Technology Center in the spring of 2011. HRDL transmits a pulse of 2-µm infrared radiation at a pulse repetition frequency of 200 Hz, velocity precision about 10 cm s-1, and range-gate resolution of 30 m. The ability of HRDL to sweep the atmosphere along both constant azimuth and elevation angles was used to develop a scanning strategy to provide a variety of high resolution boundary layer (BL) information. Velocity deficit, wake downwind extent and meandering were measured under different wind speed and BL stability conditions, but at wind directions possibly aligned along the direction of the flow from Eldorado Canyon, prevalent at the site. Results obtained from both vertical-slice scans, performed along the lidar-turbine centerline, and conical sector scans, performed in the narrow sector around wind turbine at four levels, show averaged velocity deficits of 6-8 m s-1 extending up to 10-15 rotor diameters downstream of the turbine. Profiles of wind speed, direction, and turbulence, obtained up to several km both above the ground and downstream of the turbine were used to estimate wind flow and its diurnal variations, to compute statistics and distributions of wind speed at several heights across the layer of the atmosphere swept by the turbine blades, and to monitor occurrences of the Low-Level Jet (LLJ) and other atmospheric features.

BL 25. Relative contributions of synoptic and low-frequency eddies to time-mean atmospheric moisture transport, including the role of atmospheric rivers

Matthew Newman (1), George N. Kiladis (2), Klaus M. Weickmann, F. Martin Ralph (2), and Prashant D. Sardeshmukh (1)

1CIRES Climate Diagnostics Center, University of Colorado, and Physical Sciences Division/NOAA Earth System Research Laboratory, Boulder, Colorado

2Physical Sciences Division/NOAA Earth System Research Laboratory, Boulder, Colorado

The relative contributions to mean global atmospheric moisture transport by both the time-mean circulation and by synoptic and low-frequency (periods greater than 10 days) anomalies are evaluated from the mean vertically-integrated atmospheric moisture budget based on 40 years of NCEP-NCAR Reanalysis data. In the extratropics, while the time-mean circulation moves moisture primarily zonally from one part of the ocean to another, low-frequency and synoptic anomalies drive much of the moisture transport both meridionally and from ocean to land. In particular, during the cool season low-frequency variability is the largest contributor to moisture transport into the North American Southwest, Europe, and Australia. While some low-frequency transport originates in low latitudes, much of it is of extratropical origin, due to large-scale atmospheric anomalies that extract moisture from the Northeast Pacific and Atlantic oceans. Low-frequency variability is also integral to the Arctic (latitudes > 70ºN) mean moisture budget, especially during summer when it drives poleward transport from relatively wet high-latitude continental regions. Synoptic variability drives about half of the poleward midlatitude moisture transport in both hemispheres, consistent with simple "lateral mixing" arguments. Atmospheric transport in the extratropics is also particularly focused within "atmospheric rivers" (ARs), relatively narrow poleward-moving plumes of moisture associated with frontal dynamics. AR moisture transport, defined by compositing fluxes over those locations and times where column-integrated water vapor and poleward low-level wind anomalies are both positive, represents most of the extratropical meridional moisture transport. These results suggest that understanding potential anthropogenic changes in the Earth's hydrological cycle may require understanding corresponding changes in atmospheric variability, especially on low-frequency time scales.

BL 26. Evaluation of High Resolution Rapid Refresh (HRRR) Model Changes and Forecasts During 2011

Curtis Alexander (1), Steve Weygandt (2), Stan Benjamin (2), Tanya Smirnova (1), David Dowell (2), Patrick Hofmann (1), Eric James (1), Ming Hu (1), Haidao Lin (3), John Brown (2), and Joe Olson (1). (1) CIRES, (2) NOAA ESRL GSD, (3) CIRA

The High Resolution Rapid Refresh (HRRR) is a 3-km, convection permitting model, run hourly in real-time at the Global System Division (GSD) of the NOAA Earth System Research Laboratory (ESRL). The WRF-ARW-based HRRR is run out to fifteen hours over a domain covering the entire coterminous United States (CONUS), using initial and boundary conditions from an hourly-cycled 13-km mesoscale model, formerly the Rapid Update Cycle (RUC), and currently the Rapid Refresh (RR). The RR (and RUC) includes a diabatic digital filter-based radar reflectivity data assimilation procedure to improve specification of the divergent component of horizontal wind in areas of precipitation.

HRRR gridded output is used as input to an automated convective weather forecast product known as CoSPA. During the summer of 2011, an operational performance evaluation of CoSPA was conducted by the FAA to assess its impact on air traffic management (ATM) decision-making.

In this presentation, we will include an update of the changes implemented in the real-time HRRR model for 2011, including the adoption of the RR as a parent mesoscale model, along with results from an in-house assessment of HRRR model forecasts. Forecast evaluation from 2011 will include both the cool-season and warm-season and include verification of ATM related fields including ceiling, visibility, surface winds and reflectivity (convection).

Evaluation of model changes will include regional, diurnal (valid-time) lead-time, and multi-scale stratification of verification statistics. Case studies highlighting comparisons of the HRRR with the coarser-resolution parent model (RUC and/or RR) will be presented.

Ths research is partially in response to requirements and funding by the Federal Aviation Administration (FAA). The view expressed are those of the authors and do not necessarily represent the official policy or position of the FAA.

BL 27. Investigating North Pacific air-sea interaction using a local, empirical model

Dimitry Smirnov (1), Matt Newman (1), Mike Alexander (2). (1) CIRES, (2) NOAA ESRL

The predominant view of sea surface temperature (SST) variability in the middle latitudes is a nearly passive response to unpredictable, rapidly changing atmospheric wind, temperature and moisture anomalies. However, because the heat and moisture fluxes depend on the SST itself, the system must be coupled. Focusing on the North Pacific, we analyze the extent of coupling using simple local models on daily timescales. While the predominate view holds over large portions of the basin, deviations are seen near the Kuroshio current region. In this area, the ocean significantly alters the air temperature and moisture anomalies, particularly during the boreal winter season.

BL 28. Snow and Ice Enhancements to the Land-Surface model used in WRF-based Rapid Refresh

Tatiana G. Smirnova (1,2), John M. Brown (2), Stan Benjamin (2). (1) CIRES, (2) NOAA ESRL

The Land Surface Model (LSM) described in this presentation was originally developed as part of the Rapid Update Cycle (RUC) model development effort at what is now the Earth System Research Laboratory (ESRL). The goal of this work was to provide more accurate lower boundary conditions for the Rapid Update Cycle (RUC). This LSM (henceforth, RUC LSM) has been operational as part of the RUC since 1998. The RUC LSM describes complicated atmosphere/land surface interactions in a simplified fashion so as to avoid excessive sensitivity in the RUC system to multiple poorly defined surface parameters. The simple parameterizations in RUC LSM have proved to be physically robust and capable of realistically reproducing evolution of soil moisture, soil temperature and snow in the cycled model, where surface fields are initialized from the previous 1-h model forecast. Our RUC LSM development has adapted some ideas from existing land surface schemes, but also conceived of some unique features which in our opinion can give more accurate representation of physical processes. Monitoring of model performance over the years has motivated several modifications to the RUC LSM leading to better performance. Beginning in 2002, the RUC LSM became available to the WRF community as part of the yearly WRF code releases, and is implemented in the WRF-based Rapid Refresh (RAP), which will replace RUC at NCEP in March of 2012. With the much larger RAP domain covering the whole North American continent as well as large ocean areas in high latitudes, the RUC LSM needed further validation and development for application in the tundra permafrost regions and over sea ice, including heat conduction in the sea ice, and snow accumulation and ablation on top of the sea ice. The modifications to the RUC LSM were extensively tested off-line in one-dimensional framework using data from SnowMIP2 (Snow Model Intercomparison Project for forest snow processes) experiment, then were monitored and verified in the coupled developmental version of RAP, and finally were implemented in the operational RAP at NCEP. These recent modifications to ice and snow treatment in RUC LSM and results from one-dimensional and coupled RAP validations are described in this poster.

BL 29. A Relationship Between Stochastic Forcing of Tropical SST and the North Atlantic Oscillation (NAO)

Leslie M. Hartten (1,2), Cécile Penland (2). (1) CIRES, (2) NOAA/ESRL/Physical Sciences Division

Linear Inverse Modeling (LIM) estimates the deterministic dynamics of a linear system and the statistical structure, though not the time series, of stochastic driving noise. While there already exist several methods of diagnosing plausible sources of stochasticity from data, none of these is guaranteed to reproduce dynamical consistency. In this poster, we present a dynamically consistent method of using LIM output to capture the elusive time series of stochastic forcing and apply it to seasonal sea surface temperature (SST) data. The stochastic forcing of North Tropical Atlantic SST is particularly interesting, showing a strong relation to the rapidly-varying North Atlantic Oscillation.

BL 30. Understanding the Causes of ENSO Asymmetry Using CMIP5 Runs

Tao Zhang and De-Zheng Sun. NOAA ESRL/PSD1 CIRES

The asymmetry between El Nino and La Nina events is a fundamental property of ENSO. Understanding the causes and consequences of this property of ENSO may hold the key to understand decadal variability in the tropics and beyond. Here we present a preliminary analysis of existing CMIP5 runs that is aimed to extend a previous study using NCAR models and attempt to shed more light onto the question of what are the causes of ENSO asymmetry. An underestimate of ENSO asymmetry is found to be a common bias in CMIP5 coupled models. A common bias is also found in the wind stress response to El Nino warming in the corresponding AMIP runs of these models: the response of the zonal surface wind stress in the SPCZ region is too strong. These models also have a mean precipitation in the SPCZ region that is more zonally extended. Thus it appears that the underestimate of ENSO asymmetry in the coupled models may be linked to a long-standing error in the mean precipitation distribution in the AMIP runs of the models--a more zonally extended SPCZ.

BL 31. Physical Processes Associated with Heavy Flooding Rainfall in Nashville, Tennessee, and Vicinity during 1–2 May 2010: The Role of an Atmospheric River and Mesoscale Convective Systems

Benjamin J. Moore (1), Paul J. Neiman (2), F. Martin Ralph (2), Faye E. Barthold (3)
(1) CIRES, (2) NOAA/ESRL/PSD, (3) NOAA/HPC

A multi-scale analysis is conducted in order to elucidate the physical processes that resulted in prolonged heavy rainfall and devastating flash flooding across western and central Tennessee and Kentucky on 1–2 May 2010, during which Nashville, Tennessee, received 344.7 mm of rainfall and incurred 11 flood-related fatalities. On the synoptic scale, heavy rainfall was supported by a persistent corridor of strong water vapor transport rooted in the Tropics that was manifested as an atmospheric river (AR). This AR developed as water vapor was extracted from the eastern tropical Pacific and the Caribbean Sea and transported into the central Mississippi Valley by a strong southerly low-level jet (LLJ) positioned between a stationary lee trough along the eastern Mexico coast and a broad, stationary subtropical ridge positioned over the southeastern U.S. and the subtropical Atlantic. The AR, associated with substantial water vapor content and moderate convective available potential energy, supported the successive development of two quasi-stationary mesoscale convective systems (MCSs) on 1 May and 2 May, respectively. These MCSs were both linearly organized and exhibited back building and echo training, processes which afforded the repeated movement of convective cells over the same area of western and central Tennessee and Kentucky, resulting in a narrow band of rainfall totals of 200–400 mm. Mesoscale analyses reveal that the MCSs developed on the warm side of a slow-moving cold front and that the interaction between the southerly LLJ and convectively generated outflow boundaries was fundamental for generating convection.

BL 32. Toward Understanding the Climatic Role of Tropical Cyclones Using an Atmospheric General Circulation Model: Experiment Design and Model Evaluation

Henry R. Winterbottom (1), Phillip J. Pegion (2), and Robert E. Hart (3)
NOAA ESRL/CIRES (1), NOAA ESRL/CIRES (2), Department of Earth, Ocean, and Atmospheric Sciences, The Florida State University (3)

A formal assessment and an identification for the global circulation impact of a tropical cyclone (TC) remains in the developmental stages. This area of research was first suggested by Bengtsson et al., [1982], when questions were posed regarding the role of TCs with respect to the poleward transport of heat, moisture, and momentum. To date, much attention has been paid to the role of oceanic heat transport [Emanuel, 2001; Sriver and Huber, 2007; Hart et al., 2007; Liu et al., 2008; Hu and Meehl, 2009]. Fewer studies, however, have identified an explicit role for the TC within the atmosphere, although recent work has begun to quantify the magnitude of that atmospheric footprint from reanalysis datasets [Hart et al., 2007; Schenkel and Hart, 2011]. A recent study by Hart [2011] deduced a statistical relationship between northern hemisphere TC activity (evaluated using both TC count and power dissipation [Emanuel, 2007]) and the subsequent winter climate. Hart [2011] ascertained that there exists a strong (statistical) inverse relationship between the amount of pole-ward TC power-dissipation (e.g., recurving TCs) and the 500-hPa extratropical stationary eddy-temperature flux, and speculated on the physical (and potential nonphysical) explanations for such a relationship. Indeed, the relationship was so strong that it was the most robust predictor of this measure of wind activity amidst all known teleconnection indices. These prior works provide the foundation on which to further explore the TC role in climate. Accordingly, in this study, we diagnose the climatic impact of TCs upon the Earth's general circulation using the National Center for Atmospheric Research (NCAR) Community Atmosphere Model (CAM) and the TC vortex removal procedure discussed by Winterbottom and Chassignet [2011]. A series of experiments with and without TCs will be compared. We will evaluate the mean and transient eddy fluxes as a function of a simulation with TCs and a simulation without. We will also analyze the tropical wave characteristics and the position and strength of the Hadley Cell also as functions of TC presences. Finally, we will present the initial results from this ongoing study and will provide a hypothesis for the climatic role of TCs within the Earth's general circulation.

BL 33. Upper Colorado Runoff Predictions in Support of NIDIS

Klaus Wolter (1,2,3). (1) CIRES, (2) NOAA ESRL, (3) WWA

Naturalized streamflow for the Colorado River at Lees Ferry has been processed since the Water Year of 1906. Its linkage to ENSO is complicated by highly diverse seasonal precipitation cycles in this region, as well as a switch from being typically dry (wet) with La Niña (El Niño) during fall and spring to being typically wet (dry) during winters of the same ENSO phases in the northern mountains of this basin. Both NOAA and NRCS river runoff forecasts are typically trained on actual snowpack conditions from January onward into the melt season, not ENSO or other teleconnection information. This leaves a hole of several months without any information on the upcoming streamflow season. Furthermore, Lake Powell and Lake Mead are managed jointly on a two-year schedule, leaving an additional need for forecasts into "Year 2". This poster reports on my efforts to fill this gap in predictive capabilities with statistical models, including three years of actual forecasts (rather than hindcasts).

BL 34. Ionosphere-Plasmasphere-Electrodynamics (IPE) Model: An Impact of the Realistic Geomagnetic Field Model on the Ionospheric dynamics and energetics

Naomi Maruyama(1,2), Phil Richards(3), Tzu-Wei Fang(1,2), Catalin Negrea(1,2), Leslie Mayer(1,2), Tim Fuller-Rowell(1,2), Art Richmond(4), Astrid Maute(4). (1) CIRES, (2) NOAA SWPC, (3) George Mason Univ. (4) NCAR HAO

Longitudinal variations of the observed ionospheric and plasmaspheric signatures are often associated with the forcing from the lower atmosphere, such as the longitudinal variations of the upward propagating tides. It has been difficult to separate out the relative contribution between the lower atmospheric forcing and geomagnetic field variations when interpreting the observed signatures. Furthermore, little effort has been made so far to evaluate the different responses of the dynamics and energetics to geomagnetic field variations between the ionosphere and plasmasphere in a quantitative manner. In order to quantify the impact of the geomagnetic field variations in the ionosphere and plasmasphere, we have developed the new Ionosphere-Plasmasphere-Electrodynamics (IPE) model. It consists of a physics based model of an ionosphere and plasmasphere using the IGRF geomagnetic field configuration (APEX). Furthermore, the global ionospheric potential is solved self-consistently on the same grid. In this presentation, we will make comparisons of the modeled properties of the ionosphere and plasmasphere using the full IGRF and a dipole geomagnetic field. Furthermore, we will quantify the impact of the geomagnetic field variations in observed signatures of the plasma densities and temperatures and electrodynamics.

BL 35. The Western Water Assessment RISA Program: An Overview of Recent Accomplishments and Ongoing Research.

Eric Gordon(1), Jeff Lukas(1), Brad Udall(1), Kristin Averyt(1), and Tim Bardsley(1)
(1) CIRES Western Water Assessment

The Western Water Assessment (WWA) is a NOAA-funded Regional Integrated Sciences and Assessments (RISA) program based at CIRES. WWA's broad mission is to characterize regional vulnerabilities to climate variability and change and to assist decision makers throughout Colorado, Wyoming and Utah in responding to those vulnerabilities. At the same time, WWA works to understand how decision makers acquire and make use of climate information and deal with uncertainity. As a boundary organization WWA conducts multiple research projects that integrate stakeholder needs with academic research expertise. Examples include understanding the influence of multiple drivers of snowmelt across the Up! per Colorado River Basin, assisting Southwestern tribes with climate and drought adaptation planning, examining drivers of climate adaptation at the municipal level, and assessing how water managers make use of streamflow forecasts. This poster provides an overview of the mission and goals of WWA along with brief descriptions of several recently completed and ongoing projects.